i

The Dissertation Committee for Hossein Nazari Certifies that this is the

approved version of the following dissertation:

Neuronal and Vascular Degeneration of the aging retina in the

3xTg-AD mouse

Committee:

Massoud Motamedi, PhD
Supervisor

Wenbo Zhang, PhD

Erik van Kuijk, MD, PhD

Gracie Vargas, PhD

Gerald Campbell, MD, PhD

Giulio Taglialatela, PhD

Neuronal and Vascular Degeneration of the aging retina in the

3xTg-AD mouse

by

Hossein Nazari, MD

Dissertation

Presented to the Faculty of the Graduate School of

The University of Texas Medical Branch

in Partial Fulfillment

of the Requirements

for the Degree of

Doctor of Philosophy

The University of Texas Medical Branch
May 2021

Dedication

This dissertation is dedicated to my lovely wife, Fereshteh,

and to our children, Alireza, Mohammadreza, and Eila.

I also dedicate this dissertation to my beloved father and mother, Ata and Ana.

Acknowledgements

Neuronal and Vascular Degeneration of the aging retina in the 3xTg-AD mouse

Hossein Nazari, MD, PhD

The University of Texas Medical Branch, 2021

Supervisor: Massoud Motamedi

Alzheimer's disease (AD), a progressive and irreversible neurodegenerative disease and the most common cause of dementia in the United States, is characterized by amyloid β (Aβ) and tau deposition in the central nervous system (CNS), neurovascular dysfunction, and neuroinflammation. Diagnostic modalities to detect the early phases of these CNS pathologies in preclinical AD are inadequate. Vision abnormalities are common in AD, and Aβ and tau have been detected in the retina parallel to the brain. Noninvasive detection of early AD pathologies in the retina may enable: 1) improved understanding of the biologic foundation of AD, 2) early diagnosis and monitoring, 3) AD risk stratification, and 4) monitoring response to treatments. However, retinal structural or microvascular changes in AD, that may be detectable with noninvasive depth-resolved imaging modalities, have not been fully characterized yet. In this dissertation, several aspects of retinal neurovascular degeneration in a well-characterized mouse model of AD, 3xTg-AD, have been studied. Chapter one provides a rationale for studying retinal neurovascular alteration accompanying AD. Chapter two explores retinal sublayer thickness changes by optical coherence tomography (OCT) in young to middle age transgenic and control mice and suggests that a pattern of retinal sublayer changes may detect AD's preclinical stage and distinguish AD- from aging-neurodegeneration. The third chapter summarizes the age-dependent pattern of retinal capillary layer attenuation in the transgenic model. Such

vascular degeneration may be due to amyloid and tau deposition in vessel walls and reduced metabolic demand caused by neuronal loss. Mapping out such retinal degenerative changes would aid in the noninvasive diagnosis of AD. In chapter four, a novel retinal tissue preparation protocol to investigate retinal neuronal and vascular structures without cutting through the retina and disturbing the geometric correlation of various retinal regions is introduced. The final chapter summarizes the findings of the current project and its contributions to the field. In summary, these studies describe several aspects of retinal neuronal and vascular structures from young to middle age to old age in a well-characterized murine model of AD. Our findings highlight the need for a multi-modal imaging approach for early detection of AD.

TABLE OF CONTENTS

List of Figures

List of Abbreviations

3xtg-AD   Triple transgenic mouse model of Alzheimer's disease

Aβ   Amyloid-beta

AD   Alzheimer's disease

APOE4   Apolipoprotein E4

APP-PS1   Amyloid precursor protein-Presenilin 1

BBB   Blood-brain barrier

CBF   Cerebral blood flow

CNS   Central nervous system

CSF   Cerebrospinal fluid

DVA   Dynamic vessel analyzer

DVP   Deep capillary plexus

EOAD   Early-onset Alzheimer's disease

ERG   Electroretinography

GABA   Gamma-aminobutyric acid

IACUC   Institutional animal care and use committee

IVP   Intermediate capillary plexus

INL   Inner nuclear layer

IPL   Inner plexiform layer

IS   Inner segment

LOAD   Late-onset Alzheimer's disease

MCI   Minimal cognitive impairment

NFT	Neurofibrillary tangle
NGS	Normal goat serum
NVU	Neurovascular unit
OCT	Optical coherence tomography
OCTA	Optical coherence tomography angiography
ONL	Outer nuclear layer
OPL	Outer plexiform layer
OS	Outer segment
PBS	Phosphate-buffered saline
PD	Parkinson's disease
PFA	Paraformaldehyde
PET	Positron emission tomography scan
PS	Presenilin
p-tau	Phosphorylated tau
RGC	Retinal ganglion cell
RNFL	Retinal nerve fiber layer
ROI	Region of interest
RPE	Retinal pigment epithelium
SVP	Superficial capillary layer
SD-OCT	Spectral-domain optical coherence tomography

Chapter 1 Introduction to Neuronal and Vascular Degeneration

of the aging retina in the 3xTg-AD mouse

ABSTRACT

Alzheimer's disease (AD) is a progressive and irreversible neurodegeneration and the most common cause of dementia in the United States. Pathologic hallmarks of the disease are extracellular amyloid β (Aβ) plaques and intracellular hyperphosphorylated tau tangles in the brain. Substantial evidence indicates that Neurovascular dysfunction and neuroinflammation play major roles in AD neurodegeneration. Imaging biomarkers of such neurovascular dysfunction and neuroinflammation may help with early diagnosis of AD and monitoring its progression. Retina, as an extension to the brain, is a highly vascularized neuronal tissue that is accessible to various *in vivo* imaging modalities. Aβ plaques and tau tangles have been detected in the retina in AD. Detecting such pathologies and ensuing neurovascular degeneration in the retina using noninvasive imaging tools may facilitate early diagnosis of AD and monitoring its progression. However, retinal structural or microvascular changes that could differentiate AD from other neurodegenerations including aging remain unknown.

Current dissertation summarizes several aspects of retinal neurovascular degeneration in a mouse model of AD, 3xTg-AD. We first reviewed the current state of knowledge about Alzheimer's disease and provided a rationale for studying retinal neurovascular alteration in AD. Next was a presentation of our studies on retinal sublayer thickness changes in young to middle age transgenic and control mice. The third chapter illustrated the pattern of retinal vascular attenuation in the AD transgenic model and their age-matched controls. Next, we introduced our novel retinal tissue preparation protocol to investigate retinal neuronal and vascular structures in their entirety without cutting through the retina and disturbing the geometric correlation of various retinal regions is introduced. The final chapter summarized the findings of the current project and its contributions to the field.

INTRODUCTION

      Alzheimer's disease (AD), the most common cause of progressive dementia in the United States, is a growing health issue with no available treatment for our aging society. AD's pathologic markers are widely known to be amyloid β (Aβ) plaques and hyperphosphorylated tau tangles in the central nervous system (CNS). Braak and Braak suggested that these pathologic deposits begin at a young age and progress throughout life, culminating in the debilitating disease of the elderly.[1] It is now well-recognized that CNS vasculature and neuroinflammation play central roles in initiating toxic protein deposition and propagation of resulting destructions. However, the interplay between CNS neurovascular units (NVU), composed of neurons, vessels, inflammatory cells (Figure 1), and amyloid and tau deposition, is still unclear. Besides, diagnostic modalities to study cerebral neurovasculature and inflammation are often inadequate, expensive, or invasive, and thus, not scalable for large populations. Therefore, finding new markers of CNS vascular and inflammatory structure and function that can be easily visualized and quantified is a necessity.

      The retina is a neuronal tissue accessible to noninvasive optical imaging. Hence, it may be used as a tool to study the initiation and progression of AD pathology. In the following chapters, I will summarize my studies aiming at improving the current understanding of coupling of retinal neuronal and vascular elements in a well-established AD animal model. I will provide evidence that a set of biomarkers composed of various components of retinal NVU may be an indicator of AD pathology burden in the brain and may differentiate AD from other neurodegenerative conditions.
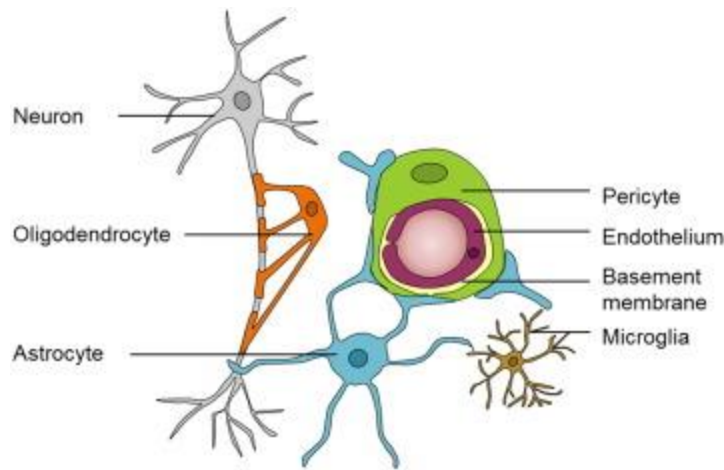
Figure 1. Neurovascular unit. NVU is an interactive network of cells (pericytes and endothelial cells), glia (microglia and astrocytes), and neurons (figure reused with permission from reference #2).[2]

HISTORY OF ALZHEIMER'S DISEASE

Ancient Greek and Romans considered loss of cognition an inevitable part of growing old. In the early 1800s, the word dementia started to appear in medical literature to indicate loss of mind. Around the same time, histologic studies linked senile dementia to brain atrophy and brain vessel changes.[3] In the early 1900s, after Bielschowsky visualized neurons using an improved silver staining, Alois Alzheimer, a German psychiatrist, described neuronal plaques and tangles in a woman who had died young from dementia associated with progressive confusion and hallucinations. This constellation of symptoms was later called Alzheimer's disease. In 1927, the substance in neuronal plaques was identified as "amyloid" due to the green birefringence of polarized light in Congo red staining. It was suggested that the amyloid plaques and neurofibrillary tangles (composed of microtubule-associated protein tau) interfered with normal neuronal function resulting in neuronal cell death.[3,4] Highly enriched amyloid β (Aβ) fibers were isolated from AD patients' meningeal vessels in 1984.[5]

Over the last four decades, it has become apparent that AD is a multifactorial disease. Although the triggering event for the deposition of misfolded proteins has remained unknown, neuroinflammation and neurovascular changes have become increasingly known to contribute to Aβ and NFT deposition and eventual neuronal

dysfunction. Searching imaging tools to identify and trace the neuronal, vascular, and inflammatory changes in AD and other neurodegenerations is an ongoing effort.

PERSONAL AND SOCIETAL IMPACT OF ALZHEIMER'S DISEASE

AD is seen in all ethnicities and involves slightly more females than males.[6] AD is the most common form of elderly dementia, accounting for about 50-75% of all cases. It is estimated that 5.7 million Americans have AD.[7] AD prevalence increases with age: only 3% of people aged 65-74 are diagnosed with AD, in contrast to 17% of those aged 75-84, and 32% of those aged 85 and older.[8] Considering all these, AD's economic impact is enormous. As the size and proportion of the population aged 65 and older continue to grow, AD's impact on society will increase dramatically unless preventive and early diagnostic measures are developed.[8] A mathematical model has projected saving up to $7.9 trillion in medical and care costs with early and accurate AD diagnosis.[9]

AD is not just an American or western world problem. World Alzheimer Report estimated that 36 million people around the world live with dementia, with a substantial worldwide cost of around $604 billion in 2010, representing 1% of global GDP (World Alzheimer Report 2011).

PATHOGENESIS OF ALZHEIMER'S DISEASE

AD's etiology and the neurodegenerative process leading to its clinical presentations are complex. There is a widespread agreement that AD develops due to multiple modifiable and non-modifiable risk factors that converge on the amyloid β and phosphorylated tau protein deposition. The amyloid hypothesis suggests that AD's neurodegenerative process ascends primarily from cytotoxic events prompted by excessively metabolized amyloid precursor protein (APP) in the amyloidogenic pathway that leads to the formation, aggregation, and deposition of Aβ plaques. APP is a plasma membrane protein with a single domain found on different cell types, including neurons, astrocytes, oligodendrocytes, and glial cells. APP is coded for by a gene located on chromosome 21, which explains why all individuals with chromosome 21 trisomy develop AD in their midlife. In physiological conditions (non-amyloidogenic pathway), APP is cleaved by α-secretase producing the fragment (s)APPα and a carboxy-terminal component

of 83 amino acids (C83) (Figure 2). The physiologic role of (s)APPα includes regulating neural excitability, improving synaptic plasticity, and increasing neural resistance to oxidative and metabolic stress. Under neuropathological situations (amyloidogenic pathway), BACE (β-secretase 1) slices APP at its N (extracellular)-terminus, and γ-secretase cleaves APP at its C-terminus. This enzyme activity yields two extracellular (s)APPβ and Aβ40/42 fragments and an intracellular C-99 fragment. The C-99 fragment transports to the cell nucleus to induce genes that promote neuronal death by apoptosis. Naturally, APP regulates neuronal survival, protection against toxic stimuli, synaptic plasticity, and cellular adhesion. However, Aβ40/42 deleteriously affects synapse function, decreases neuronal plasticity, alters energy and glucose metabolism, induces oxidative stress and mitochondrial dysfunction, and disturbs cellular calcium homeostasis.[10]

Soluble Aβ peptides are present in endosomes before the Aβ plaque appearance.[11] Failure of the perivascular wall lysosomal pathways to efficiently clear intracellular Aβ peptides foster their pathological aggregation. Thus, although Aβ overproduction is probably the main driving force for plaque formation, impaired intracellular trafficking of Aβ monomers in perivascular spaces (also called g-lymphatics) is increasingly suggested as the cause of Aβ accumulation and deposition (Figure 3).[12–14]
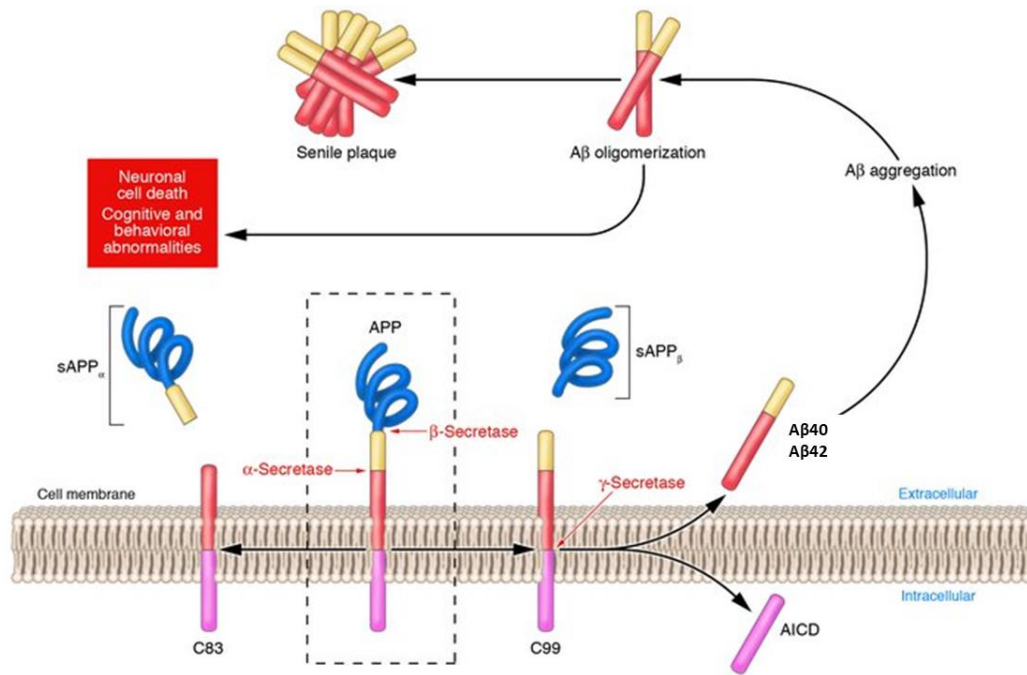
Figure 2. APP processing and Aβ accumulation. Mature APP (center, inside dashed box) is metabolized by 2 competing pathways, the α-secretase pathway that generates sAPPα

and C83 (also known as CTFα; left) and the β-secretase pathway that generates sAPPβ and C99 (right). Some β-secretase cleavage is displaced by 10 amino acid residues and generates sAPPβ′ and C89. All carboxyterminal fragments (C83, C99, and C89) are substrates for γ-secretase, generating the APP intracellular domain (AICD) and, respectively, the secreted peptides p3 (not shown), Aβ-40/42 (right), and Glu11 Aβ. Aβ aggregates into small multimers (dimers, trimers, etc.) known as oligomers. Oligomers appear to be the most potent neurotoxins, while the end stage senile plaque is relatively inert (Republished with permission of the American Society for Clinical Investigation, from reference #15; permission conveyed through Copyright Clearance Center).[15]

The role of age-related cardiovasculopathies in this process is not fully understood. The brain's high metabolic demand requires a well-controlled blood supply that is adjusted based on neuronal activity. A close metabolic and structural interdependence between astrocytes and neurons with blood vessels that forms the so-called neurovascular unit– NVU- regulates local blood perfusion by regulating blood flow to the brain, blood-brain barrier (BBB) permeability, and the chemical composition of the neuronal interstitial tissue required for neuronal circuits' proper functioning. Cellular and noncellular components of NVU, including neurons, astrocytes, vascular endothelium, myocytes, pericytes, and the extracellular matrix, are altered in AD patients [16,17] and mouse models of AD. [18,19] Among the known NVU ultrastructural changes in AD are capillary distortions, BBB dysfunction, endothelial cell mitochondria loss, thickening of the basement membrane, endothelial degeneration, degenerated pericytes, and perivascular neuroinflammation.[20] Such NVU alterations are potential biomarkers for diagnosing AD and monitoring its activity.

In contradiction to the amyloidogenic and taugenic hypothesis, clinical trials targeting amyloid and tau depositions have not been successful.[21] Thus, there is an increased realization that the role of neuroinflammation, synapse dysfunction[22], and cerebrovascular pathologies are possibly more pronounced early in the disease course. It has been suggested that neurodegenerative changes associated with AD may begin 10-20 years before AD symptoms appear.[23–26] Early pathologic changes are compensated by neuroplasticity and vascular plasticity, and for a long time, those who will develop AD in the future do not have any apparent symptoms. Nevertheless, as the pathologic burden of

AD accumulates, the patient starts to show symptoms of minimal cognitive impairment (MCI) that will gradually progress to Alzheimer's dementia. Finding new diagnostic and improving the available tools' precision and accuracy for detecting AD's early pathologic changes is the key to future treatments' success.
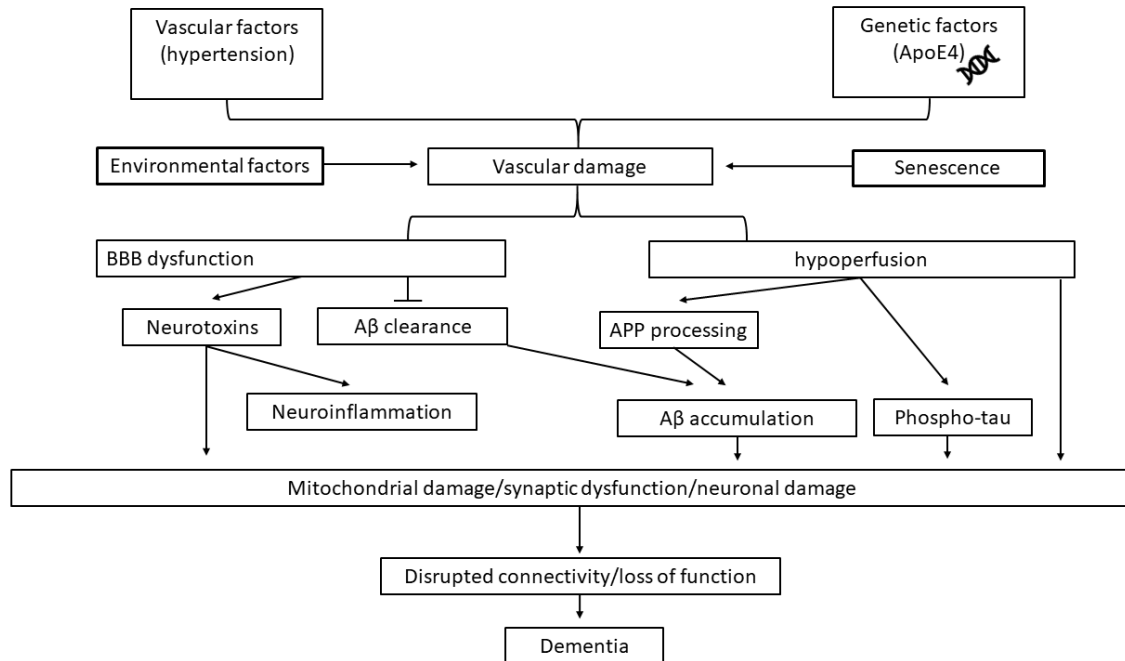
Figure 3. Alzheimer's dementia hypothesis. The vascular hypothesis of AD states that cerebrovascular damage is an initial insult that promotes Aβ accumulation in the brain (adopted with modifications from reference #2).[2]

RISK FACTORS OF AD

The most significant risk factors for late-onset AD (LOAD) are older age, having a family history of AD, and carrying the APOE-e4 gene. Individuals with a first-degree relative with AD are more likely to develop the disease. Those who have more than one first-degree relative with AD are at even higher risk.[27] Whether this increased risk is due to genetics or shared environmental and lifestyle factors, or both, is not clear. Those who inherit APOE-e4 have an increased risk of developing AD at a younger age than those with

other gene variants.[28] Cardiovascular diseases, education level and social/cognitive engagement, and traumatic brain injury (TBI) are modifiable risk factors for AD. And finally, it should be mentioned that a small percentage of AD cases (1% or less) develop due to mutations in the APP, presenilin 1, or presenilin 2 genes.[29] All of the individuals inheriting an APP or presenilin 1 genes and 95% of those inheriting a presenilin 2 gene will develop the disease.[29] Individuals with any of these three mutations tend to develop AD symptoms before age 65, sometimes as young as age 30.[9] This is commonly referred to as early-onset AD (EOAD).

CLINICAL FEATURES OF ALZHEIMER'S DISEASE

Dementia and dementia-like diseases

Dementia is a constellation of symptoms arising from neurodegeneration involving parts of the brain responsible for cognitive functions such as memory, language, and problem-solving skills. Such neurodegenerative processes will then affect essential motor functions such as walking and swallowing, and the disease will ultimately become fatal. Different forms of dementia, other than AD, that present with distinct symptom patterns and brain abnormalities include vascular dementia, dementia of Lewy body, Frontotemporal lobe degeneration, Parkinson's disease, Creutzfeldt-Jakob disease, and normal-tension hydrocephalus.[9] Very often, people with dementia symptoms have brain abnormalities associated with more than one cause of dementia. One study showed that only 30% of people with histologic features of AD had pure AD, and half of the AD patients also had brain changes compatible with vascular dementia.[30]

The primary differential diagnosis for AD and non-AD dementia includes dementia-like symptoms without the progressive brain changes caused by depression, delirium, side effects from medications, thyroid problems, certain vitamin deficiencies, and excessive alcohol use. Unlike AD and other neurodegenerative diseases, these conditions are often reversible with treatment.

Symptoms of Alzheimer's dementia

AD's symptoms include loss of ability to gain and recall new memories, declining decision-making abilities, and impaired cognition. With eventual impairment in both

declarative and non-declarative memory, an individual's capacity for reasoning, abstraction, and language will be remarkably reduced. Normal aging may be associated with nonpathological age-related changes in memory and cognition. Such changes should be differentiated from neurodegenerative dementia, which may be difficult early in the disease course. AD symptoms vary among the patients, and any combination of the symptoms mentioned above may occur. In the early stages, most individuals can function independently in many situations but may require support with some activities to remain independent and safe. In the moderate stage, patients may have difficulty performing daily routine tasks, become confused about place and time, and start having personality and behavioral changes. In the severe stage, patients require help with basic daily living activities, such as bathing, dressing, and using the bathroom. Eventually, their verbal communication ability becomes limited.[9] Physical health becomes significantly impaired in the severe stage of the disease. Eating and drinking become difficult, and patients may get aspiration pneumonia. Patients become bed-bound due to damage to motor centers. Being bed-bound increases the risk of lower extremity thrombosis, skin infections, and sepsis.

DIAGNOSIS OF ALZHEIMER'S DISEASE

AD diagnosis cannot be made with a single test. Instead, a variety of diagnostic approaches and tools are used to make a diagnosis:

1.   Comprehensive medical evaluation, including medical and family history, including psychiatric history, cardiovascular history, and history of cognitive and behavioral changes.

2.   Soliciting a history of changes in thinking skills and behavior.

3.   Cognitive tests and physical and neurologic examinations.

4.   Ruling out medical causes of dementia by blood tests and brain imaging.

Revised guidelines for diagnosing Alzheimer's disease: The National Institute on Aging (NIA) and the Alzheimer's Association have proposed revised guidelines for clinical and pathological diagnosis of AD.[31,32] The older diagnostic criteria and guidelines were based mainly on a physician's clinical judgment about the cause of an individual's symptoms,

considering reports from the patient and caregivers, cognitive tests, and general neurological assessments.[9] The updated revised guidelines incorporate the same steps for diagnosis but also incorporate biomarker tests. Brain imaging modalities to detect the progression to AD include magnetic resonance imaging (MRI), magnetic resonance spectroscopy (MRS), and positron emission tomography (PET). In a study to estimate the progression rate from minimal cognitive impairment (MCI) to dementia, the model that best predicted progression to dementia included age, sex, hippocampal volumes in MRI, N-acetylaspartate (NAA)/creatine (Cr) on MRS, and the presence of cortical infarctions.[33]

A noninvasive, easily executable, convenient, and inexpensive diagnostic modality is the key for timely diagnosis and follow-up of patients with preclinical and clinical AD. Future treatments to slow or stop AD's progression and preserve brain function will be most effective when administered early in the disease porgresion. A noninvasive and simple diagnostic tool for detecting and following early AD biomarkers in individuals with MCI or preclinical AD would allow testing if an experimental therapy can delay or prevent symptoms in such at-risk individuals. Such diagnostic modalities would boost future therapeutic trials' success by providing a means to follow the effect of emerging treatment modalities.

TREATMENT OF ALZHEIMER'S DEMENTIA

No effective medication is currently available to slow or stop AD's neurodegenerative destruction. In the decade of 2002-2012, 244 drugs for AD were registered with clinicaltrials.gov. Only one of these 244 drugs (memantine) completed clinical trials and received approval from the US Food and Drug Administration (FDA).[9] Factors that contribute to the difficulty of developing effective treatments for AD include 1) lack of reliable and convenient disease biomarkers, 2) lack of animal models that closely resemble the manifestation of AD in human, allowing for pre-clinical evaluation of the safety and efficacy of promising therapeutic agents, 3) slow pace of clinical study recruitment, and 4) long time needed to observe whether an investigational treatment affects disease progression.[9] Retinal biomarkers that can noninvasively probe subtle signs of AD progression may help monitor potential treatment effects.

Despite the lack of effective therapies, studies have consistently shown that lifestyle modification and active management of AD and other dementias can improve the quality of life for affected individuals and their caregivers.[34]

ANIMAL MODELS OF ALZHEIMER'S DISEASE

Our current knowledge of the pathologic changes associated with AD and their biological and genetic pathways has been gained through studying genetically modified AD animal models. None of the existing animal models of AD fully reproduce AD's complete spectrum; they repeat the disease's critical pathologic aspects reasonably well. Despite the abundance of mouse models of AD for over two decades, clinically proven treatments are not available yet. The lack of translation of knowledge from the preclinical models to the clinical phase has multiple aspects, including 1) mouse models do not recapitulate all pathologic aspects of the disease. Transgenic mice may overproduce amyloid, tau, or APP, but only a few of them harbor the transgenes expressing both amyloid and tau proteins. 2) AD is a disease of elderly when comorbid cardiovascular diseases and normal aging neurodegeneration contribute to AD pathogenesis. Many of these aging neuronal and vascular changes cannot be recapitulated in a 2–3-year life span of a mouse. 3) Despite all the similarities, there is a lack of substantial cell and synaptic loss in animal models of AD, suggesting that animal models better represent the disease's preclinical stage.

Other than many transgenic rodent models of AD that represent EOAD, AD research is performed in late-onset AD models (ApoE KO mice), fruit fly models of AD, and nontransgenic models (injecting Aβ into the brain, using cholinotoxins, and using naturally long-living animals that show senescence neurodegenerations) too. Below, the main features of transgenic mouse models of AD (both APP and tau transgenic models) are summarized, and the justification for using 3xTg-AD in the current study is presented.[35,36]

PDAPP transgenic mice: generated by a PDGF-driven human APP (PDAPP) shows astrocyte reactivation before plaque formation. It starts to develop plaques,

dystrophic neurites, and more reactive astrocytes and microglia at 6 months. This model has far less neuronal loss compared to AD and does not have tau pathology.

Tg2576 transgenic mice: This line has two Swedish mutations that express APP_{695} isoform with multiple fold increase in $A\beta_{1-40}$ and $A\beta_{1-42/43}$. Brain pathologic and behavioral changes are similar to patients with AD. However, neuronal loss is low, and there are no tau pathologies.

J20 transgenic mice: This model presents with very early cognitive deficits and shows a high level of $A\beta$. Plaques appear at the age of 5-7 months, but a significant neuronal loss has been found at age 3 months, before the appearance of plaques.

APP/PS1 transgenic mice: mutations in PS1 account for the majority of EOAD. However, PS1 overexpression is not enough to produce amyloid pathology, and a simultaneous APP mutation is needed. Cerebral amyloid deposits are seen at 6-8 weeks of age in this model.

5xFAD transgenic mice: This mouse co-expresses five FAD mutations that accelerated $A\beta$ plaque formation. $A\beta$ plaques begin to deposit at the age of 2 months. Activated astrocytes and microglia are seen at the age of 2 months, with a gradual increase with age.

Tau transgenic mice: Tau plays a significant role in AD pathogenesis. However, early transgenic models did not include tau expression. 3xTg-AD was developed by inserting two transgenes containing the APP Swedish mutant and a tau mutant (P301L) into a homozygous presenilin 1 mutant (M146V) mouse and displayed progressive histopathologic and behavioral abnormalities such as concurrent senile plaques and neurofibrillary tangles formation and synaptic dysfunction that progress in an age-related manner and closely mimic the neurodegenerative process in human AD.[37–40] The 3xTg mouse has been extensively studied and its brain lesions, retina pathologies, and behavioral changes have been well characterized. High levels of $A\beta$ and tau deposition are found in the 3xTg-AD mouse brain. Besides, the synaptic loss was observed even before $A\beta$ and tau accumulation.[37,38] Retinal presentation of 3xTg-AD mouse recapitulates many of the characteristic pathologic aspects of the human AD disease in retina too. [37,38,41–45]

Limitations of animal models. Although our current knowledge about AD originates from studies on animal models, AD models have significant limitations.

Transgenic mouse models of AD have been extensively used; however, mouse neurons are generally resistant to Aβ toxicity. Besides, mice retina cannot mount an inflammatory response like the human retina.[46] Furthermore, although animal models of AD may manifest some key features of AD-related pathologies; they miss AD's environmental and cardiovascular risk factors.[47] The pathogenesis of AD-like features in 3xTg-AD mimics early-onset AD (EOAD) (such as patients with Down syndrome who are born with an extra copy of amyloid precursor protein (APP) genes) more closely compared to those with late-onset AD (LOAD).[25] Also, limitations of translating mouse OCT and OCTA studies to human disease conditions should be considered.[41] Rodents, unlike the human, do not have macula and FAZ that is shown to present AD pathologies significantly more than the other parts of the retina.[39] On the other hand, the mouse retina's layered structure with a trilaminar arrangement of its capillary layers is almost identical to the human retina, and similar degenerative processes occur in murine models.[48]

OCULAR MANIFESTATIONS IN ALZHEIMER'S DISEASE

The retina shares embryological origin, cellular elements, and physiological properties (such as a blood-tissue barrier) with the brain. A wide range of visual dysfunctions has been reported in patients with AD, and multiple histology studies have revealed structural changes in the retina, including the deposition of Aβ (though structurally different from Aβ plaques seen in the brain)[49], hyperphosphorylated tau, and APP in individuals involved with the disease.[41,49–53,54,55] Animal studies and histopathologic evidence from human samples suggest that these functional and structural retinal changes parallel brain pathologies of AD. Thus, it is conceivable that the retina could serve as a window for studying neurodegeneration caused by AD.[55–57] Besides, retinal vasculature, which can be visualized and monitored noninvasively via multi-modal imaging tools, may serve as biomarkers of brain vasculature and enable monitoring of AD neurovascular pathologies.[43–46]

The retina, consisting of three neuronal and two synaptic layers, is a highly organized neural tissue (Figures 4 and 5). Retinal cellular and synaptic layers consist of (from innermost layer to out): the retinal nerve fiber layer (RNFL), retinal ganglion cell layer (RGC), inner plexiform layer (IPL), inner nuclear layer (INL), outer plexiform layer

(OPL), outer nuclear layer (ONL), and photoreceptor outer segments (OS) (Figure 4).[62] Having a high metabolic demand, a rich and highly connected capillary plexus supplies blood perfusion to the retina. In both mouse and human, blood vessels that nourish the retina follow retinal cellular and synaptic organization and form three vascular network layers, or plexuses, that run parallel within the retina and connect by inter-plexus vessels. Three retinal vascular networks extend from the optic nerve head to the retinal periphery.[63–66] Central retinal artery supplies the superficial vascular plexus (SVP) composed of larger arteries, arterioles, capillaries, venules, and veins. SVP is mainly located within RNFL and GCL. The intermediate vascular plexus (IVP) is located between the IPL and INL, and the deep vascular plexus (DVP) is situated in the OPL (Figure 6).[67] Vertical capillary connections from the SVP provide for IVP and DVP perfusion.[63–66] This retinal vascular pattern is highly preserved across mammals, including rodents, monkeys, and humans.[63–69] Because of the inability of fluorescein angiography to depict the three-dimensional aspect of retinal capillary plexuses, *in vivo* investigation of these vascular layers has not been possible until the recent development of OCTA.[68,70–72]

The mouse retina doesn't have a macula like the human retina; otherwise, it is organized similar to the human retina and serves as an excellent model for exploring the physiology of vision and dissecting the pathologic mechanisms mediating retinal disease. Similar to the human, the mouse retinal vessels develop in an overlapping stepwise process that starts with the radial expansion from central retinal vessels onto the surface of the retina that forms the SVP, followed by vascular sprouting deep into the retina to develop the IVP and DVP along with numerous cellular and molecular cues orchestrated by the vascular, neuronal, Muller, and glial (microglia and astrocyte) components.[69,73–76]
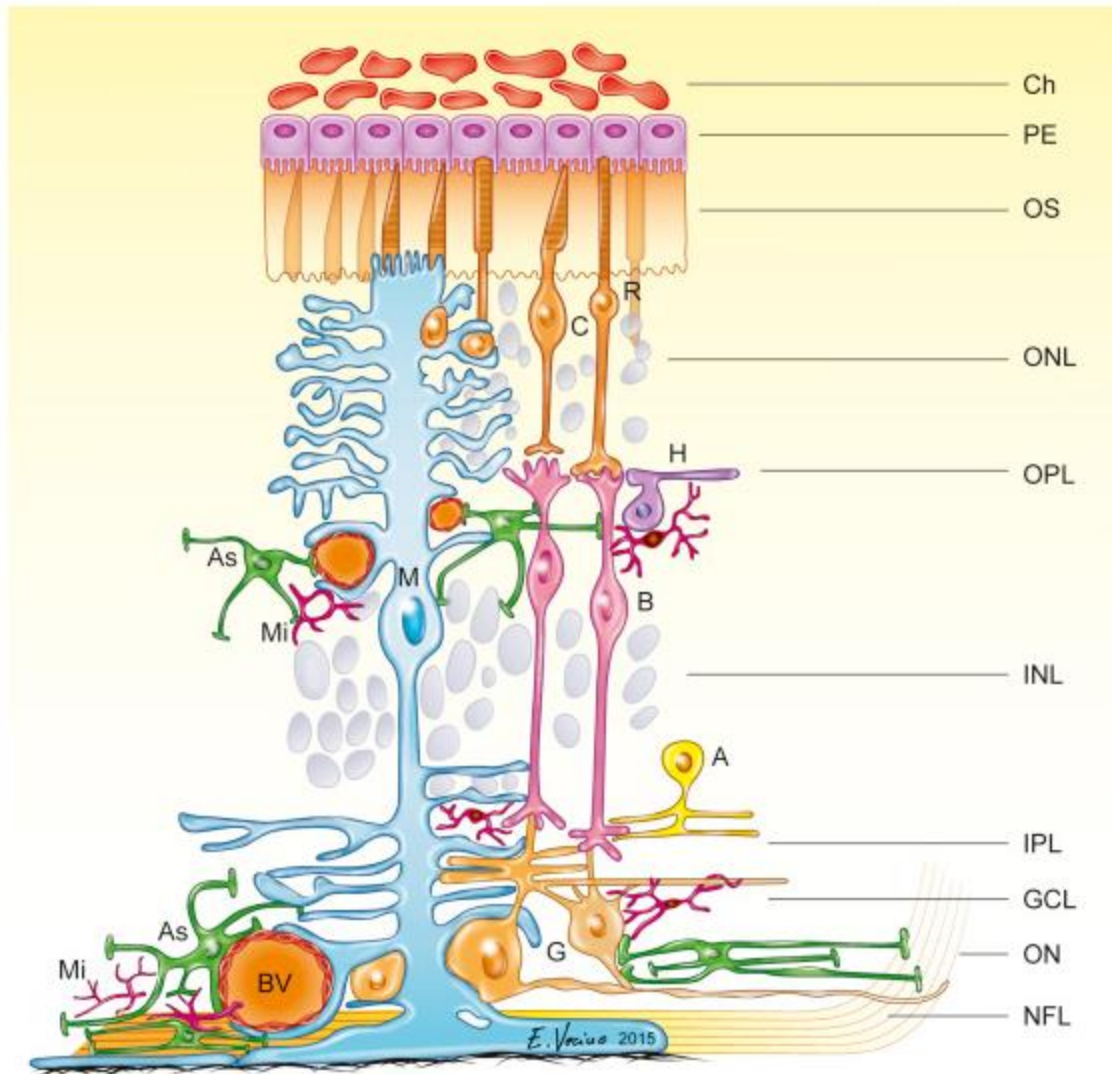
Figure 4. Schematic drawing of the cellular components of the retina. Note the interactions between the cells and blood vessels (BV). Amacrine cells (A), astrocytes in green (AS), bipolar cells (B), cones (C), ganglion cells (G), horizontal cells (H), Müller cells in blue (M), microglia in red (Mi), rods (R), cones (C). Note the location of the different layers of the retina (from the most internal to the outer layers): optic nerve (ON), nerve fiber layer (NFL), ganglion cell layer (GCL), inner plexiform layer (IPL), inner nuclear layer (INL), outer plexiform layer (OPL), outer nuclear layer (ONL), outer segment layer (OS), pigment epithelium (PE), choroid (Ch) (Figure reused from reference #76 under Creative Commons License).[76]
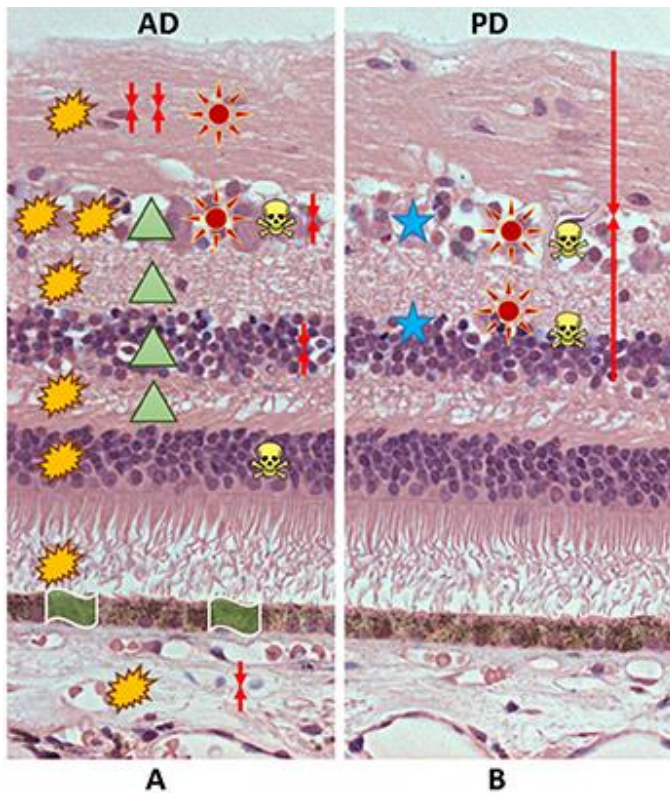
Figure 5. Histologic locations for toxic proteins. Proposed histologic locations for toxic protein deposition and resulting degenerative consequences in the retina in the process of AD and PD (reproduced with permission from reference #77 under Creative Commons Attribution License).[77]
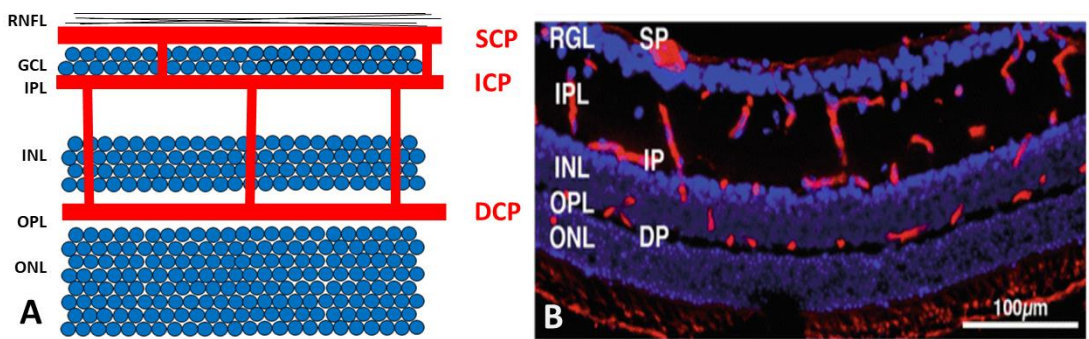
Figure 6. Cellular and vascular organization in retina. Organization of the cellular and vascular elements in mouse and human retina. A. Cartoon illustration of the retina, showing its organization. B. Cross-section of a mouse retina stained with DAPI and GS-B4 (section B used with permission from reference #67).[67]

Visual function in Alzheimer's disease

Multiple visual disturbances, including visual processing and integration dysfunctions, have been described in individuals with AD. Impaired contrast sensitivity is common in AD and worsens with AD's progression.[78] In advanced AD, disturbed facial recognition, self-identification, and prosopagnosia (abnormal recognition of familiar faces) may interfere with daily life.[79] Other visual function disturbances recognized in patients with AD include decreased visual acuity and difficulties in writing and reading, and fluctuations in color perception.[80–82] Further, pupil size, pupil reaction to light and near, and ocular motility abnormalities have been reported in AD patients.[83,84] Finally, visual field loss mainly occurs in the inferior quadrant (that may correlate with more severe GCL damage in the superior quadrants).[85] To clarify the longitudinal pattern of these clinical findings with ocular imaging features in various clinical stages of MCI and AD, we need large-scale prospective clinical studies.

Ocular imaging studies in Alzheimer's disease

FUNCTIONAL IMAGING STUDIES

Besides visual function tests such as visual acuity, contrast sensitivity, color vision, and visual field tests, a host of indirect evidence confirm retinal neuronal and vascular dysfunction in AD. Increased permeability of the blood-retinal barrier (BRB) has been shown in models of retinal degeneration.[86] Retinal perfusion is considered a marker of retinal function. For example, Gameiro et al. studied retinal blood flow using Retinal Function Imager and showed decreased tissue perfusion and tissue volume in clinical AD patients.[87] Further evidence for vascular disruption of retinal vascular comes from more recent OCTA studies that will be discussed in detail in section b-ii below.

Common epidemiological and cardiovascular risk factors are shared between AD and vascular dementia (VaD). The presence of regional brain microvascular abnormalities and regional cerebral hypoperfusion in preclinical AD suggested AD as a "vascular disease."[74] Indeed, patients with AD show evidence of cerebrovascular abnormalities such as decreased cerebral blood flow, BBB dysfunction, altered trophic factors, and reduced

clearance of toxic proteins. Thus, experts have proposed brain vascular density and structure as potential biomarkers of AD. However, detailed cerebral vascular imaging is a challenge partly because of the brain being encased in a bony skull and the limited sensitivity of current imaging methods to reveal the cerebral vascular map and the dynamic changes in cerebral vessels in detail. Because of the shared developmental, structural, and physiologic processes between the retina and the brain, retinal microvasculature has been proposed as a potential biomarker for cerebral vessels. OCTA is a noninvasive optical imaging tool that provides depth-resolved volumetric information from the choroidal and retinal microcirculation and offers a possible way to detect microvascular changes in AD.

STRUCTURAL IMAGING STUDIES

In vitro histopathological assessment of AD-induced structural changes in the retina

Neurodegenerative loss of RNFL and RGC was detected in the 1980s. Still, it was not until 2011 that Aβ plaques were identified from postmortem retina tissues of individuals with confirmed AD.[39,52] Importantly, the retinal Aβ burden correlated with the severity of brain plaque pathology.[88] Interestingly, retinal Aβ plaques were smaller than CNS plaques and were found nonuniform in superior and inferior quadrants and mid- to far-peripheral regions of the retina.[88,89] These regional and geometric patterns may have implications in noninvasive optical imaging detection of AD's retinal biomarkers. Studies by den Haan et al. on human retina tissue from individuals with confirmed AD have shown that Aβ deposits were found in various retinal cell layers, mostly in INL. Amacrine cells, Muller cells, and horizontal cells showed immunoreactivity to Aβ.[90] A leading group led by Koronyo-Hamaoui reported more prominent Aβ deposits in RNFL and GCL of the central retina.[49] The same group has recently reported significant deposition of Aβ in retinal vascular lumen associated with loss of pericytes.[91] Similarly, hyperphosphorylated tau has been identified in the retina in colocalization with retinal neuronal loss.[90] Asanad et al. examined retina samples from AD patients and observed significant RNFL thinning in the peripapillary area and significant GCL and IPL thinning in the parafoveal area.[92] Outer retinal layers were thinner than controls, though the thinning was less pronounced than the inner retinal layer thinning.[92]

In vivo non-invasive depth-resolved imaging of retina

OCT imaging in AD

Optical coherence tomography (OCT) is an essential component of ophthalmic diagnosis and evaluation due to its non-invasiveness and high spatial resolution that approaches 2-3 µm. This resolution is close to conventional histology resolution and better than other imaging modalities such as PET, CT, or MRI. Based on their development time-line and scanning speed, OCT imaging machines include time-domain (TD-capturing approximately 400 A scan per second), spectral-domain (SD-capturing 20000-50000 A-scans per second) and swept-source (SS-capturing 100,000–400,000 A-scans per second) OCT. SD-OCT is the most commonly used OCT in clinical practice and is available in almost all retina clinics nationwide.

OCT scans show the retina's layered structure (Figure 7) and provide retinal sublayer thickness, macular volume and thickness, and choroidal volume and thickness. While some studies have not detected any difference in total retinal thickness between AD patients and controls with normal cognition,[93,9495] most studies have shown reduced retinal thickness in patients with AD, and in some instances, in individuals with MCI. It is often a challenge to compare AD OCT studies (with occasional contradictory findings) because of the variation in OCT instrumentation and segmentation protocols, variation in sample size, and variable criteria for classifying participants to normal, MCI, and AD. However, it is almost consistent that retinal thinning is often limited to inner retinal layers, and the outer retina is mostly preserved.[96] Looking into more detailed thickness maps that include retinal sublayers, RNFL thinning is most commonly reported from AD patients. Depending on retinal segmentation protocol, some animal studies have not reported RNFL thickness separately and included it in ganglion cell-inner plexiform layer (GC-IPL), a three-layer structure referred to as the ganglion cell complex (GCC). Total retinal thickness decreases from young age to middle-age, then to MCI, and then to clinical AD. In multiple studies, patients with MCI were often reported to have significantly reduced RNFL thickness compared to healthy controls.[97–99] When it comes to AD, retinal thickness often correlates with the severity of AD. Salobrar-Garcia and colleagues found that macular thickness was thinner in patients with moderate AD than those with mild AD. In turn, those with mild AD had a thinner macula compared to cognitively normal controls.[74] Other studies have also confirmed that patients with AD have a significantly thinner retina than healthy controls and MCI patients.[97,100–102] While some studies reported more pronounced thinning

in the superior quadrant RNFL, others have not seen any difference in RNFL thickness from various retinal quadrants.[89,94,103–106] In a population-based study that enrolled about 3300 patients, RNFL thinning was associated with an increased risk of dementia.[107] Thus, total and retinal sublayer thickness may represent a marker of cognitive status in the elderly. It should be noted that retinal thickness change is a combination of degenerative changes caused by AD and normal aging and associated neuroinflammatory trophic changes. Furthermore, it has been shown that retinal thickness changes span a spectrum, thus may not differentiate milder forms of AD from MCI.[108]

Two recent systematic reviews have summarized various OCT studies quite comprehensively. Chan et al. reviewed 30 eligible studies involving 1257 AD, 305 MCI, and 1460 cognitively normal individuals. AD subjects had significant GC-IPL and GCC and RNFL thinner than MCI and controls.[109] However, these differences were less pronounced between individuals with MCI and normal cognition.[109] Similarly, Song et al. reviewed OCT/OCTA studies in AD that included a total of 6757 individuals encompassing 2350 AD, 793 MCI, and 2902 controls.[110] Song et al. reported that most studies noted a significant structural and functional decline in AD compared to normal controls. Studies including MCI yielded more mixed results, but a similar declining pattern was noted in many studies. OCT and OCTA findings correlated with neuropsychological and neuroimaging findings of AD.[111]
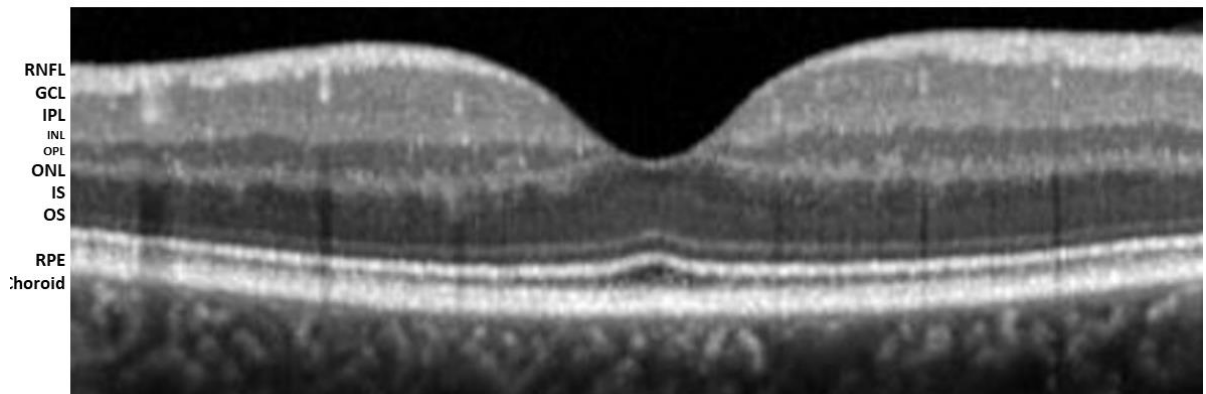
Figure 7: Optical coherence tomography scan through fovea in a healthy individual. Retinal neuronal and synaptic layers are well depicted in this scan.

Another layer of complexity comes from the fact that retinal thickness changes are not specific to AD and can be seen in normal aging and various neurodegenerative and neuroinflammatory diseases. In one study, patients with AD, PD, and LBD all had reduced RNFL thickness than healthy controls.[74] A system of biomarkers that may encompass a weighted scoring for retinal sublayer thickness may be a better diagnostic and follow-up tool for AD neurodegeneration. Such biomarker systems may be refined using machine learning methods and artificial intelligence.[74]

The choroid is thinner in patients with AD compared to healthy controls, supposedly due to the vasculopathy triggered by Aβ deposition in choroidal vasculature,[112–115] similar to the cerebral vascular changes described in AD.[116,117] Animal studies have supported this hypothesis by showing inflammatory responses that led to neurodegeneration and regression of the choroidal vasculature.[118]

OCTA imaging in AD

In the past few years, there has been a surge of OCTA-based studies investigating retinal vascular parameters, including retinal vessel density, retinal perfusion density, and foveal avascular zone (FAZ) size. Other parameters studied sparsely include retinal vessel fractal dimensions, vessel caliber, vessel branching, blood flow velocity, and retinal oximetry. However, such studies have resulted in variable, inconsistent, and sometimes contradictory results making it difficult to draw a clear conclusion about retinal vascular changes in AD and their utility in diagnosis and following AD's progression or response to treatments. In patients with MCI and clinical AD, most OCTA studies have revealed reduced vessel density and perfusion density in both the superficial capillary plexus (SVP) and deep capillary plexus (DVP).[119–126] Below, relevant OCTA studies on patients with AD or MCI are summarized.

One of the first OCTA studies in AD came from a rare pair of 96-year old female monozygotic twins discordant for AD.[127] The twin with advanced AD had a significantly reduced SVP density and a larger FAZ.[127] Another early study reported by Bulut et al. was performed on 26 confirmed AD patients and 26 healthy controls.[119] It showed that retinal vascular density was lower and FAZ was significantly enlarged in AD.[119] Although outer retinal flow and choroidal flow were lower, the difference was not significant. The small

number of subjects in this study may have impacted this nonsignificant difference.[119] Similarly, Lahme et al. studied AD and healthy subjects with OCTA and found decreased superficial retinal flow density in AD. Decreased flow correlated with MRI findings but did not correlate with Aβ and tau levels in the CSF.[126] Zabel et al. compared OCTA parameters in patients with AD, glaucoma, and healthy controls. In AD, DVP density was lower, and FAZ was enlarged compared to glaucoma and healthy controls.[124] Besides, SVP density was lower in AD and glaucoma compared to controls.[124] Zhang et al. showed decreased SVP density in the parafoveal area in early AD patients, but DVP was not studied.[128] Similarly, Yoon et al. did not evaluate DVP in their patient population, consisting of AD, MCI, and cognitively normal controls.[120,121] In their study, macular SVP vascular density and flow density was lower in AD, but there was no difference between these parameters between MCI and controls.[120,121] Besides, participants with AD showed decreased GC-IPL in inferior and inferonasal quadrants.[120] Jiang et al. studied both SVP and DVP and showed that retinal vascular networks decreased in both vascular plexuses.[122,123] Also, they showed that DVP density correlated with GC-IPL thickness.[122]

O'Bryhim et al. initially published a well-designed study on individuals with preclinical AD in 2018.[119] They reported an increased FAZ and a decreased inner foveal thickness in subjects with preclinical AD who had PET and/or CSF biomarkers of AD. In a three-year follow-up study on a subset of the original study population, enlarged FAZ was confirmed again. Although there was a trend for inner and outer retinal thinning, FAZ size and retinal layer thicknesses did not change significantly after three years of follow-up.[129] The authors note that this was a pilot study, and their sample size was small. The authors are planning to publish a five-year follow-up report from the same study population.

As noted above, multiple papers report decreased vascular density in SVP and DVP in patients with AD. Yet, few publications report no change or decreased vascular density in AD. Querques et al. and Haan et al., in two separate studies, reported that retinal vascular density did not differentiate individuals with AD, MCI, and normal cognition.[130,131] In Querques et al.'s study, individuals with AD and MCI had retinal vascular dysfunction as determined by Dynamic vessel analyzer (DVA), but OCTA parameters were not differentiating as mentioned above. Although their sample size was small, only studying

12 individuals with AD, the finding may suggest that the retinal vessels' functional alterations precede their morphological changes.[130] Besides, van de Kreeke et al. showed increased vessel density and no difference in FAZ size in healthy individuals who were positive for Aβ in PET scan and concluded that retinal vessel density was higher in preclinical AD.[132] Other than using different OCTA image acquisition and segmentation protocols, a possible reason for such inconsistency is that almost all these studies investigated vascular density, flow density, and other OCTA parameters in SVP and ignored IVP and DVP,[121,125,126] or lumped both IVP and DVP in one layer, likely due to the limited resolution of their OCTA devices.[119,130]

The radial peripapillary capillaries (RPCs), too, have been studied in patients with AD. The RPC is located in the superficial retina, like SVP, but has intercapillary connections than the SVP; thus, RPC is likely more susceptible to vascular dropout.[133] Like retinal capillary plexus analysis, quantification of RPC in AD patients is controversial and complicated with variable segmentation and analysis methods. AD patients and cognitively-normal controls did not have significantly different peripapillary vascular densities in two separate studies.[124,134] In contrast, Lahme et al. reported decreased peripapillary vessel density in patients with AD.[126]. With the current data, it is impossible to conclude if OCT-A could identify the preclinical stage of AD or MCI.[135] Similarly, there is no conclusive evidence supporting the association between AD and impaired peripapillary vascularity.[135]

In summary, OCTA has been promising to detect retinal capillary network alterations and may prove useful in the diagnosis and follow-up of patients with AD. Despite little controversies, patients with AD have shown an enlargement of the foveal avascular zone,[119,120,136] reduced capillary density in SVP [119,120,122,128,136,137] and DVP,[121,125] and decreased vascular density and flow parameters in patients with AD.[119,120,126,128] Such changes may be explained by the accumulation of Aβ and tau within the retinal capillaries, amyloid angiopathy, or decreased metabolic demand due to neuronal cell loss.

Future studies should focus on improving instrumentations, recruiting larger study populations with a more extended follow-up period, and validating the initial promising data in the preclinical AD. Such an approach is necessary for developing a possible non-

invasive imaging retinal biomarker to identify individuals with early AD who may eventually benefit the most from potential treatment.[135]

One of the limitations of OCTA in analyzing the vascular size and density is that OCTA, due to the limitations in its lateral resolution, overestimates the size of retinal capillaries.[65,70,138–140] In contrast to OCTA, retinal capillaries appear smaller and more spaced in histologic studies. Yu et al. studied microperfused human retina by confocal microscopy and reported that the DVP covered about 17% of the field of view, whereas, in the OCTA study by Lavia et al., DVP covered 30% to 35% of the field.[70,139]

Imaging neuroinflammation and metabolism in the retina

Inflammatory microglia density, activation, and distribution have been studied in a mouse model of AD in which microglia were tagged with green fluorescent protein (GFP). In this study, in vivo microglia counts corresponded well with ex vivo counts on retinal flat-mounts.[141] In the 3xg-AD model, retinal microglia assume an anti-inflammatory phenotype in presymptomatic stages of AD but express pro-inflammatory features in advanced stages. Evaluating retinal metabolism and oxygen consumption are among the approaches adopted by some researchers. Autofluorescence shows oxidative damage and photoreceptor turn around in a noninvasive way. Fluorescent lifetime imaging ophthalmoscopy (FLIO) is an advanced imaging method that measures endogenous fluorophores' fluorescent intensity decay. It has been shown that FLIO signals correlate with CSF AD biomarkers and GC-IPL thickness in OCT in individuals with preclinical AD.[142] In another comparative study, FLIO parameters correlated with cognition and $A\beta$ and hyperphosphorylated tau concentration in CSF.[143] Another novel imaging approach is DARCs (the detection of apoptotic retinal cells) that uses fluorescent-labeled annexin to visualize apoptotic cells in individual RGCs. DARCs has shown RGC loss at least 18 months before the OCT signs of RNFL loss in glaucoma,[144] but the utility of this method in AD hasn't been explored yet.

NEUROVASCULAR COUPLING IN ALZHEIMER'S DISEASE

Microvascular changes, including increased capillary tortuosity, capillary rarefaction, thickened basement membrane, and "string vessels," have been commonly

noted in the AD brain.[145] Some studies have shown that AD patients have Aβ production similar to normal controls but decreased clearance rates than non-AD individuals.[146] Besides, vascular function is impaired in AD, as demonstrated by a direct correlation of BBB permeability with the severity of AD dementia.[147] However, BBB dysfunction in MCI and normal aging has been reported too.[148,149] Further evidence for the contribution of vascular insufficiency to AD pathology comes from the association of cerebrovascular disease and cardiovascular risk factors with AD's development.[150,151] It is also known that cardiovascular risk factors such as hypertension promote amyloid deposition, supposedly due to defective Aβ clearance.[152] In turn, amyloid impairs endothelial function and cerebrovascular autoregulation, promotes vasoconstriction, and induces vascular oxidative stress.[145,153–155]

While interstitial fluid (ISF) of the white matter is directly drained into the cerebrospinal fluid (CSF), the ISF of gray matter drains via perivascular spaces alongside cerebral vessels called glymphatics. In LOAD, cerebrovascular pulsatility is impaired, so the latter drainage pathway functions less efficiently, possibly contributing to Aβ deposition. In patients with AD, the progression of intracerebral amyloid deposition correlated with the extent of white matter hyperintensities, a marker for small vessel disease, supporting the hypothesis that impaired amyloid clearance via perivascular drainage may contribute to Aβ deposition.[156] The deposition of misfolded proteins contributes to synaptic loss and neuronal death that, in turn, causes further vascular dysfunction and altered vascular dynamics. Such interaction, also known as neurovascular coupling, is suggested to be the core pathogenesis of AD and a potential target for diagnostic and therapeutic developments. However, studying neurovascular coupling in the brain is a challenge mostly due to the limitation of current imaging tools for investigating cerebral capillaries.

As discussed before, the similarities between the retina and brain in terms of common embryologic origin, similar histological and physiological features, and comparable layered structures suggest the retina as a tool for studying neurovascular coupling in AD. Retinal neuronal and vascular elements can be visualized, quantified, and monitored noninvasively and in-vivo with advanced retinal optical imaging tools.

OBJECTIVES:

Amyloid-β and tau deposition, neuroinflammation, and neurovascular dysfunction all contribute to the pathogenesis of AD. However, the link between various components of this pathogenesis system is not fully elucidated. Revealing this link increases our understanding of AD and its initiation and progression, which in turn opens new avenues for novel therapeutics and provides potential targets for efficient diagnostics. Thus, there is an urgent need to clarify the interplay between various neuronal, glial, and vascular elements of the so-called neurovascular unit in the CNS in AD. The retina, an extension of the CNS that is easily seen and examined by noninvasive imaging tools, frequently manifests pathologic events similar to AD neuroinflammation and neurodegeneration. AD neuropathology may be seen and detected noninvasively in the retina.

In this work, we aimed to probe various neuronal and vascular structures of the retina in 3xTg-AD and age-matched non-AD control mice (C57BL/6J) to understand changes in these neuronal and vascular structures as they age and if such changes are detectable with noninvasive optical imaging. We first evaluated retinal sublayers in a large group of young to middle age transgenic and control animals. We determined that a combination system of retinal sublayer thickness changes is a better marker to identify AD progression and differentiate it from neurodegeneration caused by normal aging. Besides, we showed that retinal sublayer changes occur parallel to the loss of RGCs in the retina. We then performed immunofluorescent studies on retinal vascular layers in young, middle-aged, and old transgenic and control mice to differentiate retinal capillary changes caused by normal aging and AD pathology. Differential age-associated changes in the retinal capillary plexuses in nontransgenic and transgenic mice paralleled reported metabolic demand in retinal layers and Alzheimer's pathology burden in the retina. Besides, vascular changes detected in our histology approach were in alignment with the pattern of retinal vascular changes reported by most OCTA studies. We further developed a novel method to study retinal vascular network in intact, whole retina that enables us to explore retinal capillary plexus in their undisturbed natural state. This method allows us to study retinal vessels without the distortion caused by conventional tissue preparation methods and offers a novel way to study hyaloid vessels in their pristine natural state. Such studies are valuable for understanding hyaloid and retinal development in normal and disease states. Further

work to correlate retinal vascular changes with the pattern of retinal vessels detected noninvasively using OCTA has been initiated. Altogether, these studies confirm that noninvasive retinal imaging may differentiate AD neurovascular degeneration from age-related neurodegeneration. Our original work further identifies the connection between retinal neuronal and vascular elements in AD and possibly other neurodegenerative diseases. Findings from our studies pave ways for developing a better biomarker system for AD diagnosis and monitoring.

Chapter 2 Monitoring retinal sublayer thickness as a biomarker for Alzheimer's disease progression in young to middle age triple transgenic mouse model of AD

ABSTRACT

Purpose: Neuronal loss due to Alzheimer's Disease (AD) starts 15-20 years before its clinical presentation. Retinal thinning detectable by optical coherence tomography (OCT) is consistently reported in AD. We studied retinal sub-layer thickness in young to middle-age mouse model of AD.

Methods: We measured retinal sublayer thicknesses using annular spectral domain-OCT scans in young to middle-age (6-60 weeks) triple transgenic mouse model of AD (3xTg-AD, 109 eyes from 60 animals) and control mice (C57BL/6, 72 eyes from 40 animals). Retinal flat mounts were immunostained with anti-TUJ1 antibody, and retinal ganglion cells (RGC) were quantified. Brain sections and retina flat mounts were immunostained with Aβ-42 6E10 antibody.

Results: Total retinal thickness did not change from young to middle age in transgenic and control animals (p=0.479). Retinal nerve fiber layer (RNFL) thickness decreased (linear regression model, p=0.0002) from young to middle-age in transgenic (-0.1491μm/week, p<0.0001), but not in control, (-0.0271μm/week, p=0.2525) animals. Ganglion cell-inner plexiform layer (GC-IPL) thickness decreased in control but not in transgenic animals (p=0.0072). Other retinal sublayers did not change differently in transgenic and controls. RGCs were significantly attenuated in 8- and 12-month-old transgenic animals compared to age-matched controls (p=0.0426 and p=0.0002, respectively). Aβ-42 6E10 staining was noted first in the 4-month-old retina and 8-month-old brain sections.

Conclusion: Retinal neurodegeneration in middle-age AD model was detectable with retinal sublayer thickness measurement using OCT. RNFL, but not GC-IPL, thickness reflected AD-related neurodegeneration, possibly due to the compensatory increase in GC-IPL thickness in the AD model.

Translational Relevance: Retinal sublayer thicknesses may show Alzheimer's disease-related neurodegeneration in middle age and differentiate it from neurodegeneration caused by aging.

INTRODUCTION

Alzheimer's disease (AD) affects millions of people worldwide and has no treatment available despite decades of research.[157] The deposition of extracellular amyloid-β (Aβ) plaques and intraneuronal hyperphosphorylated tau tangles are believed to be the leading causes of neurodegeneration and loss of mental abilities in AD.[157,158] AD is typically a disease of elderly, however, neuroimaging studies such as magnetic resonance imaging (MRI) and positron emission tomography (PET) scan, cerebrospinal fluid (CSF) analysis, and histology studies on the genetically at-risk population who developed AD later in their life indicate that the deposition of Aβ and tau starts in midlife, decades before dementia becomes clinically apparent.[159,160] The success of future treatments for AD depends on detecting such at-risk individuals. However, MRI, PET scan, and CSF analysis are expensive or cumbersome methods, not suitable for screening healthy, middle-aged, at-risk individuals or for the daily care of millions of patients with confirmed AD. As a result, AD's diagnosis is almost always delayed until the appearance of clinically detectable cognitive decline when no therapeutic intervention could reverse the amount and impact of neuronal loss. Thus, a non-invasive and easily executable method for the detection of preclinical AD is an absolute necessity.

The retina is an extension of the central nervous system (CNS) and shares embryological origin, cellular elements, and physiological properties (such as a blood-tissue barrier) with the brain. The retina is easily accessible for examination and imaging via non-invasive optical diagnostic devices. Visual symptoms such as diminished spatial contrast sensitivity, color discrimination, and visual integration are common in patients with AD.[161,162] Widespread retinal ganglion cell loss, and optic nerve axonal degeneration were first found in postmortem analysis of patients with AD in the 1980s.[52,53] More recently, amyloid and tau deposits, pericyte loss, axonal transport impairment, and microglia reactivation have been detected in the retina from both animal models of AD and

AD patients.[39,40,42,49,91,163] Such similarities between the retina and brain physiology and pathologies have encouraged finding methods to detect and monitor AD through retinal imaging. An ideal tool for such non-invasive detection is optical coherence tomography (OCT), a non-contact optical imaging method that generates cross-sectional high-resolution tissue images. OCT utilizes a scanning near-infrared beam of light that penetrates through the retina, retinal pigment epithelium (RPE), and choroid, and an interferometer processes the reflected light to reconstruct the depth and volume profile of selected retinal locations.[109] Multiple OCT-based studies have shown cross-sectional and volumetric retinal changes, mostly thinning of retinal nerve fiber layer (RNFL), in patients with AD and the transitional stage before clinical AD, known as mild cognitive impairment (MCI).[164–167] Although there is a consensus about said functional and structural ocular abnormalities in patients with AD, it is not resolved whether AD-related retinal changes can be detected in normal middle-aged individuals who will eventually develop clinical AD in their elderly. This question can be answered by longitudinal OCT studies on a cohort of normal individuals with an enhanced risk of developing AD to find a subset who will progress to preclinical and clinical AD.[23,168] However, such a study has not been done yet. Many OCT studies on mouse models of A have studied retinal thickness changes in advanced pathologic stages of the disease[169,170]; however, and longitudinal analysis of layers from young to middle age to old age are sparse.[57,171] In an OCT study on 4- to 16-months old triple transgenic mouse model of AD (3xTg-AD), progressive age-dependent thinning of the inner retina was detected, suggesting that preclinical AD can be identified and monitored noninvasively.[57] However, RNFL thickness, which has been consistently shown thinning in AD human studies[39,109,165,172], was not analyzed. Besides, no study has shown retinal sublayer changes and concurrent GC loss in the same group of young and middle-age AD model animals.[173–175] We aimed to fill these gaps by OCT-assisted analysis of retinal sublayers and correlating OCT findings with histologic evidence of retinal neurodegeneration and retinal and brain deposition of Aβ in young to middle-age 3xTg-AD model. We observed that total retina thickness remained stable up to middle age in transgenic mice. RNFL thickness and not GC-inner plexiform layer (GC-IPL) thickness decreased in transgenic mice compared to controls. Parallel to such RNFL thinning, immunofluorescent studies on flat-mount retina preparations showed significant RGC loss

in 3xTg-AD mice compared to age-matched controls. These findings support monitoring retinal sublayers, including RNFL and GC-IPL as a biomarker to differentiate AD-related neurodegeneration in the preclinical stage of the disease from neurodegeneration caused by normal aging.

MATERIAL AND METHODS

The University of Texas Medical Branch (UTMB) Institutional Animal Care and Use Committee (IACUC) approved all the experiments. Animal use and care were per the ARVO statement for animal use in ophthalmic and vision research. Two to five mice were housed in a single cage.

Animals. Sixty triple transgenic B6; 129-Psen1tm1Mpm Tg(APPSwe,tauP301L)1Lfa/Mmjax (3xTg-AD) mice and forty C57Bl/6 J control mice between the ages of 6 to 60 weeks were used for this study. The original line of 3xTg-AD mice was obtained from The Jackson Laboratory (Bar Harbor, ME) and bred and maintained at UTMB animal facilities with genotyping confirmation of the mutations in randomly selected progenies. Only female mice were used in the experiments as they have shown less variable and more severe disease phenotype compared to their age-matched males.[176] OCT imaging was performed in the morning or early afternoon, and the animals were returned to their housing unit the same day. The investigators were not blind to the study groups during in-vivo imaging sessions.

OCT imaging. Animals were anaesthetized with an intraperitoneal injection of a 60 mg/kg Ketamine and a 0.5 mg/kg Dexmedetomidine combination to ensure movement restriction during imaging procedures. Pupils were dilated with topical 1% tropicamide and 2.5 % phenylephrine drops. Eye surfaces were lubricated using Systane eye drop (Alcon, Fort Worth, TX). Following pupil dilation, the mice were positioned into an animal Imaging Mount and Rodent Alignment System (AIM/RAS) setup that allowed x, y, and z-axis manipulation to align the eyes properly. Bioptigen spectral-domain ophthalmic imaging system (SDOIS) (Bioptigen, Inc., Durham, NC) that uses an 840 nm probe providing a 5 micrometer (µm) axial resolution was used to obtain spectral-domain-OCT images. Optic nerve head (ONH) was visualized, centered, and focused within the viewing pan depicting a three mm×3 mm, 50-degree field of view.[177] Then, the Bioptigen annular

scanning protocol centered on the ONH was run. The scan captured a 0.4 mm width circle encompassing 1000 B scans, each comprised of 150 A-scans. One investigator performed all OCT scans for consistency. Eyes were excluded from the study if vitreous opacities or optic nerve head vascular anomalies obstructed the retina.

Bioptigen's Envisu Diver Analysis Software, a built-in automated retinal thickness analysis tool for small animals, was used to populate a retinal sublayer segmentation output that identified boundaries of these eight retinal layers: RNFL, ganglion cell + inner plexiform layer (GC-IPL), inner nuclear layer (INL), outer plexiform layer (OPL), outer nuclear layer plus inner segments (ONL+IS), outer segments (OS), and RPE (Figure 8). We further defined inner retina (IR) as the sum of RNFL, GC-IPL, and INL thickness and outer retina (OR) as the sum of OPL, ONL+IS, and OS.[177] RPE layer thickness stability was considered as an internal control for the validity of the measurements in different ages.[178]
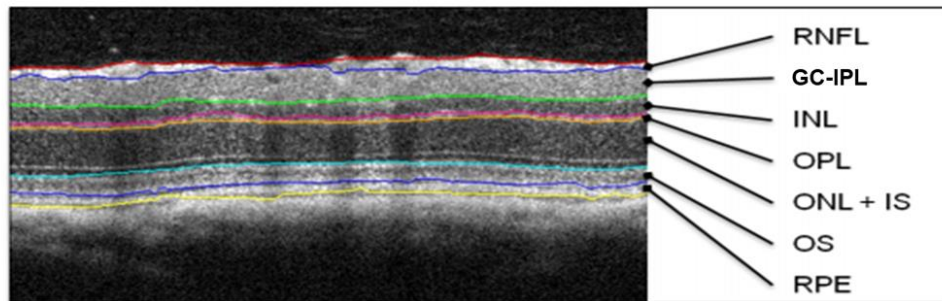
Figure 8. Representative automated retinal layer segmentation by Bioptigen Envisue imaging system used in this study. RNFL: retinal nerve fiber layer; GC-IPL: Ganglion cell + inner plexiform layer; INL: inner nuclear layer; OPL: outer plexiform layer; ONL+IS: outer nuclear layer + inner segment; OS: outer segment; RPE: retinal pigment epithelium.

Immunostaining. Three 3xTg-AD and three control eyes in each age group of 4-, 8-, and 12-months were used for retinal flat mount immunostaining for RGC quantification. Animals were anesthetized as described above and euthanized by cervical dislocation. After euthanasia, the animals were perfused with 30-50 ml of ice-cold Phosphate-buffered solution (PBS) and then with 30-50 ml of freshly prepared 4%

paraformaldehyde (PFA). Both eyes were enucleated and were immediately immersed in ice-cold Hanks' balanced salt solution (HBSS). Only one eye from each animal was used for immunostaining. Under a dissecting microscope, a circumferential incision was made around the limbus, and the cornea, iris, lens, and vitreous body were removed. The eyecups were washed in PBS three times for 5 minutes each time and were incubated in 4% PFA for 10 minutes, followed by carefully dissecting the retina from RPE, choroid, and sclera. Four to five radial cuts were made in the retinal periphery to mid-periphery, and the retina was spread on a glass slide, RGC side up. The samples were then permeabilized with 0.2% Tween-20 in PBS for 20 minutes at room temperature (RT). After washing with PBS (3 times, 5 minutes each time), retina flat mounts were incubated with 5% normal goat serum (NGS) in PBS containing 0.25% Triton X-100 for 1 hour (RT) and incubated overnight at 4°C with anti-human TUJ-1 (Abcam, ab80579, 1:200). Following incubation with the primary antibody, the tissue was washed three times with PBS (5 minutes each time) and probed with mouse-specific fluorescent-labelled Alexa Fluor 546 secondary antibodies (Life Technologies, 1:200) for 3 hours (RT). Slides were washed with PBS, mounted with ProLong Gold Antifade medium (ThermoFisher, P36930), and covered with a cover glass. Under 10x viewing lens, four 100x100 µm regions of interest (ROI) (one ROIs per retina flat mount petal)[179,180] from retinal mid-periphery were imaged using Zeiss LSM 510 scanning confocal microscope. RGC number was counted by two independent observers who were blind to the genotype and age groups. There was a strong linear correlation between the two observers' cell counts (Pearson correlation coefficient of 0.9816).

3xTg-AD mouse is a well-established model for AD pathologies where Aβ and tau deposition in the retina has been established before.[42] Only representative retina flat mounts and brain sections from transgenic and control mice in each of 4-, 8, and 12- month old age group were immunostained for Aβ-42, and no quantifications were performed. Aβ-42 staining of retina flat mounts followed the immunostaining method described above with anti-Aβ-42 6E10 (BioLegend #803002, 1:300) and Alexa Fluor 488 (Thermo Fisher Scientific, #A32723, 1:500) as primary and secondary antibodies, respectively.

Brain tissue was collected and fixed in 4% PFA for 24h and then immersed in 30% sucrose solution for three days. [45] The brain samples were sliced at 30 µm using Cryostat

(Thermo Shandon) and mounted onto a glass slide, incubated in 0.25% Triton-X100 for 1 hour, blocked by 5% NGS- 0.1% Triton-X100 for 1 hour, and then incubated with primary antibody against human Aβ-42 6E10 (1:300) at 4°C overnight. The samples were then washed in PBS (3 times, 5 minutes each) and probed with Alexa Fluor 488 secondary antibody (Thermo Fisher Scientific, #A32723, 1:500). Hoechst stain was used for nucleus staining. Slides were covered with a coverslip and were imaged with a Zeiss LSM 510 scanning confocal microscope.

Data analysis and statistics. Retinal layer thicknesses were populated by the OCT machine's auto-analysis software that provides minimum, maximum, mean and standard deviation (SD). We performed the stratified analysis by fitting a linear regression model on each genotype separately with mean thickness measurements as response and age (in weeks) as an independent variable. Coefficient and p-value are reported to evaluate the impact of age on measurements. A greater than 0 coefficient implies positive impact (when age increases, measurement also increases); a significant p-value suggests the coefficient is different from 0, in other words, age has some impact (positive or negative) on measurements. To further compare the differences in age impact between control and transgenic groups, we fit a combined linear regression model with both genotypes and age-by-genotype interaction. All comparisons were performed within and between the groups, and all reported p-values were two-sided with p<0.05 considered statistically significant. A significant p-value suggests differences in age impact between genotypes. When appropriate, p-values are corrected with Bonferroni procedure for family-wise error rate. All analyses were performed using SAS version 9.4 (SAS Inc., Cary, North Carolina). All graphs were made using Python (Python Software Foundation. Python Language Reference, version 3.7).

RESULTS

Retinal sublayer thickness measurements from a total of 60 (109 eyes) 3xTg-AD and 40 (72 eyes) control mice were analyzed. Total retina thickness did not change significantly from young to middle age in transgenic (-0.02 µm/week, p=0.4850) and control (-0.07 µm/ week, p=0.1803) animals. A linear regression model with interaction

term showed no difference in total retinal thickness between transgenic and control animals (p=0.4790) (Figure 9A). RNFL thickness decreased significantly from young to middle age in transgenic animals (-0.1491 µm/week, p<0.0001), but not in controls (-0.0271 µm/week, p= 0.2525). A linear regression model with interaction terms showed that RNFL thickness in transgenic mice decreased faster than RNFL thickness in controls (p=0.0002) (Figure 9B). In contrast, GC-IPL thickness decreased significantly in control animals (-0.13 µm/week, p=0.0196) but not in the transgenic group (0.05 µm/week, p=0.174). A linear regression model with interaction term showed that GC-IPL thinning in control animals was significant compared to transgenic animals (p=0072) (Figure 9C). INL thickness change was minimal in both transgenic (-0.05 µm/week, p=0.0181) and control (-0.04 µm/week, p=0.1071) mice. A linear regression model with interaction term showed no difference in INL between transgenic and control animals (p=0.9152) (Figure 9D). OPL did not show a noticeable change in control (-0.01 µm/week) or transgenic (0 µm/week) animals. A linear regression model with interaction term showed no difference between transgenic and control animals (p=0.5220) (Figure 9E). ONL+IS thickness did not change significantly in transgenic (0.04 µm/week, p=0.0526) or control animals (0.05 µm/week, p=0.1027). A linear regression model with interaction term showed no difference in ONL+IS between transgenic and control animals (p=0.8360) (Figure 9F). OS thickness did not change significantly in transgenic (0 µm/week, p=0.6793) or control animals (0 µm/week, p=0.7896). A linear regression model with interaction term showed no difference in OS thickness between transgenic and control animals (p=0.9296) (Figure 9G). RPE thickness did not change significantly in transgenic (-0.01 µm/week, p=0.2364) or control animals (0.01 µm/week, p=0.1443). A linear regression model with interaction term showed no difference in RPE thickness between transgenic and control animals (p=0.9457) (Figure 9H).

Inner retinal thickness decreased significantly in control animals (-0.11 µm/week, p<0.0051) but not significantly in transgenic animals (-0.05 µm/week, p=0.0640). Linear regression model with interaction term showed no difference in inner retinal thickness between transgenic and control animals (p=0.1880) (Figure 10A). Outer retinal thickness did not change significantly in transgenic (0.04 µm/week, p=0.1132) or control animals (0.04 µm/week, p=0.2152). Linear regression model with interaction term showed no

difference in outer retinal thickness between transgenic and control animals (p=0.9286) (Figure 10B).

RGCs were counted in flat-mount projections (Figure 11A). RGC numbers decreased significantly in transgenic and control animals from 4 to 12 months of age (Figure 11B). RGC numbers were not significantly different between transgenic and control 4-month-old animals (p=0.5996). However, 3xTg-AD animals had a significantly lower RGC count than controls in 8-month-old and 12-month-old groups (p=0.0426 and p=0.0002, respectively) (Figure 11C).

We did not observe any human Aβ-42 staining in control animals (0/3 in 4-, 8-, 12-month-old control groups). Aβ deposition was detected in the extracellular space of retinal ganglion cells in the 4-month-old 3xTg-AD retina (Figure 12). Aβ deposition in RGC increased with increasing age, and larger aggregates were noted from 4 to 12 months of age. Immunostaining of the brain sections from the same 4-month-old 3xTg-AD mice did not show Aβ deposition (Figure 12). Aβ deposition was observed in brain sections of all (3/3) 8-month-old mice. Aβ deposition increased in distribution and intensity in 12-month-old mice (3/3).
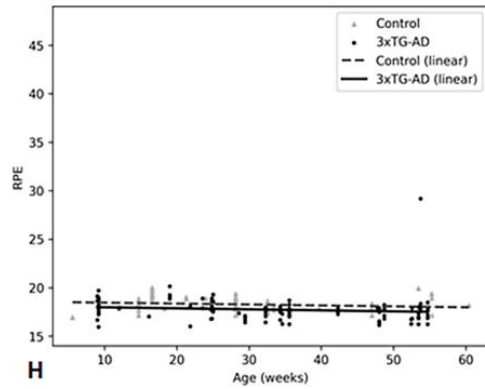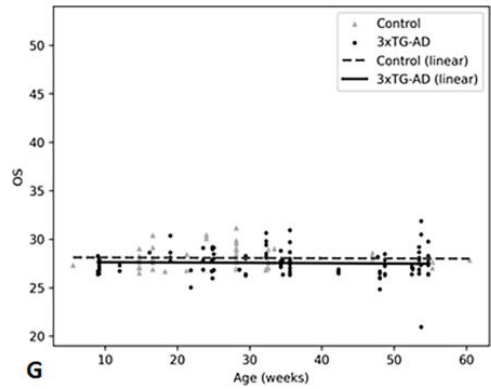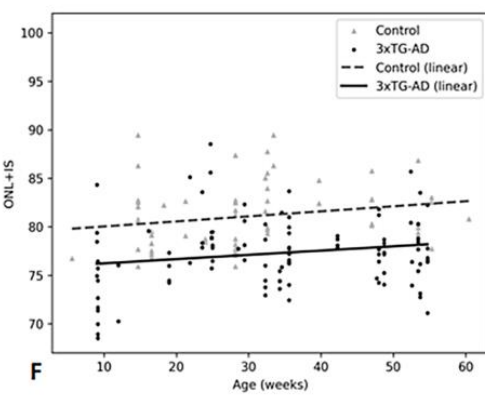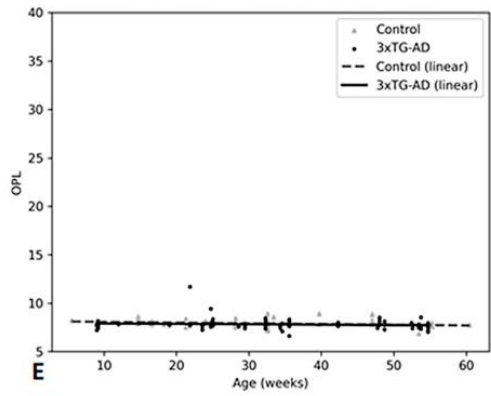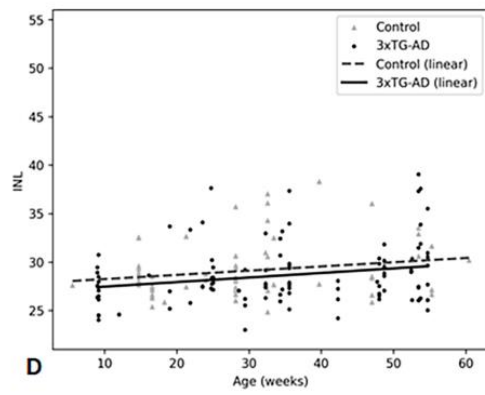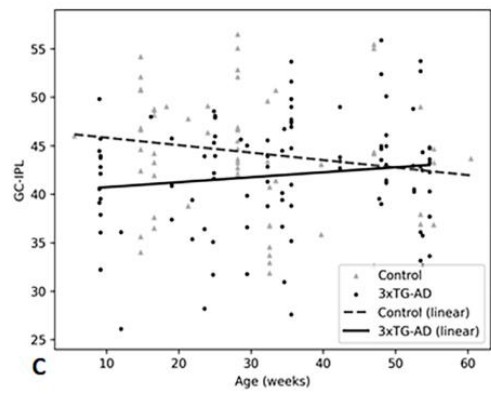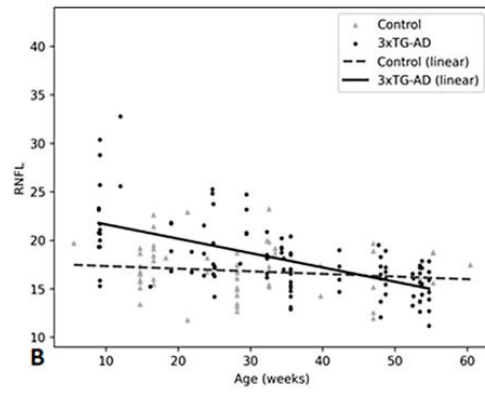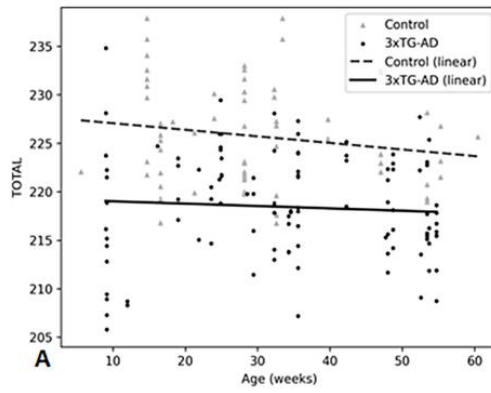
Figure 9. Retinal sublayer thickness changes in young to middle-age in 3xTg-AD and control mice. Total retinal (TOTAL), retinal nerve fiber layer (RNFL), ganglion cell + inner plexiform layer (GC-IPL), inner nuclear layer (INL), outer plexiform layer (OPL), outer nuclear layer + inner segment (ONL+IS), outer segment (OS), and retinal pigment epithelium (RPE) thickness in young to middle-age 3xTg-AD and control mice. RNFL thickness decreased from young to middle age 3xTg-AD, but not in control animals (A). GC-IPL thickness decreased in control, but not in 3xTg-AD, animals (B). Although there was a trend for increasing or decreasing thickness from young to middle-age, changes were not significant in INL (C), OPL (D), ONL+IS (E), OS (F), and RPE (G) thicknesses. There was no significant difference between the 3xTg-AD and control eyes in INL (D), OPL (D), ONL+IS (E), OS (F), and RPE (G) thickness changes from young to middle-age.
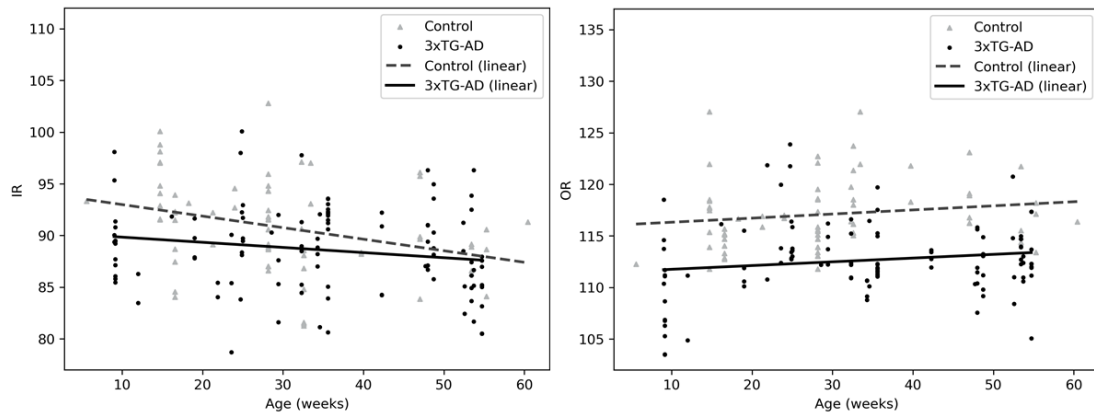
Figure 10. Inner and outer retinal layer thickness in young to middle age 3xTg-AD and control mice. Inner retina (IR) is defined as the sum of retinal nerve fiber layer, ganglion cell-inner plexiform layer, and inner nuclear layer thickness, Outer retina (OR) is defined as the sum of inner nuclear layer, outer plexiform layer, outer nuclear layer + inner segment, outer segment, and retinal pigmented epithelium thickness. Inner retinal thickness (A) was stable in young to middle age transgenic animals, but IR thickness decreased significantly in control eyes. There was no significant difference between the two groups. Outer retinal (B) thickness change was not significant from young to middle age in transgenic and control groups.
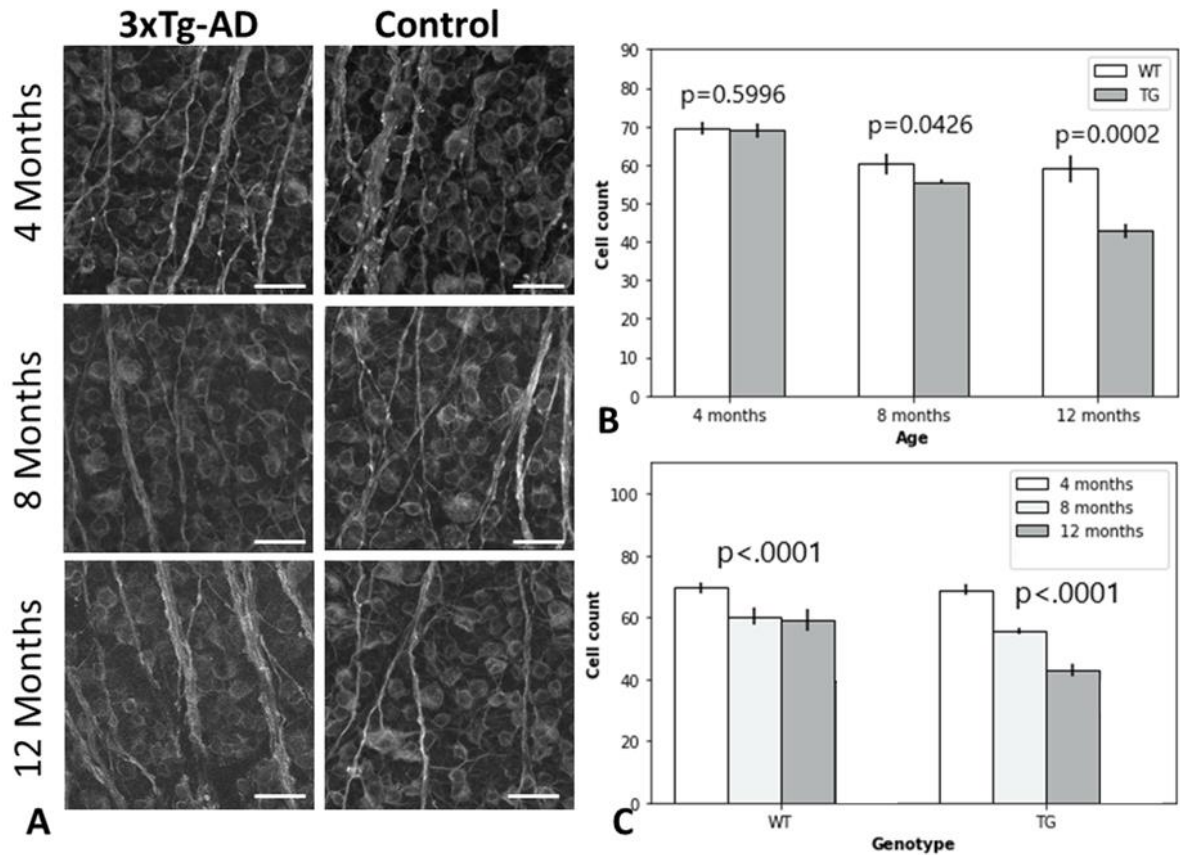
Figure 11. Retinal ganglion cell quantification from young to middle-age 3xTg-AD (TG) and control (WT) mice. The ganglion cell layer was stained with anti-TUJ-1 antibodies. GC density was quantified in 4-, 8-, and 12-month-old 3xTg-AD and control mice (A). While there was no significant difference in GC density between the transgenic and control animals at age 4 months, the GC number was significantly lower in transgenic eyes than their controls at age 8 months and 12 months (B). Ganglion cell numbers decreased significantly in both groups as their age advanced (C). (scale bar: 20 µm)
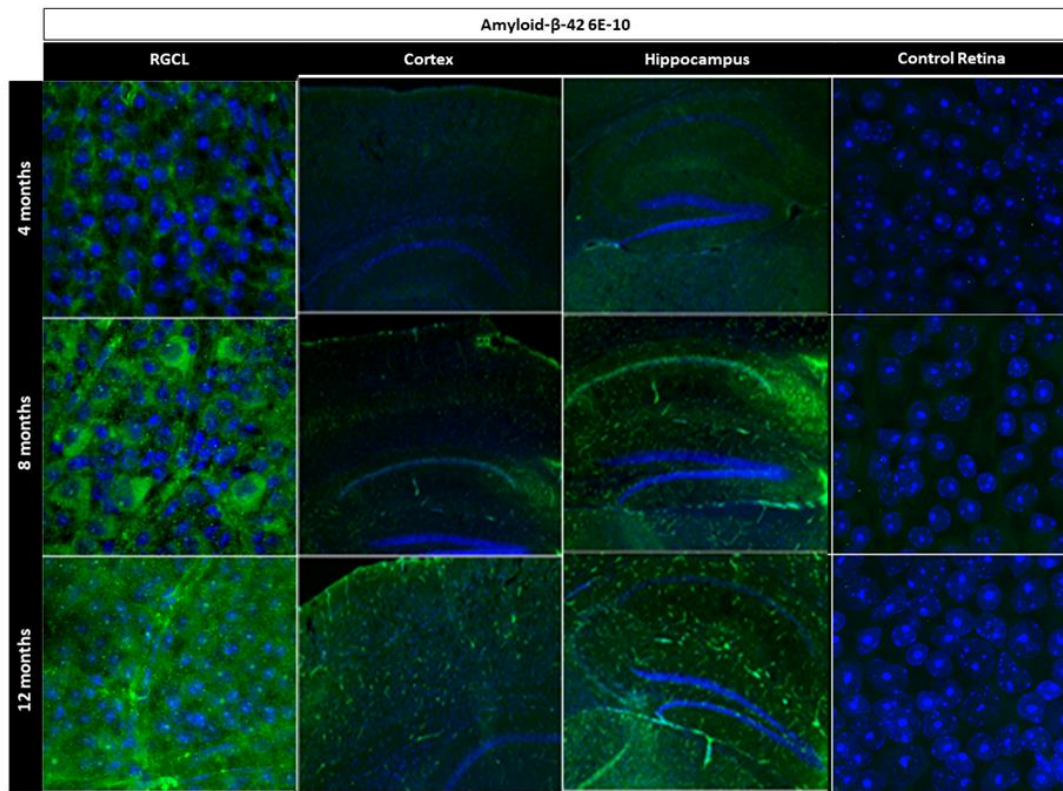
Figure 12. Amyloid-β 42 (Aβ-42) immunostaining of retina flat-mount and brain sections. Transgenic and control retina and transgenic hippocampus and cortex sections from 4-, 8-, and 12-month-old mice were stained for Aβ-42. 3xTg-AD retina flat mounts were positive for Aβ-42 in 4-, 8- and 12-month-old mice. Immunoreactivity to Aβ-42 increased in the ganglion cell layer with age. No Aβ-42 positivity was detected in the control retina (scale bar: 20 µm). Aβ-42 positivity was not detected in the cortical sections of 4-month-old mice but was noted in cortex and hippocampus sections at 8-month and 12-month-old transgenic mice (scale bar: 200 µm).

DISCUSSION

Preferential involvement of inner retinal layers has been consistently reported in transgenic mouse models of the disease.[57,170,171,181,182] However, the changes involving distinct retinal sublayers have not been consistent among these studies. Chiquita et al. studied 3xTg-AD mice at 4-, 8-, 12-, and 16- months of age and showed GC-IPL thinning in the transgenic model.[57] Although this may seem contradictory to our findings, the results

are possibly more similar when the difference in retinal sublayer segmentation methods is considered. Chiquita et al., similar to Harper et al. and Gardner et al., included RNFL thickness within GC-IPL thickness, likely because their segmentation method did not differentiate RNFL from other inner retinal layers.[57,181,182] So, it is possible that the changes in RNFL thickness have influenced the amount of change that occurred in GC-IPL thickness. While Chiquita et al. reported GC-IPL thinning from 4 to 8 months of age, GC-IPL thinning did not progress from age 8 to 12 months. Although Chiquita et al. did not explain such lack of time effect on GC-IPL thickness,[57] it could be due to the thickening effects of the simultaneous increase in AD-related inflammatory burden in retinal nuclear layers that neutralizes the thinning effect of AD neurodegeneration. Neurodegeneration, neuroinflammation, and neurovasculapathy ensue simultaneously, but possibly at a different rate, in AD, and their effect on retinal sublayers vary depending on the predominance of neuronal, glial, and vascular components in each of these layers.[42] RNFL is mostly acellular, unlike GC-IPL, and may not be influenced by the trophic processes such as microglia activation,[77] neuronal swelling[183] and Müller cell hypertrophy.[42,184] Such inflammatory processes may offset volume loss associated with neurodegenerative cell death in AD.[102] Lim et al. also showed progressive RNFL thinning but stable total retinal thickness in 6 to 17 months old 5xFAD mice that may similarly imply the variable impact of AD pathology on different retinal sublayers.[171] Human OCT studies have suggested that neuronal loss may eventually overwhelm the concurrent trophic inflammatory processes in advanced AD. A comparison between MCI and clinical AD by Ascaso et al. found that total macular thickness remained stable while RNFL thinning occurred in the preclinical stage of AD (MCI); however, in advanced AD, both total macular and RNFL thicknesses declined.[102] In summary, these studies may indicate that RNFL, which is devoid of major cellular elements, may be less influenced by the inflammatory-trophic processes in early AD. As a result, RNFL may better represent the neurodegenerative process in preclinical AD.

Both human and animal studies have shown retinal RGC loss in AD.[40,51,102,175,185] However, we are not aware of other studies showing OCT-based retinal thickness changes and concurrent RGC loss in the same animal AD models. While RGC loss occurred in both 3xTg-AD and control mice, the RGC loss rate was more remarkable in 3xTg-AD animals,

as shown before.[173–175] The trend of RGC loss and RNFL thinning were parallel, indicating that RNFL thickness is a surrogate marker of ganglion cell loss caused by AD neurodegeneration. Two possible mechanisms have been proposed for RNFL thinning in clinical and preclinical AD: 1) Retrograde loss of ganglion cell axons due to the central involvement of visual pathways in CNS.[186] 2) *In situ* retinal neural loss caused by AD pathology as evidenced by observing retinal neuronal death occurring adjacent to Aβ plaques.[91,173,175,187–189] Our findings did not directly differentiate between retrograde versus *in situ* retinal neurodegeneration. Confirmation of such *in situ* retinal neuronal loss in AD may prove retina as a suitable tool to study local medication delivery for neuroprotection.

The longitudinal correlation of AD pathologies in the brain and retina has been debated. Georgovsky et al. showed that Aβ deposition occurred in APP/PS1 model's brain and retina in parallel.[170] In contrast, Chiasseu et al. showed an age-related increase in retinal tau deposition and a reduction of RGC numbers in 3xTg-AD mice as early as three months of age, preceding tau aggregation in the brain.[40] In another study, Koronyo-Hamaoui et al. observed retinal Aβ deposition in a double transgenic mouse model as early as 2.5 months of the age preceding brain Aβ aggregates seen in 5-month-old animals.[39] In our study, Aβ-42 deposits were noted in the 4-month-old 3xTg-AD mouse retina; but Aβ-42 deposition in the brain sections was first detected at eight months. Similarly, Cho et al. did not observe 6E10-positive plaques in the brain of 5-month-old 3xTg-AD mice but detected diffuse plaques in 7-month-old animals.[190] These observations agree with Chiasseu et al. and Koronyo-Hamaoui et al. findings that retinal AD pathologies precede the brain pathologies; thus, supporting retinal screening as a potential method to identify early AD. Identifying such healthy individuals in the preclinical stage of AD before their neuronal loss reaches a threshold to present as MCI or clinical AD is the key to modify risk factors and implement potential treatments.

We observed an age-related RGC loss and a corresponding GC-IPL thinning in C57BL/6J mice. Similarly, Shariati et al. showed ganglion cell complex thinning on their OCT analysis of 3- to 12-month old C57Bl/6 mice.[191] Cenni et al. also observed that the density of ganglion cells in wild-type murine eyes declined from $112,000 \pm 17,400$ at birth to $45,000 \pm 4000$ by 6 to 8 months of age.[192] Also, Samuel et al. showed that total retinal, ganglion cell layer, and inner plexiform layer thicknesses decreased by about 15% from

young (3 to 5 months) to old (24 to 48 months) C57BL/6 mice.[193] Taken together, these findings corroborate a moderate attrition of RGC with normal aging that is reflected as GC-IPL thinning in OCT scans. The pattern of retinal sublayer thickness changes may help to noninvasively differentiate neurodegenerative and neuroinflammatory conditions from neurodegeneration caused by normal aging.

This study has several limitations, including the choice of C57BL/6J as controls. 3xTg-AD mouse has been developed on C57/129 SVJ genetic background; however, C57BL/6J has been widely used as controls in previous studies on 3xTg-AD mice.[42,171,194–196] The difference in total retinal, RNFL, GC-IPL, and ONL+IS thicknesses in the younger mice may have originated from such difference in 3xTg-AD and C57BL/6J genetic background. Alternatively, the neuroinflammatory and vascular processes that had already started before our measurements may have contributed to such differences. Regardless, we drew our interpretations based on the slope of changes from young to middle age within each transgenic and control group, not the absolute amount of the changes. Translating mouse OCT studies to human bears some limitations.[41] Rodents, unlike the human, do not have macula where AD pathologies concentrate,[39] however, the layered structure of the mouse retina is otherwise identical to the human retina, and similar degenerative processes occur in murine models too.[48] Also, rodent models of AD may manifest AD-related pathologies, but they miss environmental and cardiovascular risk factors of AD.[47] However, such environmental and cardiovascular risk factors are probably less pronounced in young and middle-age at-risk individuals. OCT scans from very thin mouse retina tissue are inherently prone to segmentation errors and motion artifacts (for example, when differentiating very thin layers such as RNFL from GC-IPL); however, our results showed a significant trend for thickness changes in transgenic and control groups. The discrimination and quantification of such changes in the thicker human retina are potentially more feasible and less prone to errors. GC density decreases toward the periphery; however, GC density is relatively consistent in areas with equal distance from the optic nerve,[197] and we measured GC density in areas equidistance from the optic nerve head. The choice of animal model in the current study may increase the translational value of our findings. 3xTg-AD mouse is born with no Aβ and tau pathologies and develops an increasing Aβ and tau burden in the CNS, resulting in progressive neurodegeneration and

behavioral and cognitive abnormalities, arguably similar to human AD disease.[37,38,41–45] We used an annular OCT scan protocol with automated segmentation and thickness averaging that has been shown to minimize biased measurements possibly seen in manual segmentations.[191] While some reports[198,199] have shown significant RNFL thinning in superior quadrant compared to the other quadrants of the retina, most studies, including a meta-analysis of the studies that measured RNFL thickness in AD, reported a balanced loss of RNFL in all quadrants.[102,200] Thus, we only analyzed the average retinal sublayer thickness based on the annular scans and did not differentiate between the quadrants.

Conclusion Our study offers a robust analysis of retinal sublayer thicknesses in young through middle-age triple transgenic mouse model of AD. The total retinal thickness stayed stable but RNFL, and no other retinal sublayers, thinned out progressively as 3xTg-AD mice aged through their midlife. The thickness of RNFL in 3xTg-AD retina was quantifiable with non-invasive OCT imaging and correlated with the reduction in retinal GC numbers and an increasing retinal and brain AD pathology load. Retinal Aβ-42 deposition appeared before the appearance of such depositions in the brain, as reported in similar studies.[40,42,173] Our data supported OCT-based non-invasive monitoring of retinal sublayers as a possible biomarker for AD progression in midlife, as a potential component of a decision-making tree to differentiate AD-related retinal changes from retinal changes associated with normal aging, and as a likely outcome measure in future preclinical treatment interventions. Our finding should be validated in human.

Chapter 3 Retinal vascular plexus attenuation in the triple transgenic mouse model of Alzheimer's Disease

ABSTRACT

Purpose: Retinal vessel structure and function may be markers for cerebral vascular pathology in Alzheimer's disease (AD). However, differentiating age- versus AD-related retinal vascular changes is unresolved. To answer this question, we studied superficial (SVP), intermediate (IVP), and deep (DVP) vascular plexuses in young to old triple transgenic mouse model of AD (3xT-AD).

Methods: Retinal flat-mounts from young, middle-age, and old 3xT-AD (transgenic) and C57BL/6j (control) mice were immunostained for collagen-IV. The number of vessel intersections and endpoints and total vascular length were quantified, as vascular density parameters, in SVP, IVP, and DVP using AngioTool. Mixed effect linear regression modeling was used to detect the difference among groups.

Results: All three layers had equal densities in young 3xTg-AD and control animals. In control animals, IVP and DVP densities decreased by aging (-14.1% to -32.36% change from young to old, $p<0.05$). In the transgenic group, all three layers' densities decreased by aging (-12.03% to -48.68% change from young to old, $p<0.05$). The number of SVP intersections was lower in the old transgenics than the old controls ($p=0.028$). DVP vessel length and the number of intersections were lower in the old transgenics than the old controls ($p=0.037$ and $p=0.016$, respectively).

Conclusion: Vascular rarefaction with natural aging and AD occurs differentially in retinal capillary plexuses. Vascular densities correlated with the reported AD pathologic burden and metabolic changes in the retina. SVP and DVP may serve as indicators for AD-related vascular attenuation and differentiate AD-related vasculopathy from age-related neurodegenerations.

INTRODUCTION

Cerebral vessels are increasingly known as significant contributors to the pathogenesis of Alzheimer's disease (AD). Amyloid β (Aβ) and tau accumulation in cerebral and leptomeningeal capillaries, loss of pericytes, attenuation of endothelial tight junctions, impaired vasoregulation, and disrupted blood-brain barrier are among vascular pathologies identified in the AD brain.[2,201–205] Besides, acquired and genetic risk factors of AD are closely linked to vascular dysfunction.[2,205,206] Thus, there is a strong belief that cerebral vascular biomarkers indicate AD pathology's severity and progression in the brain.[203,205] Indeed, imaging modalities such as arterial spin labeling magnetic resonance imaging (ASL-MRI) have shown that cerebral blood flow (CBF) is defective years before AD's clinical presentation and CBF abnormalities increase as patients progress to clinical disease.[207] However, such expensive and time-consuming vascular imaging methods are not suitable for screening millions of AD patients and at-risk individuals.

The retina is an extension of the central nervous system (CNS), shares many structural and functional properties with the brain, and is readily visible using noninvasive optical imaging modalities. Retinal vasculature is organized in three layers: superficial vascular plexus (SVP), located within the retinal nerve fiber (RNFL) and ganglion cell (GCL) layers, intermediate vascular plexus (IVP), located between the inner plexiform (IPL) and inner nuclear (INL) layers, and deep vascular plexus (DVP), situated between the INL and outer plexiform layer (OPL).[67,69,139,208] SVP is mainly composed of main retinal arteries, veins, and arterioles; IVP is mainly composed of arterioles and capillaries; DVP is formed by a rich capillary network and collecting venules.[209,210] Connecting arteries and veins travel between these vascular layers.[209,210]

Retinal vascular abnormalities in senescence correlate with hippocampal microvascular abnormalities and cognitive impairment, suggesting that retinal vascular structure and function may indicate brain neurodegeneration.[211–213] In AD, histopathologic studies on animal models and human samples show amyloid and tau deposition in retinal and brain vasculature and comparable perivascular neuroinflammation.[39,188,214–216] Besides, noninvasive optical imaging studies with OCTA show retinal vascular changes in preclinical and clinical AD supporting the idea that retinal vessels change in AD may correlate with brain pathologies.[87,119,121,122,126,130,132,133,217] However, these findings have

sometimes been contradictory,[130,132] and differentiating the extent of Alzheimer's-related retinal vascular changes from vascular alterations due to aging and cardiovascular diseases have remained unresolved. Besides, although it has been shown that retinal blood flow in each vascular plexus is differentially regulated and tightly coupled with metabolic demand in their respective retinal layers,[218] it is unclear if retinal vascular distribution follows the variable burden and vulnerability of retinal vascular and neuronal layers to Alzheimer's pathology. To answer these questions, we investigated, for the first time, retinal vascular distribution in young, middle age, and old age groups in an AD mouse model and its controls. We used the 3xTg-AD model because it expresses both amyloid and tau pathologies and closely mimics AD's cerebral and retinal pathologic manifestations in human.[38,40,57] Using an immunofluorescent approach combined with tissue optical clearing to easily visualize deeper retinal vascular layers for confocal microscopy and vascular quantification, we showed that all three vascular layers attenuate from young to old age in the AD model retina. SVP and DVP densities were significantly lower in old transgenic than age-matched control eyes. Our data suggested SVP and DVP vascular density as a marker for AD.

METHODS:

Animals and their care. The University of Texas Medical Branch (UTMB) Institutional Animal Care and Use Committee (IACUC) approved all animal experiments. Mice were maintained with food and water access ad libitum and on a 12-hour light and dark cycle.

The triple transgenic B6; 129-Psen1tm1Mpm Tg(APPSwe,tauP301L)1Lfa/Mmjax (3xTg-AD), and C57BL/6j mice were used for the studies. The original line of 3xTg-AD mice was obtained from The Jackson Laboratory (Bar Harbor, ME) and maintained at the University of Texas Medical Branch animal facility with genotyping confirmation of the mutations in randomly selected progenies. 3xTg-AD mice will be referred to as "transgenic" in this manuscript. C57BL/6j mice served as controls. Animals were grouped into three age groups of 2-month-old that will be called "young," 8-14-month-old that will be called "middle-age," and 18-20-month-old that will be called "old. Only female mice were used in this study.[219]

Retinal flat-mount immunofluorescent staining and optical clearing.
Anesthesia was induced by an intraperitoneal injection of a 60 mg/kg Ketamine and a 0.5 mg/kg Dexmedetomidine combination followed by cervical dislocation for euthanasia. Then, cardiac perfusion was performed using 20-40 ml of ice-cold PBS, followed by 20-40 ml of freshly prepared 4% paraformaldehyde (PFA). Both eyes were enucleated and were immediately immersed in ice-cold PFA 4% for overnight fixation. Then, under a dissecting microscope, an incision was made around the limbus, and the cornea, iris, lens, and vitreous body were removed. The retina was carefully dissected from the underlying retinal pigment epithelial (RPE), choroid, and sclera. Retina tissue was then washed in PBST (PBS containing 0.3% Tween 20) and incubated in PBST containing 5% normal goat serum for 4 hours at room temperature (RT) or overnight at $4°$C. A 48-hour incubation with anti-mouse anti-collagen IV antibody (Abcam, ab19808, 1:200 in PBST containing 5% normal goat serum) at RT followed. Following incubation with the primary antibody, the retinas were washed with PBST and probed with fluorescent-labeled secondary antibodies (Alexa Fluor 546, 1:200, Life Technologies) for 12 hours at RT. The samples were washed with PBS, and then 2,2′-Thiodiethanol (TDE) tissue clearing method was applied as described in detail before.[220] In brief, each sample was incubated at room temperature in an increasing concentration of TDE that started with 10% TDE in PBS for 1 hour and then in progressively increasing TDE solution concentrations, in 10% increments, up to 60% TDE. Retinal tissue generally started to clear after incubation in 50% TDE solution. Retina samples were placed on a glass slide, and four to six radial cuts were made to spread them flat with retinal ganglion cell side up. The samples were then mounted with 60% TDE solution and covered with a cover glass.

Microscopy. A confocal microscope (LSM880, Carl Zeiss) equipped with 405, 488, 561 nm lasers with a ×20 air objective (20×/0.8) was used for imaging. Midperipheral fields (0.5-1.5 objective distances from the optic nerve head margin) were selected while focusing only on the superficial microvascular plane (Figure 13). Two non-overlapping regions of interest (ROI) from each petal (eight ROIs in total for each sample) were imaged. After selecting each field, the focal plane was reset to the superficial vascular plexus. Z-stacks encompassing all three retinal vascular networks (usually 40-60 µm in thickness) were captured at 1 µm intervals. Initially, four 413 x 413 µm squares were scanned and

stitched with Zen lite (blue edition; Carl Zeiss Meditec) to create a composite 810 x 810 µm picture. Since image quality was poor at some areas of this larger square, only one of the 413 x 413 µm captures from each area was used for final quantification. The contrast and brightness of the images were adjusted within ZEN lite (blue edition; Carl Zeiss Meditec). The average projection orthogonal views of each SVP, IVP, and DVP layer were extracted and saved as .tif files.

Vascular quantification. Images with faint vascular outlines were opened in the Microsoft Paint program, and vessels were traced manually[65,221] with a 10-15-pixel width Wacom Intuos pen. The orthogonal views were subsequently processed by AngioTool 0.5a, a Java-based publicly available open-source software accessible from the National Cancer Institute (https://ccrod.cancer.gov/confluence/display/ROB2).[222] AngioTool has been used to study retinal capillary plexus, post-embryonic retinal vascular development, and choriocapillaris.[222,223] AngioTool quantifies vascular network morphological and spatial parameters such as ROI area, vessel area, vessel density, the total number of intersections, total vessel length, and the total number of endpoints based on a set of user-defined intensity, vessel diameter, and particle size thresholds. These parameters were optimized to delineate the vascular structure in different retinal vascular layers.[222–224] The analysis of vessel structure in AngioTool is summarized here in the following steps: 1. Enhancement of vessel structure with the multiscale Hessian analysis and smoothing with a recursive Gaussian filter. 2. Segmentation and skeletonization of the vessels. 3. Calculation of the morphometrical parameters. First and second-order retinal arteries and veins were studied in a pilot analysis of the pictures and were found to have a diameter greater than 30 pixels. Any vessels wider than 30 pixels were filtered out from the quantification, and retinal arterioles, venules, and capillaries were quantified.[209,210] Because collagen IV antibody stains both intact and degenerated vessels, we set a lower width limit of 5 pixels to eliminate degenerated vessels from quantification. AngioTool quantification was performed by a trained investigator who was blind to the age and genotype assignment of the samples. One or two senior investigators reviewed faint and noisy images to adjudicate the vessel's outline in doubt. Vessel intensity was set at 20-50 for all images (on a scale of 0-255). The option checkboxes, "Remove small particles" and "Fill holes," were selected if the immunofluorescent artifacts were seen as small particles

on the background or small holes within the thickness of the vessels (Figure 14).[222] We analyzed three density parameters: total vessel length (TL-linear pixel length), the total number of intersections (TI), and the total number of endpoints (EP) (Figure 2B).[224–226] Total vessel length was calculated as the sum of all the vessels length defined by the distance between two vessel intersections or between an intersection and an endpoint. Since some images were manually enhanced for the analysis using a digital pen, as described above, vessel diameter and total vessel area were excluded from the analysis.

Data analysis and statistics. Descriptive statistics, including means and standard deviations, were used to describe the sample population. The study outcomes were modeled to detect differences among groups using mixed-effects linear regression for accounting for repeated observations within the subject. Since all subjects contributed multiple biological samples from each eye, 3-level models were initially employed with subject id as first, eye (right/left) as second, and observation as the third level with each subsequent level being nested within the previous one. Initial analysis revealed that the second level (eye) did not contribute significantly to the observed variation in any of the outcomes; therefore, in the final analyses, 2-level models were employed using random intercept for subject id to account for repeated observations within subjects. Mixed-effect linear regression modeling was performed using the R package *nlme.*[227] All analysis were performed using the *R language for Statistical Computing*.[228]
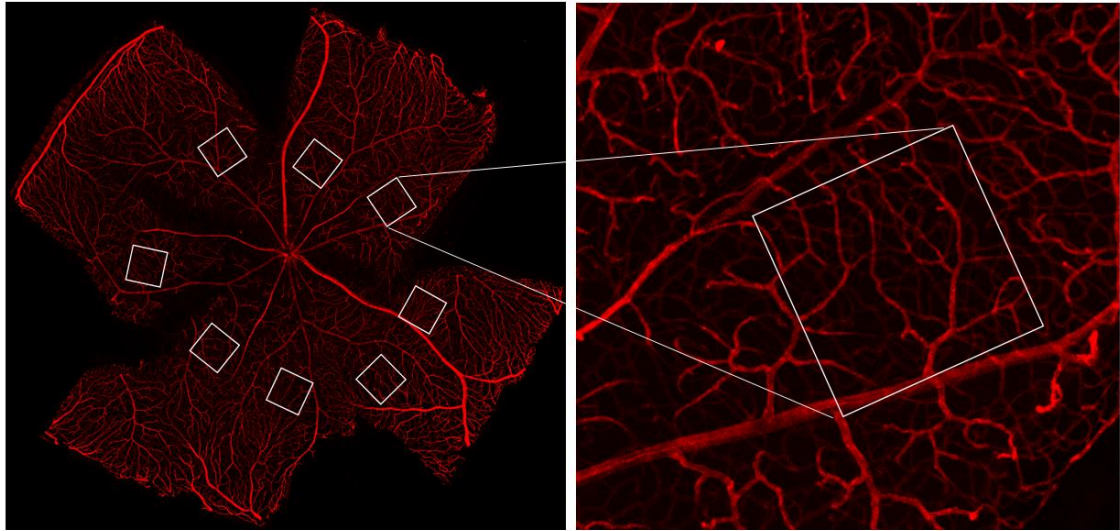
Figure 13. Retinal flat-mounts were stained for collagen IV. Eight non-overlapping regions of interest (ROI) from the midperipheral retina were imaged (A). Tissue optical clearing allowed better visualization of intermediate and deep vascular plexuses for AngioTool analysis. B demonstrates a magnified orthogonal view of all three layers from a representative ROI. The orthogonal projections of each superficial, intermediate, and deep vascular plexuses were created with ZEN Lite, and the layers were analyzed using AngiTool (20x, scale bar 1000µm) (Figure 14).
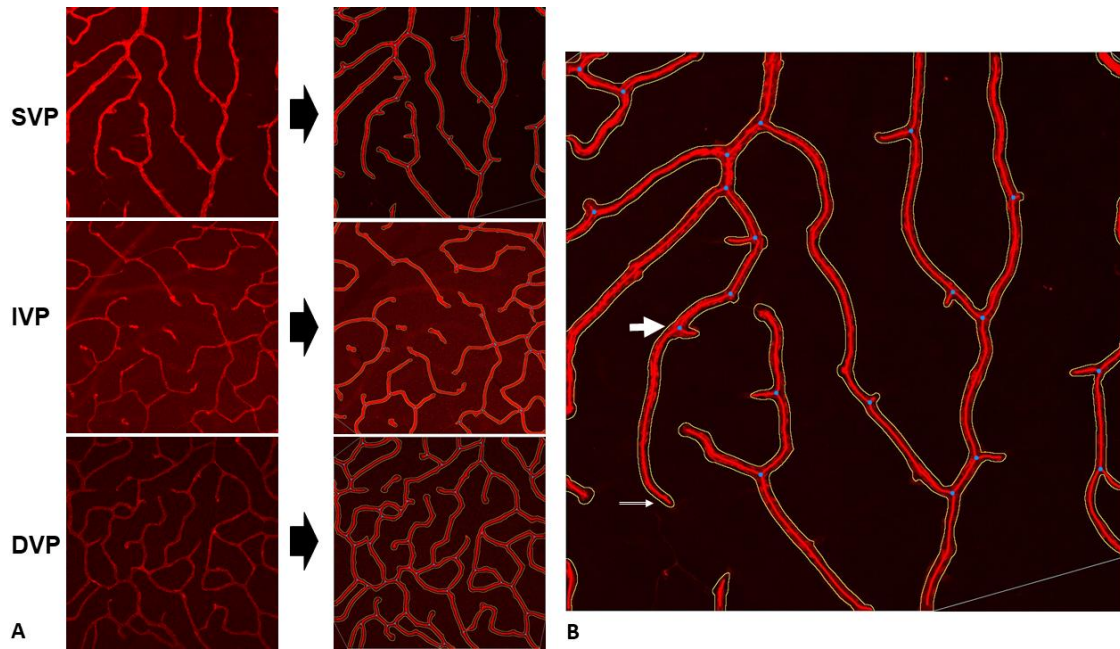
Figure 14. Representative superficial (SVP), intermediate (IVP), and deep (DVP) vascular plexus views before and after AngioTool analysis (A). Vessel outlines and intersection points were highlighted. Only vessels with 5-29-pixel diameter were filtered for detection. Intersections (thick arrow) and end points (thin arrow) were detected by AngioTool. Total vessel length is the sum of vessel lengths in each field.

RESULTS:

Table 1 shows the comparisons between various age and genotype groups in regard to vascular density parameters.

Superficial vascular plexus (Figures 15 and 16)

In the SVP, the total number of intersections (TI), total vessel length (TL), and the total number of endpoints (EP) decreased by age in the transgenic group but not in the control group. The relative difference of the total number of SVP intersections (TI) in old relative to young subjects was -34% in the transgenics (p=0.004) and -18.64% in the controls (p=0.181). The relative difference of the total SVP vascular length (TL) in old relative to young subjects was -20.66% in the transgenics (p<0.001) and -5.96% in the controls (p=0.7). The relative difference of the total number of endpoints (EP) of SVP in

old relative to young subjects was -32.23% in the transgenics (p=0.006) and -16.10% in the controls (p=0.161).

In young subjects, the SVP total number of intersections (25.5±4 in 3xTg-AD and 22.3±5 in control eyes; p=0.336), total vessel length (7717±1154 for 3xTg-AD and 7409±1605 control eyes; p=0.347), and the total number of endpoints (39.2±9 for 3xTg-AD and 37.2±7 for control eyes; p=0.319) were not statistically different between 3xTg-AD and control groups.

Similarly, in the middle age group, SVP parameters did not differ by mice genotype (TI: 19.9±4 in 3xTg-AD and 20±3 in control eyes; p=0.955; TL: 6766±660 in 3xTg-AD and 7014±1097 in control eyes; p=0.699; EP: 30±6 in 3xTg-AD and 31.9±4 in control eyes; p=0.578).

Regarding the SVP in old subjects, the total number of intersections (16.3±1 in 3xTg-AD and 18.3±1 in controls; p=0.028) was lower in 3xTg-AD relative to controls. In contrast, total vessel length (6135±281 in 3xTg-AD and ±196 in controls; p=0.065) was marginally lower in the old transgenic group, and number of endpoints (26.9±2 in 3xTg-AD and 30.2±4 in controls, p=0.156) did not differ by mice type.

Table 1: Comparison between vascular density parameters and respective p values. Significant values presented as bold. A mixed-effects linear regression model was used to account for repeated observations within the subject.

	P values	Total Number of Intersections	Total Vessels Length	Total Number of End Points
SVP	WT young vs middle vs old	0.181	0.7	0.161
	TG young vs middle vs old	**0.004**	**<0.001**	**0.006**
	WT young vs TG young	0.336	0.347	0.319
	WT middle vs TG middle	0.955	0.699	0.578
	WT old vs TG old	**0.028**	0.065	0.158
IVP	WT young vs middle vs old	**0.041**	0.14	0.393
	TG young vs middle vs old	**0.026**	**0.001**	0.111
	WT young vs TG young	0.432	0.86	0.355
	WT middle vs TG middle	0.47	**0.02**	0.967
	WT old vs TG old	0.208	0.596	0.919
DVP	WT young vs middle vs old	**0.001**	**0.018**	**<0.001**
	TG young vs middle vs old	**0.004**	**0.001**	**0.023**
	WT young vs TG young	0.759	0.98	0.403
	WT middle vs TG middle	0.438	0.1	0.558
	WT old vs TG old	**0.037**	**0.016**	0.312

SVP	Young	Middle age	Old
3xTg-AD			
C57BL/6j			
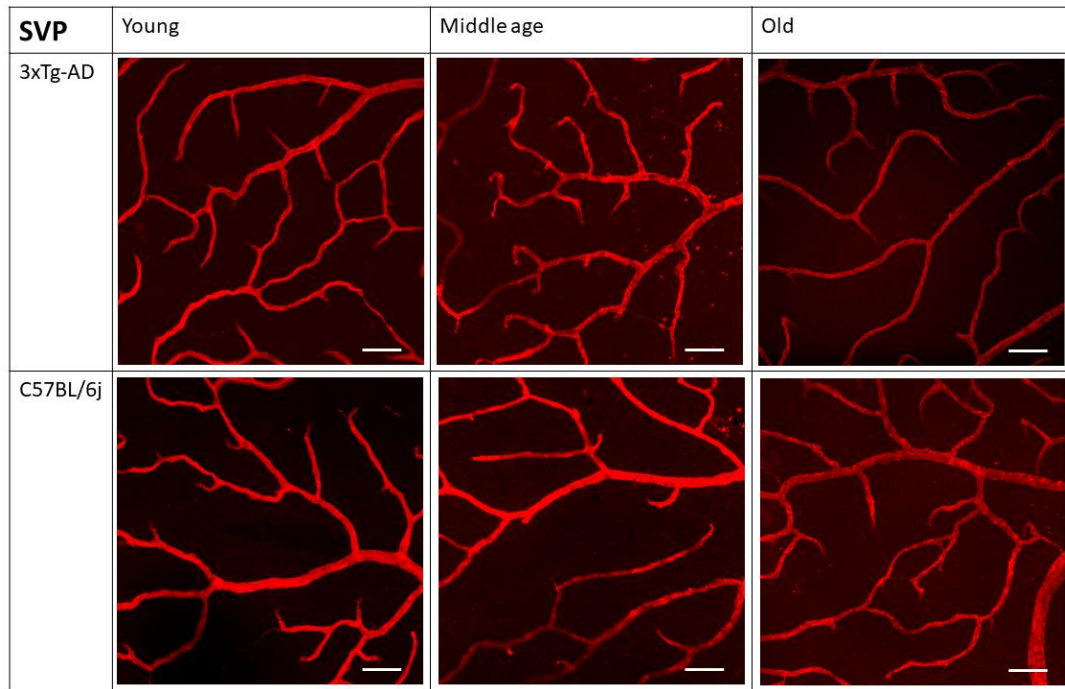
Figure 15. The vascular wall was stained with anti-collagen IV antibody. Tissue clearing was applied, and images were captured by LSM880, Zeiss confocal microscope. Representative images from superficial vascular plexus (SVP) in young, middle-age, and old transgenic and control mice (20x, scale bar 50 µm).
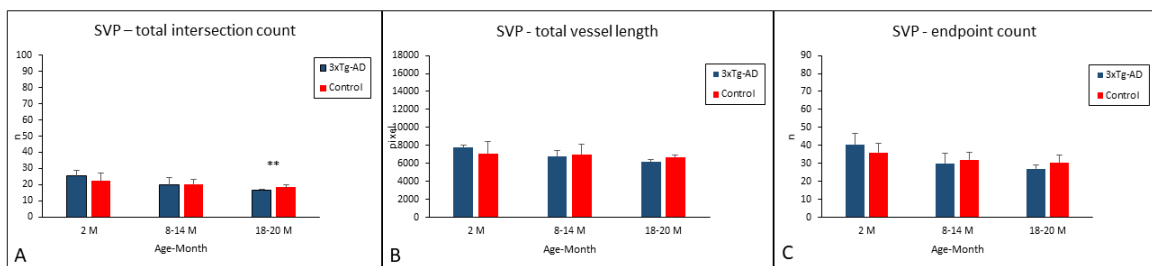
Figure 16. Bar graph representing SVP TI, TL, and EP in young, middle-age, and old transgenic and control eyes. A significant difference is marked by ** (p=0.028).

Intermediate vascular plexus (Figures 17 and 18)

In the IVP, TI, TL, and EP differed by age in transgenic and control groups. The relative difference of the total number of IVP intersections in old relative to young subjects was -31.44% in the transgenics (p=0.026) and -30.97% in the controls (p=0.041). The

relative difference of the IVP total vessel length in old relative to young subjects was -13.04% in the transgenics (p=0.001) and -14.24% in the controls (p=0.14). The relative difference of the total number of IVP endpoints in old relative to young subjects was -24.4% in the transgenics (p=0.111) and -12.92% in the controls (p=0.0393).

In young subjects, IVP parameters total number of intersections (33.5±10 in 3xTg-AD and 28.5±8 in control eyes; p=0.432), total vessel length (9308±1731 for 3xTg-AD and 9262±1816 control eyes; p=0.86), and the total number of endpoints (62.2±19 in 3xTg-AD and 56.5±14 in control eyes, p=0.355) were not statistically different between the 3xTg-AD and control groups.

Similarly, in the middle age group, IVP TI and EP did not differ by mice genotype (TI: 20.9±1 in 3xTg-AD and 21.4±2 in control eyes; p=0.47 and EP: 49.9±3 in 3xTg-AD and 50±7 in control eyes; p=0.967). IVP TL was significantly lower in the middle age transgenic than the middle age control groups (7217±301 in 3xTg-AD and 7949±492 in control eyes, p=0.02).

Regarding the IVP in old subjects, the total number of intersections (23±3 in 3xTg-AD and 19.7±5 in control eyes; p=0.208), total vessel length (8070±689 in 3xTg-AD and 727±1111 in control eyes; p=0.596), and the number of endpoints (48.5±3 in 3xTg-AD and 47.7±2 in control eyes; p=0.919) did not differ between the transgenic and control groups.
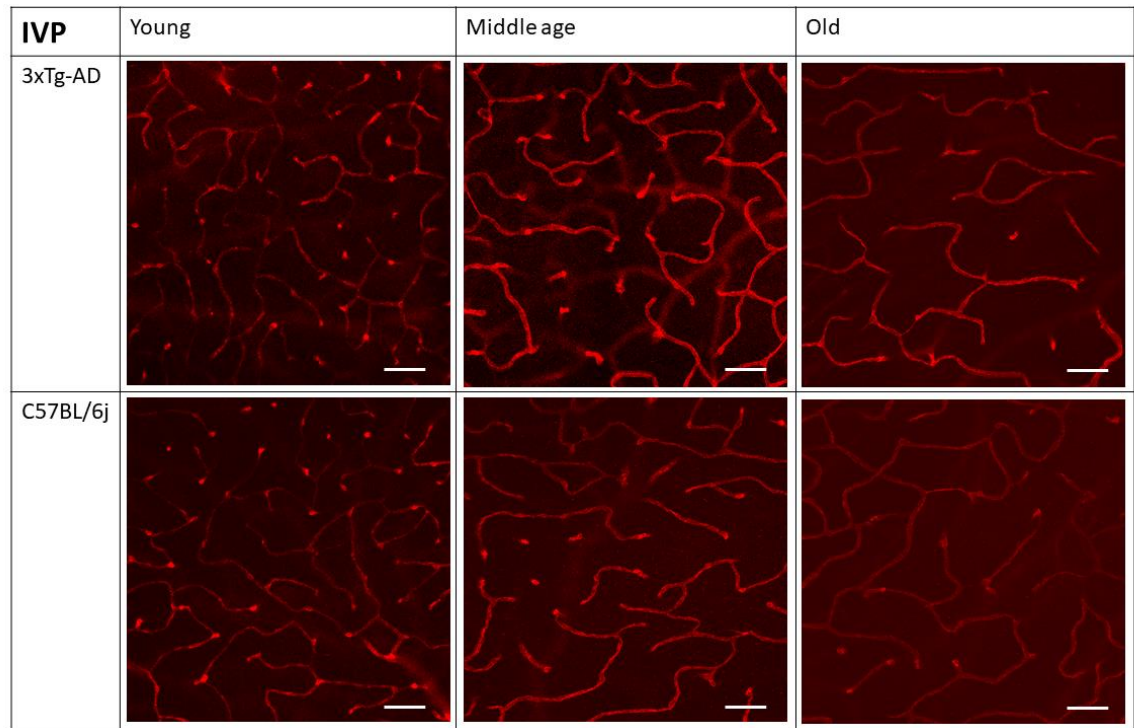
Figure 17. Vascular wall was stained with anti-collagen IV antibody. Vascular wall was stained with anti-collagen IV antibody. Tissue clearing was applied, and images were captured by LSM880, Zeiss confocal microscope. Representative images from intermediate vascular plexus (IVP) in young, middle-age, and old transgenic and control mice (20x, scale bar 50 µm).
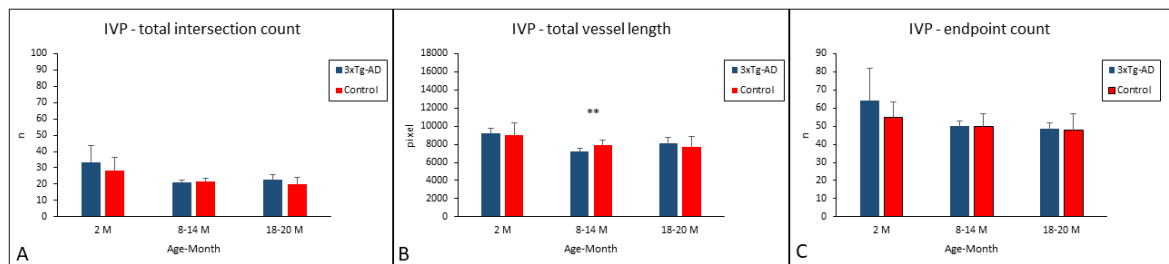
Figure 18. Bar graph representing TI, TL, and EP in IVP layer in young, middle-age, and old transgenic and control eyes. A significant difference is marked by ** (p=0.02).

Deep vascular plexus (Figures 19 and 20)

In the DVP, TI, TL, and EP differed by age in transgenic and control groups. For TI, the relative difference in old relative to young subjects was -48.7% in the transgenics (p=0.004) and -32.7% in the controls (p=0.001). For TL, the relative difference in old relative to young subjects was -24.0% in the transgenics (p=0.001) and -14.1% in the controls (p=0.018). For EP, the relative difference in old relative to young subjects was -26.9% in the transgenics (p=0.023 and -30.5% in the controls (p<0.001).

In young subjects, DVP total number of intersections (79.7±21 in 3xTg-AD and 76.2±3 in control; p=0.759), total vessel length (14628±1600 in 3xTg-AD and 14952±1331 in control; p=0.98), and the total number of endpoints (62.2±13 in 3xTg-AD and 67.0±13 in control, p=0.403) were not statistically different between the 3xTg-AD and control groups.

Similarly, in the middle age group, DVP parameters did not differ by mice genotype (TI: 49.5±7 in 3xTg-AD and 53.6±8 in control, p=0.438; TL: 11438±1133 in 3xTg-AD and 12869±1291 in control, p=0.1; EP: 50.5±6 in 3xTg-AD and 49.3±4 in control, p=0.558).

Regarding the DVP in old subjects, the number of intersections (40.9±1 in 3xTg-AD and 51.6±10 in controls; p=0.037) and total vessel length (11262±571 in 3xTg-AD and 12869±1291 in controls; p=0.016) were significantly lower in 3xTg-AD relative to controls. In contrast, the number of endpoints (46±3 in 3xTg-AD and 47.6±5 in controls; p=0.312) did not differ by mice type.
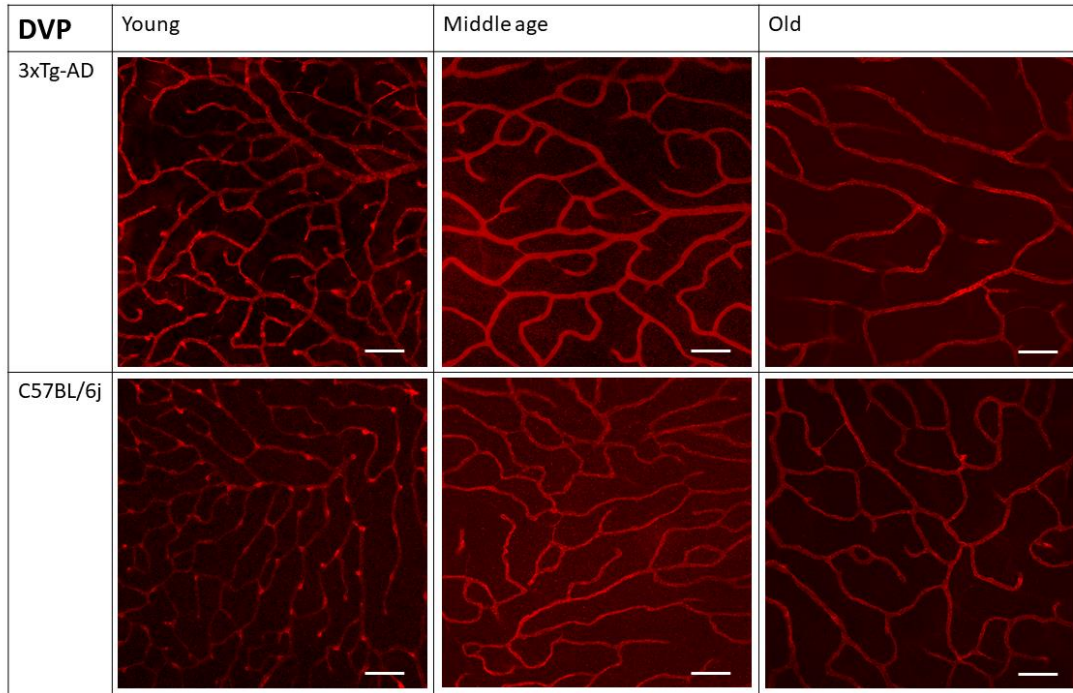
Figure 19. The vascular walls were stained with anti-collagen IV antibody. Tissue clearing was applied, and images were captured by LSM880, Zeiss confocal microscope. Representative images from deep vascular plexus (DVP) in young, middle-age, and old transgenic and control mice (20x, scale bar 100 µm).
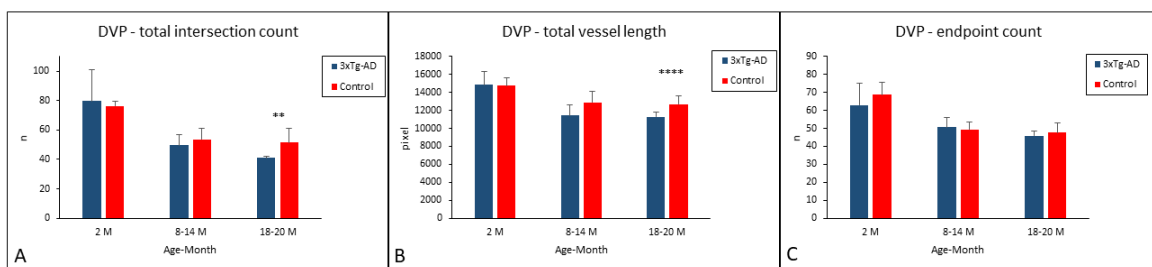
Figure 20. Bar graph representing TI, JD, TVL, and AVL DVP layer in young, middle-age, and old transgenic and 3xTg-AD eyes. Significant differences are marked by ** (p=0.037) and **** (p=0.016).

DISCUSSION

Structural and functional abnormalities of cerebral vessels are common in AD. Indeed, vascular dysfunction has been proposed to contribute heavily to the initiation and propagation of Alzheimer's pathology.[88] Similarly, retinal vascular changes are commonly reported in histopathology studies and OCTA scans from individuals with AD. However, OCTA studies have been inconsistent, showing decreased,[119,120,126,128,217] equal,[130] or even increased[132] retinal vascular densities, highlighting the uncertainty about the extent of retinal vascular changes in AD and their correlation to the disease pathology in the brain. Our study provides robust histopathologic evidence that may help mitigate this uncertainty. We quantified retinal SVP, IVP, and DVP densities in young, middle age, and old AD transgenic and control mice using a novel approach. DVP and, to some extent, IVP densities decreased by natural aging in control animals. However, all three retinal vascular plexuses, SVP, IVP, and DVP, attenuated in transgenic group. We found that SVP and DVP densities were significantly lower in old transgenic mice compared to their age-matched controls. Although IVP density was lower in middle age transgenic animals compared to middle age controls, no difference was noted in IVP density between the old transgenic and control groups. Thus, we propose that SVP and DVP densities are markers of AD-related vascular rarefaction in the retina, as shown by most human OCTA studies.

More than a histopathologic confirmation for OCTA studies, our study reveals the pathophysiologic consequences of AD and senescence in the retina. The underlying mechanistic pathways for the loss of retinal vascular density in AD are complex and not fully understood. However, it is evident that retinal vascular distribution and flow couples with respective retinal layers' metabolic demand in the short and long terms. Kornfield and Newman showed different vascular diameter and flow changes in three retinal vascular layers immediately after a flicker light stimulation.[218] Retinal vascular density changes with long-term alteration of metabolic demand too, as shown by the loss of DVP parallel to the rate of photoreceptor loss in a rodent model of retinitis pigmentosa, a photoreceptor degeneration disease.[221] In the 3xTg-AD mice where inner and middle retina deposition of tau and amyloid and the resulting GCL and INL degeneration are more prominent,[91,188,216] SVP and DVP attenuation in old animals possibly match altered metabolic demand caused by the AD neurodegeneration.[187,220] Besides, retinal vascular attenuation in the AD model

may be influenced by the availability of local trophic factors too. In one study, it was noted that RGC detects metabolic stress and orchestrates SVP remodeling in response to vascular growth factors.[229] Thus, SVP thinning in the AD model may be secondary to a combination of disturbed RGC-mediated vascular growth, decreased metabolic demand due to RGC loss, and amyloid- and tau-mediated vascular damage. Similarly, decreased DVP density in the aged 3xTg-AD is possibly secondary to decreased metabolic demand[70,221] and capillary occlusion due to amyloid and tau deposition in and around deep retinal capillaries[188,230,231] (equivalent to cerebral vascular pathologies seen in AD).[57,140,230,232] It is also possible that DVP, as a network of endcapillaries within the retina's trilaminar vascular system, is more vulnerable to reduced blood flow and vessel drop out than SVP and IVP.

Although aging and cardiovascular diseases usually cause diffuse cerebral vascular pathologies,[233] Alzheimer's-related cerebral vasculopathy are skewed toward areas with a higher amyloid and tau burden, such as the hippocampus.[231,234–237] It appears that a similar pattern is seen in the retina. In the retina, amyloid and tau deposition are concentrated in GCL, inner and outer plexiform layers, and INL,[187,216] perfused by SVP, IVP, and DVP. IVP, which supplies for the metabolic activities in IPL and INL and assumes a transitory network to transfer blood to DVP, is a very reactive layer in response to metabolic demands.[238] Although the estimated blood volume in IVP is significantly less than SVP and DVP, IVP flow increases in response to the light stimulus significantly more than the other layers.[218] IVP's better response to increased metabolic demand may be derived from the stimulus type (for example, flicker light stimulates middle retinal neurons served by IVP),[239] or, it may alternatively show differential autoregulation pathways in retinal vascular plexuses and, possibly, differential pathologic burden around these vessels. IVP attenuation from young to old age occurred in both transgenic and control animals. IVP density was lower in middle age transgenic animals than controls, but it was not different between old transgenic and control groups. This observation may be due to a faster IVP attenuation in AD transgenic retina from young to middle age compared to middle age to old age. It may also show a comparable aging and AD degenerative burden on bipolar and amacrine cells located in INL[75] and higher IVP resilience to AD metabolic insult in older transgenic animals.[218]

Decreased SVP and DVP density in 3xTg-AD animals is likely associated with compromised retinal vascular function caused by amyloid and tau deposition.[91,216] Such altered retinal vascular function (that may include blood-retinal barrier dysfunction, increased vascular leakage, and toxic protein accumulation) possibly contributes to the retinal thickness and volume as quantified by OCT and OCTA. Retinal thickness is determined by the sum of its vascular and neuronal mass. Then, it is conceivable that SVP atrophy contributes to inner retinal thinning detected by OCT in patients with AD.[102] Meanwhile, a simultaneous increase in vascular permeability due to the amyloid/tau vasculopathy counters the thinning effect of degenerative processes, highlighting that a combination of complex trophic and atrophic processes will ultimately determine the retinal sublayer thicknesses.

Aging is the most significant risk factor for AD, possibly because age-related cerebral neuronal and vascular changes predispose individuals to AD neurodegeneration. Similarly, senescence-associated retinal vascular changes may contribute to or exacerbate AD-related pathology in the retina. However, isolating aging- versus AD-related changes in retinal vascular studies is a challenge. Histology studies on human and mouse retina have shown that aging degeneration, unlike Alzheimer's pathology, primarily affects outer retinal layers.[240,241] Thus, a relatively stable SVP, mildly attenuated IVP, and severely attenuated DVP in nontransgenic animals, as observed by us and others,[221] may be explained by natural aging-associated outer retinal degeneration and the resulting decline in outer retinal metabolic demand. However, in contrast to animal studies, OCTA studies on human have found that all three superficial, intermediate, deep capillary plexuses attenuate in the parafoveal retina with natural aging.[70,242] Absence of a macula in rodents and the relative discordance between the histologic and OCTA approaches may explain these seemingly contradictory observations. Nevertheless, vascular attenuation accompanying natural aging should be considered when studying retinal vascular changes in neurodegenerative diseases.

Our study has some limitations. Creating orthogonal projections of retinal vascular plexuses, manual corrections, and quantifications were all standardized but not automated in our research. However, retinal vascular layer segmentation cannot be reliably automated due to SVP and IVP's proximity.[70] Interlayer connecting arterioles penetrate retinal layers

vertical to the imaging plane, so their junctions were not seen and quantified with our method. Besides, some endpoints reflect a vessel when it bends vertically to continue as an interlayer connecting arteriole.[209,210] Thus, the values we quantified are approximations of retinal vascular density that should be interpreted with such methodology limitations. Aβ deposition in the retina is location-dependent, with arguably more deposition in the superior retina.[88] As a result, retinal vascular changes may also vary by geographic area.[88,91] Although we captured images from multiple ROIs distributed 360 degrees around the retina to account for possible regional variations in retinal vascular densities, the whole-retina vascular analysis would be a better approach. Our study has multiple strengths, including the choice of the 3xTg-AD mouse model that expresses both amyloid and tau pathologies and mimics AD pathology more closely to human disease.[37,38] Tau deposition in vascular wall contributes to cerebral vascular changes in AD models,[216] and it is essential to have both Aβ and tau pathologies when modeling retinal vascular changes in AD.[231] Imaging deeper retina with conventional confocal microscopy is possible[209,210] but often compromised due to the optical diffraction from retina's inner nuclear and plexiform layers.[224] We applied a modified tissue optical clearing method to render deeper retinal vasculature visible for better vascular quantification.[220] Finally, semiautomated vascular quantification using AngioTool[222,223] is more reproducible than the manual tracing of the vessels as used before.[221]

 Conclusion. Amyloid and tau deposition have been studied extensively as the underlying pathologic mechanism of neurodegeneration and neuroinflammation in AD. However, the role of vascular dysfunction in AD pathogenesis is increasingly known. Aging is the leading risk factor for AD, and aging-associated vascular changes may contribute to such predisposition. Whether vascular changes are the initiating triggers for toxic protein deposition and neurodegeneration, or a result of decreased demand from neuronal loss, or a combination of each phenomenon is unknown. Cerebral blood flow abnormalities may precede the degeneration of neurons and synapses in the AD brain,[243] and individuals with preclinical AD show decreased retinal vascular density.[122,132,244] However, the extent of age-related versus AD-related retinal vascular pathologies is not clear yet. While our findings need validation in human, we showed for the first time in an animal model of AD that more significant SVP and DVP rarefaction might differentiate

age-related versus AD-related vascular attenuation. Future studies should investigate whether retinal and cerebral vascular changes precede or follow the depositions of Aβ and other AD pathologies.

Chapter 4 Intact Whole Retina Imaging

ABSTRACT:

The interplay between retinal neuronal and vascular structures during development and diseases is best explored by probing the morphologic and molecular targets in an intact whole retina. However, immunofluorescent imaging of intact whole retina imaging is hindered by the opaque coatings of the eyeball, i.e., sclera, choroid, and retinal pigment epithelium (RPE), and the light-scattering properties of retinal cellular layers that prevent the transmission of confocal microscope light through the full retinal thickness. Currently available pigment bleaching and tissue clearing protocols are mostly not suitable for imaging endogenous fluorescent molecules such as green fluorescent protein (GFP) in the intact whole retina. Presented here is an intact whole eye immunofluorescent imaging protocol that combines surgical dissection of the sclera/choroid/RPE layers with a modified tissue clearing and lightsheet fluorescent microscopy (LSFM). Surgical removal of sclera/choroid/RPE offers an unprecedented view to the vascular and neuronal elements of the retina and vitreous in their intact, uncut organization. The clearing method allows microscope light penetration through retinal layers, and LSFM provides a robust tool for three-dimensional visualization of neuronal and vascular pathways involved in physiologic and pathologic states.[a]

---

[a] Reused with permission from: Hossein Nazari, Maxim Ivannikov, Lorenzo Ochoa, Gracie Vargas, Massoud Motamedi. Microsurgical Dissection and Tissue Clearing for High Resolution Intact Whole Retina and Vitreous Imaging. *J Vis Exp*. 2021:e61595. doi:10.3791/61595

INTRODUCTION:

The interaction between retinal neuronal and vascular elements is important for retina biology in health and disease states. [245,246] Conventional histology studies of retinal vasculature and neurons are currently performed with physical sectioning of paraffin- or cryo-fixed retinas or retina flat preparations. However, tissue sectioning disrupts retina neuronal and vascular continuity, and although three-dimensional reconstruction of the adjacent retina sections is suggested as a possible solution, it is subject to errors and artifacts. Retina flat-mount preparations, too, markedly disturb the integrity of retinal vascular and neuronal elements and the geographic connection between adjacent retinal areas.[247] Alternatively, the intact whole retina has been recently used to visualize retinal neuronal and vascular elements in their natural anatomic position where they extend their projections in all three dimensions.[247–250]

In intact whole retina imaging, fluorescent signals from the vascular and neuronal elements of adjacent retina areas (tiles) of an intact whole retina are captured using a Lightsheet microscope and then these tiles are "stitched" together to reconstruct a three-dimensional view of the entire whole retina.[247–250] Intact whole retina imaging provides an unprecedented view to the retina to study the pathogenesis of retinal vascular, degenerative, and inflammatory diseases.[247–250] For example, Prahst et al. showed a previously "un-appreciated" knotted morphology to pathological vascular tufts, abnormal cell motility, and altered filopodia dynamics and oxygen-induced retinopathy (OIR) model using live imaging of a whole intact retina. [247] Similarly, Henning et al. and Chang et al. showed the complex three-dimensional retinal vascular network in an intact whole eye.[248,249] Vigouroux et al. used an intact whole eye imaging method to show the organization of the retina and visual projections in the perinatal period.[250] To create such an unprecedented 3D views of the retina, intact whole retina imaging protocols have overcome two major limitations: 1) opaque and pigmented coatings of the eyeball (sclera, choroid, and RPE) and 2) limited penetration of the microscope light into full retina thickness due to the light scattering properties of retinal nuclear and plexiform layers. Henning et al. and Vigouroux et al. applied H2O2 bleaching of choroid/RPE pigments to be able to image an intact retina.[248,250] However, bleaching is not suitable for animal strains with endogenous fluorophores such as green fluorescent protein (GFP) or after in-vivo immunofluorescent

staining.[248,250,251] In addition, Henning et al.'s method of H2O2 treatment was carried out in aqueous conditions, which may generate microbubbles that result in retinal detachment. In addition, the H2O2 treatment was performed at 55°C, further deteriorating tissue antibody affinity. In addition, bleaching may damage the retina, eliminate endogenous and in-vivo stained fluorophores, and introduce heavy autofluorescence originating from oxidized melanin.[252] Other depigmentation protocols for eye sections using potassium permanganate and oxalic acid were able to remove RPE pigments in embryonic sections, but this depigmentation method also has been shown to reduce the efficacy of immunolabelling.[253,254] Prahst et al. and Chang et al. removed sclera and choroid and cornea to render a whole retina reachable to microscope light.[247,249] However, removing cornea, lens, and peripheral retina may distort peripheral retinal and hyaloid and peripheral retinal vessels and disrupt vitreous and hyaloid vessels that make these methods unsuitable for studying hyaloid vasculature.

Intact whole eye imaging protocols include tissue optical clearing to overcome the light scattering properties of retinal layers. Tissue optical clearing renders the retina transparent to microscope light by equalizing the refractive index of a given tissue, here retina, across all its cellular and intercellular elements to minimize light scattering and absorption.[255] Choroid and RPE should be removed or bleached before tissue optical clearing is applied to the retina as the pigmented coatings of the eyeball (choroid and RPE) are not efficiently cleared.[224,256–262]

The development of vitreous and hyaloid vascular system in diseases such as retinopathy of prematurity (ROP), persistent fetal vasculature (PFV), Norrie Disease, and Stickler Disease is best studied when retina and hyaloid vessels are not disrupted in tissue preparation.[263–267] The existing methods for intact whole retina imaging either remove the anterior segment of the eye, which naturally disrupts the vitreous and its vasculature, or apply bleaching that may remove endogenous fluorophores. There is a lack of published methods to visualize vitreous body and vasculature in their intact, untouched condition. We describe here a whole retina and vitreous imaging method that consists of the dissection of pigmented and opaque coatings of the eyeball, a modified tissue optical clearing optimized for retina, and lightsheet fluorescent microscopy. Sample preparation, tissue optical clearing, lightsheet microscopy, and image processing steps are detailed below.

a)   **Protocol:**

All experiments were approved by the University of Texas Medical Branch Institutional Animal Care and Use Committee (IACUC). Animal use and care were in accordance with the ARVO statement for the use of the animals in ophthalmic and vision research.

All the materials that are needed to carry out this procedure are listed in the Table of Materials. Wear powder-free gloves during all the steps. For steps 6 and 7 of the protocol, also refer to the official microscope operating manual.

1. **Preparation of the animals**

    1.1.   Euthanize the experimental mouse (age and sex preference based on the purpose of study) with the appropriate use of anesthetic medication based on applicable Institutional Animal Care and Use Committee approved protocol (a combination of Ketamine 60 mg/kg and Dexmedetomidine 0.5 mg/kg was used here). Immediately proceed to stabilize the animal on a platform for dissection and heart perfusion.

    1.2.   Dissect the abdomen and thorax to expose the heart. Cardiac perfusion will be performed by transfusing the heart via a 27-gauge needle placed in the left ventricle and creating a small (~1mm) incision in the right atrium to allow egress of blood.[268] First, transfuse 30-50 ml of ice-cold phosphate balanced saline solution (PBS) and then 30-50 ml of freshly prepared 4% paraformaldehyde (PFA). A successful PFA transfusion will be noted by observing muscle twitches throughout the body and tail. Proceed to the enucleation step.

2. **Eyeball enucleation and fixation**

    2.1.   Use a curved jeweler's forceps to gently push over the upper or lower eyelid to force the eyeball out of its socket. Use another set of forceps to puncture the conjunctiva from the side and hold the globe from the optic nerve side. Slowly lift the globe from its socket until it is severed from the optic nerve.

    2.2.   Transfer the globe to a tube containing freshly prepared ice-cold 4% PFA. Label the tube accordingly. Allow the globe to stay in 4% PFA in a 4° fridge for 12 hours (overnight).

3. **Dissection of the sample (Figure 21 and 22)**

    3.1.   Under a stereomicroscope, locate the cornea-sclera junction (Figure 21-a)

and, using the sharp cutting tip of a 30-gauge needle, make a very superficial cut at the sclera about 0.5- 1 mm behind the cornea-sclera junction (Figure 21-b). Advance one of the blades of a sharp tip dissecting scissors through the incision that is just made into the potential space between the sclera/choroid/RPE and retina (Figure 21-c). Advance the scissors and cut circumferentially until the sclera/choroid/RPE can be peeled off the outer surface of the retina (Figure 21-d and 21-e). Radial relaxing cuts can be made on the sclera/choroid/RPE to facilitate the process of circumferential cutting and subsequent peeling of the optic nerve and sclera/choroid/RPE. Small patches of RPE (Figure 21-f) can be removed using a wet size 1 painting brush. Transfer the whole intact eyeball to a tube containing PBS. Proceed immediately or preserve in 4°C for next day immunolabeling.

NOTE: It is important to perform this step slow and gently. The dissector should be constantly careful to avoid puncturing the retina. The first few cuts are more critical to avoid cutting through the retina.

NOTE: Marks may be placed on the eyeball after enucleation and then after dissection to preserve the orientation of the eye if needed.

NOTE: The protocol may be paused here, and the samples may be preserved overnight in a 4°C fridge before proceeding to the next steps.

4. **Vascular staining**

4.1.   Permeabilize the tissue by immersing it in PBS containing 0.2% Tween-20 at room temperature for 20 minutes.

4.2.   Wash the sample with PBS 3 times on a shaker for 10 minutes.

4.3.   Incubate the sample with 5% normal goat serum (NGS) in PBS containing 0.25% Triton X-100 at room temperature for 1 hour.

4.4.   Incubate with the primary antibody at 4°C overnight. Here, an anti-mouse Collagen IV antibody was used (1:200 prepared in PBS containing 0.2% Tween-20).

4.5.   Wash with PBS 3 times, each for 5 minutes.

4.6.   Incubate the sample with fluorescent-labeled secondary antibodies. Here, an anti-rabbit Alexa Fluor 568 was used for 12 hours at 4 degrees (1:200 dilution in PBS containing 0.2% Tween-20).

4.7.   Wash with PBS 3 times, each for 1 hour, and proceed with tissue clearing steps.

5. **Optical Clearing with 2,2′-thiodiethanol (TDE)**

   5.1.   Prepare working TDE concentrations by stock TDE solution with PBS for a final concentration of 10%, 20%, 30%, 40%, 50%, and 60% volume to volume (v/v). Prepare at least 2 ml of solution for each eye sample to allow enough excess volume to penetrate the tissue.

   5.2.   Incubate the samples in a 6- or 12-well plate well at an increasing concentration of TDE. Start with immersing the intact whole eyeballs in 10% TDE solution for 2-4 hours on a shaker at room temperature. Successively, transfer the sample to a higher TDE concentration each for 2-4 hours.

   NOTE: Retina starts to clear at 40%-50% concentration, but maximum clearing occurs after incubation in 60% solution. Retina becomes less transparent at 70% and higher concentrations.

   NOTE: The clearing process may be stopped overnight at any of the successive clearing exchange steps.

   Whole eye imaging using a lightsheet microscopy

   5.3.   Mount the samples based on your lightsheet microscope platform. Cleared eye preparations can be imaged using a variety of commercial or custom-built confocal and lightsheet microscopes. In this protocol, a dual-side illumination lightsheet microscope has been used. Follow your microscope and acquisition software instructions to properly mount the sample and set up acquisition parameters, including Lightsheet alignment and illumination and detection optical paths.

   5.4.   Immerse the sample within the Lightsheet microscope chamber in 60% TDE solution (the final clearing concentration).

   Note: Use the final TDE concentration (60%) in the microscope chamber. Use a plastic transfer pipette to transfer the globe. The pipette tip should be cut, and the opening may be widened with a second pipette to avoid damage to the sample with sharp edges.

   Note: Separation of illumination and detection optical paths in lightsheet microscopy improves both the imaging speed and the signal-to-noise ratio compared to point-scanning confocal microscopy and, thus, is the preferred method for imaging large samples.

NOTE: Use low resolution and magnification imaging (5x, NA 0.16) to image cellular morphology and cellular process tracing, especially when combined with tiling. Use high resolution and magnification imaging (20x, NA 1.0) to image both cellular morphology and large sub-cellular organelles such as nuclei and mitochondrial clusters.

NOTE: In most cases, image intensities can be well represented by 8-bit digitization (256 shades), which will save disk space and image processing time for large imaging volumes.

NOTE: Whole eye samples can be glued to a hypodermic needle tip or to a custom-built platform depending on the type of lightsheet microscope (as was done here), or coverslip-bottom dishes filled with the clearing solution and agarose support blocks for imaging in an inverted confocal microscope.

NOTE: Be extra gentle while placing the needle mounted sample into the microscope chamber as touching the walls may cause dislodge the sample from the needle tip.

6. **Post-acquisition image processing**

6.1.   Post-acquisition processing depends on the type of file and software compatible with imaged files.

NOTE: Apply deblurring or deconvolution to further augment the raw images before proceeding with stitching the imaged tiles. Weiner filter can be applied to deblur the images. Alternatively, images can be iteratively deconvolved after denoising with the Richardson-Lucy deconvolution and a theoretical or experimentally measured PSF using modeling tools such as the ImageJ PSF generator plugin.[269]

NOTE: Stitching of pre-processed z-stacks and affine and non-rigid volume transformations followed by multi-view volume registration and fusion can be performed using a variety of commercial or public-domain software packages (ImageJ – BigStitcher plugin).[270]

REPRESENTATIVE RESULTS:

A zero-angle projection of the peripapillary vascular network and microglia is shown in Figure 23A. Also, intact whole retina microglia distribution in a CX3CR1-GFP mouse is presented in Figure 23B. A major advantage of the method presented here is its

ability to image innate fluorophores. Figure 23C, D show microglia in representative Z projections (green channel) from samples prepared with the current method of intact whole eye imaging (Figure 23C) and flat-mount preparations (Figure 23D). Microglia were quantified and compared in randomly selected regions of interest from the intact whole retina and flat-mount preparations. No statistically significant difference was noted between the flat-mount and intact whole retina imaging in terms of microglia numbers (Figure 23E). All representative images in Figure 23 were captured from the CX3CR1^{-GFP} mouse retina.

GFP-tagged microglia (green channel) and the vascular network (red channel) in a CX3CR1-GFP mouse retina that was imaged using the current intact whole retina imaging protocol is further described in Supplemental Video 1. Endogenous and in vivo staining fluorophores would have been bleached if the pigment bleaching methods used by Henning et al.[248] and Vigouroux et al.[250] were used to remove choroid and RPE pigmentation. Supplemental Video 2 shows a view of the hyaloid vessels and retrolental vascular plexus in their natural state. It should also be noted that removing the anterior segment of the eye as described by Prahst et al.[247] and Chang et al.[249] would have disturbed the hyaloid vessels.
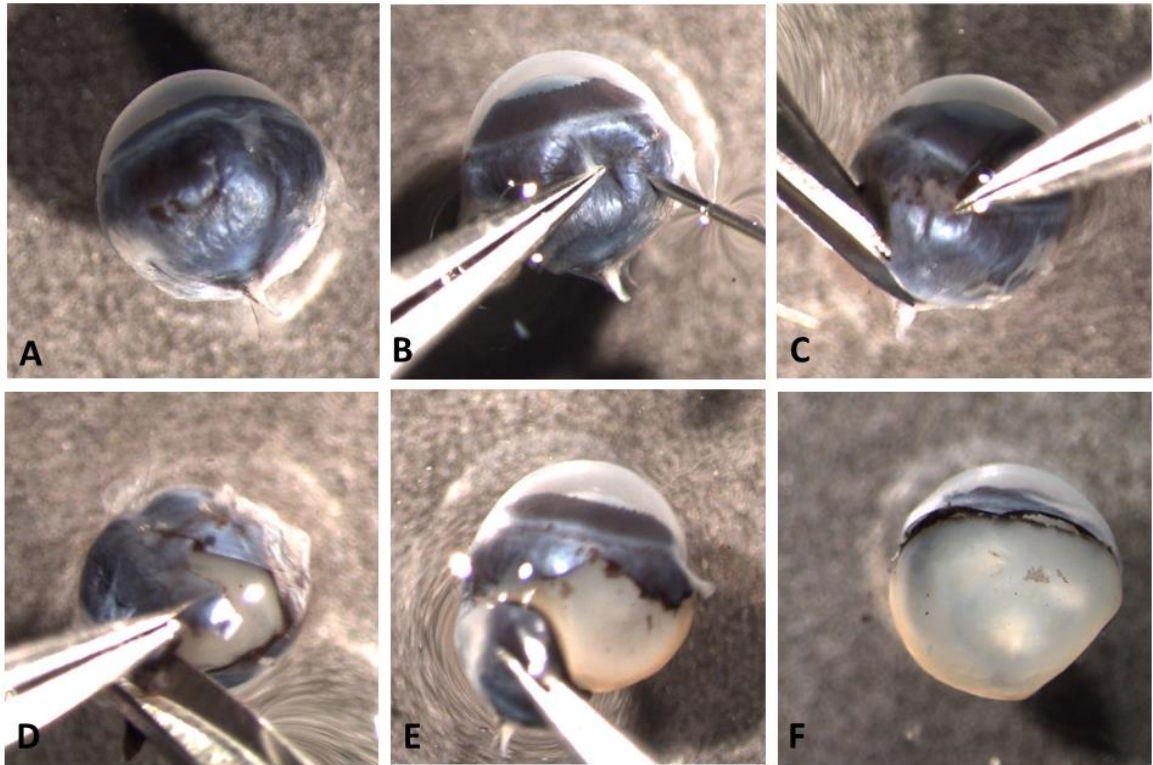
Figure 21. Dissecting out sclera/choroid/retinal pigment epithelium. Removal of outer opaque and pigmented layers allows optical imaging of retina and vitreous cavity without interference from these pigmentations.
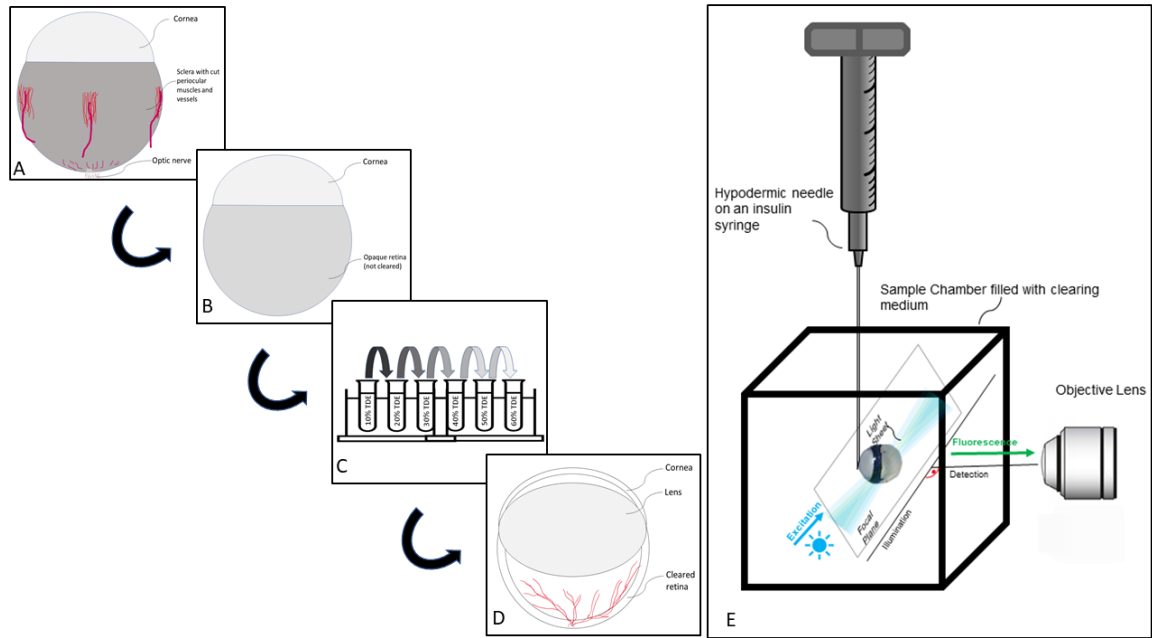
Figure 22. Cartoon depicting the steps to dissect sclera/choroid/retinal pigment epithelium and mounting the intact eyeball to the lightsheet microscopy platform.
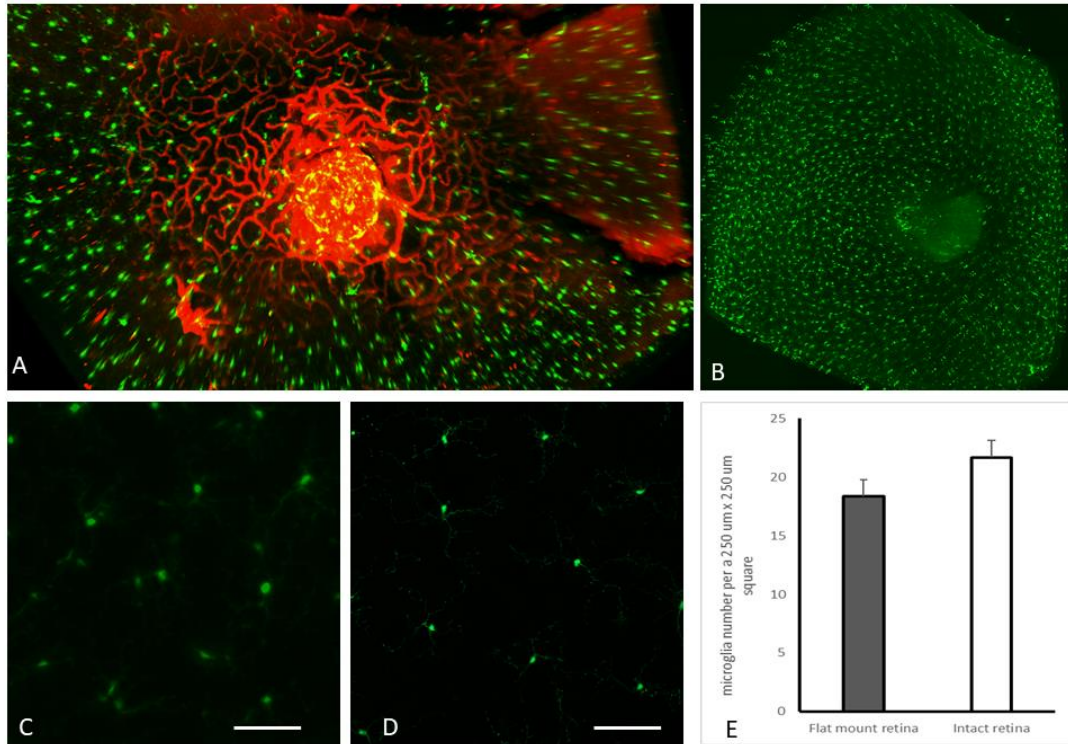
Figure 23. Representative results for intact whole retina imaging. (A) Zero angle projection of the peripapillary vascular network and microglia in an 8-month-old female CX3CR1^{-GFP} mouse intact whole retina. (B) Flat projection of the green channel showing microglia distribution in an intact whole retina from an 8-month-old female CX3CR1^{-GFP} mouse. Peripheral retina was distorted in this flat projection of the cup shaped intact retina. (C-D). Representative 250 μm x 250 μm square flat projection from an intact whole retina scans (C) and flat-mount preparation (D), both from 8-months old female CX3CR1^{-GFP} mice (scale bar 50 μm). (E) Retinal microglia enumeration in flat-mount preparations versus intact whole retina imaging using Lightsheet fluorescent microscope: Three regions of interest (ROI) were randomly selected from the mid-peripheral retina for microglia quantification. Orthogonal projections of the entire retina thickness in green channel were prepared for each ROI. Microglia numbers were counted within ImageJ. A two tailed Student's t-test did not show statistically significant difference in the number of microglia in flat-mount and intact whole eye preparations.

Supplemental video 1:

Intact whole eye imaging of a CX3CR^{-GFR} mouse. Retinal vessels are visualized in their entirety. Imaging was performed without a need for choroid/RPE pigment bleaching. In this GFP-tagged mouse (and similar strains with innate fluorophores), choroid/RPE bleaching would have removed the GFP-tagged microglia signals. In this video, the three-dimensional depiction of retinal microglia distribution shows the strength of this method in detecting microglia distribution and activation. Microglia morphology may be better visualized in higher resolution still images using this technique.

Supplemental video 2:

Hyaloid vasculature and retrolental vascular plexus in a 4-day old mouse. Anterior segment of the eyeball including cornea, iris, and lens are not removed so the vitreous cavity and its vasculature are not disturbed.

DISCUSSION:

Retina and vitreous development and pathologies are best studied with intact whole retina imaging techniques where retina is not cut for sections or for flat-mount preparations. Existing intact whole eye imaging methods either use pigment bleaching that removes innate fluorophores or remove the opaque coatings of the eyeball (RPE, choroid, and sclera) along with cornea and lens that may disturb peripheral retina and vitreous body. Chang et al. and Prahst et al. removed the outer coatings of the eyeball but also removed cornea that possibly disrupts vitreous and hyaloid vasculature and peripheral retina.[247,249] Alternatively, Henning et al. and Vigouroux et al. used pigment bleaching to render choroid and RPE transparent to microscope light.[248,250]

Pigment bleaching protocols remove GFP and other innate/endogenous fluorophores as well as the fluorophores used for *in-vivo* staining.[251] One of the advantages of the current method is that no bleaching is used. Instead, we dissected out sclera/choroid/RPE but left the cornea, iris, and lens untouched. By not removing the anterior segment of the eye, peripheral retina and hyaloid vessels can be visualized in their undisturbed state. The majority of the existing methods described for studying hyaloid vessels in diseases such as PFV and ROP involve dissecting anterior segment of the eye that disturbs the vitreous body and inevitably hyaloid vasculature.[266,267]

All the current methods for intact whole eye imaging, including ours, use tissue optical clearing, a method used to match a tissue's refractive index to the surrounding medium to minimize light scattering and absorption.[255,271] Three major tissue clearing approaches include hydrophobic, hydrophilic and hydrogel-based methods. [257,271–273] Tissue clearing in the current intact whole eye imaging methods is time consuming, taking 3 to 7 days.[249,250] Our protocol uses 2,2′-thiodiethanol (TDE) as a glycol derivative hydrophilic clearing agent and the process of clearing can be completed in less than two days without quenching the fluorescent proteins.[274] TDE is miscible with water in any ratio that makes it possible to create a gradient of concentration to allow penetration of this high refractive index solution into the tissue. The intact whole retina was immersed in an increasing concentration of TDE to achieve a refractive index gradient that gradually equalized the tissue's refractive index and rendered it clear. TDE does not quench the fluorescence of various fluorophores unlike some other clearing methods such as CLARITY and CUBIC.[275] In addition, TDE does not have the potential to damage equipment, as is the case for organic solvent based clearing agents such as benzyl benzoate/benzyl alcohol (BABB). It also prevents the growth of contaminating organisms that can be seen in fructose based SeeDB clearing method.[275]

Lightsheet Fluorescent Microscopy (LSFM) offers a high temporal and spatial resolution by viewing the sample from different angels (isotropic resolution-multiview imaging mode).[276] LSFM operates based on a thin sheet of light that is directed through the sample to excite fluorophores only in a thin imaging plane that in turn allows lower phototoxicity and photobleaching, faster imaging, and higher contrast due to the minimal out of focus excitation. Imaging of the dissected and optically cleared whole murine eyes could be performed using one of the many commercially available LSFM or confocal microscopes. In the current method, LSFM allowed a fast and detailed view to retinal neurons and vessels and allowed quantitative analysis of vascular thickness, vascular arborization, and vessel tortuosity indices.

The current method is applicable -with modifications- to intact whole eye samples from other rodent and non-rodent eyes. Two critical steps for the success of the current methods is good surgical dissection of the ocular coatings and tissue optical clearing. Dissecting sclera/choroid/RPE layers in a small rodent eye maybe technically difficult and

one should be careful not to cut through peripheral retina when dissecting sclera/choroid/RPE. However, this technique requires the same set of skills used for retina flat-mount preparation and, in our experience, essential dexterity can be acquired after performing the dissection steps on three to five eyes.

In summary, the method described here combines pieces of the previously described techniques is optimized for imaging molecular and structural targets including those of innate and in-vivo staining fluorophores in an intact whole retina and vitreous. This method addresses some of the limitations of the existing whole retina preparation methods and is unique in providing an unprecedented view to hyaloid vasculature (supplemental video 2).

Acknowledgments:

Chapter 5 Discussion and Future Direction

ABSTRACT:

Our studies provided insight into differentiating age- and AD-related retinal neuronal and vascular changes in a well-established mouse model of AD and were compatible with the findings from the majority of current OCT and OCTA studies in terms of retinal sublayer thickness and retinal vascular density changes in AD. Besides, the whole-retinal imaging method we introduced a novel method to study the regional variability of the retinal vascular and cellular components. The retinal structure and function have many common pathways to change in response to the wide varieties of neurodegenerative and neuroinflammatory diseases. As a result, there is an overlap between the retinal neuronal and vascular changes caused by natural senescence and pathologic neurodegeneration. Considerable evidence indicates that no single image-based biomarker would differentiate AD from aging and other neurodegenerations. Thus, it is imperative to combine multiple biomarkers to detect preclinical and clinical AD progression and differentiate it from retinal changes caused by normal aging. Using a well-established mouse model of AD, we recognized a combination of retinal structural and functional biomarkers that may help differentiate age-dependent changes in multi-layered components of the retinal neurovascular unit in AD. Such changes were detected noninvasively in middle age and old 3xTg-AD animals, a preclinical model simulating clinical stages of AD in human. Based on the observations summarized in this chapter, we confirmed that the retina goes through a complex structural and functional AD-induced changes in middle age and old AD; thus a multimodal approach to interrogate various neuronal and vascular components of the retina is required to identify alterations in various retinal neurovascular components as a method for reliable noninvasive AD diagnosis, monitoring and differentiating it from other conditions leading to retina neurodegeneration.

Utilizing noninvasive retinal imaging for Alzheimer's disease diagnosis and monitoring has received increasing attention because of a growing body of studies that indicate a relationship between retinal structure and function and AD progression. The retina is part of the CNS and is directly connected to the brain via neuronal axons. Retinal neurons, neuronal connections, and vascular supply are organized in layers, much like the brain cortex. From developmental biology, physiology, and pathology standpoints, the retina and brain share many similarities. Considering these similarities and the eye's transparent media, retinal imaging and functional studies could illustrate the CNS's normal physiology and pathologies. Indeed, many retinal abnormalities (i.e., structural and functional alterations) can be detectable and visualized with noninvasive high resolution imaging modalities such as OCT and OCTA in individuals with stroke, multiple sclerosis, Parkinson's disease, and Alzheimer's disease. However, the ability of these imaging modalities for early diagnosis of neurological diseases and establishing a longitudinal correlation with their progression has not been yet fully demonstrated in pre-clinical and clinical studies. Besides, concurrent cardiovascular risk factors, systemic disease, and aging neurodegeneration overlap with the retinal imaging findings that have been reported as potential markers for CNS diseases. In the field of Alzheimer's disease, a continuous effort is focused on establishing a set of AD-specific retinal structural or microvascular patterns that reflect AD pathology in at-risk and diseased individuals and distinguish AD from non-AD neurodegeneration.

In the current project, novel animal studies were conducted to further explore the potential for applications of noninvasive retinal imaging for detection of retinal neuronal and vascular degeneration in a mouse model of AD. Our goal was to untangle the interaction between the retina's neuronal, vascular, and glial elements in AD and identify a set of neuronal and vascular imaging biomarkers for AD neurodegeneration. We used the 3xTg-AD model that expresses both amyloid and tau pathologies and mimics many pathologic features of the disease. First, we showed that the RGC population declined from young to middle age in the mouse retina. Such reduction was more pronounced in 3xTg-AD mice compared to age-matched nontransgenic controls. Loss of RGC population was parallel to increased deposition of Aβ in the retina and brain. Most importantly, retinal

sublayer analysis by OCT showed a significant decrease in RNFL thickness in the 3xTg-AD model. GC-IPL thickness remained stable from young to middle age in transgenic animals, while GC-IPL thickness decreased in control animals. We hypothesized that a compensatory retinal thickening due to neuroinflammation and neurovascular changes was the likely cause for relatively stable GC-IPL thickness in the transgenic model. These compensatory changes neutralized RGC loss due to AD pathology. We further confirmed RNFL thickness as a potential biomarker for detecting AD and monitoring its progression, as reported by a host of histopathology and OCT studies. We concluded that a set of changes in retinal sublayers might be a better biomarker to identify the preclinical stage of AD and differentiate AD neurodegeneration from normal aging or even other non-AD neurodegenerations.

Furthermore, studies were designed and conducted in the 3xTg-AD model to assess age-dependence of AD-induced changes in retinal vascular distribution and density. While it is well-recognized that the cerebral vascular changes are a hallmark of AD and its progression but a noninvasive, sensitive, cost effective and convenient imaging modality to quantify and follow such changes in the brain is not available yet. Changes in retinal vasculature, which can now be imaged noninvasively with OCTA and DVA, has been found to correlate with AD's neuronal and vascular pathologies in the brain. Nevertheless, such correlations have been controversial at times, and the sequence of retinal vascular changes and amyloid and tau pathologies in the retina and brain is not fully known. The uncertainty about such vascular changes originates partly from the lack of previous histologic studies on retinal vascular distribution in mouse models of AD. We analyzed the trilaminar retinal vascular network in young, middle age, and old 3xTg-AD and control mice to explore these questions. Each of the three retinal vascular plexuses had its distinct distribution and branching pattern (Chapter 3, Figure 2). Consistent with the observations made by Duggan et al.,[208] and as shown in chapter 3, figures 3, mouse SVP consisted of large arteries and veins that branched out to form arterioles and possibly capillaries. SVP sent anastomosing penetrating branches that extended through the GCL into the IPL and formed IVP that, in turn, extended connecting branches deeper through the INL into OPL to form DVP (supplementary video). IVP consistently appeared less dense with more isolated looping branches and formed fewer junctions than DVP (Chapter 3, figures 5 and

7).[65,208] DVP was a heavily branching network of capillaries with frequent loops and closed circles. In the AD brain, too, cerebral capillaries may appear convoluted, looped, or tortuous.[231,234–236,277] Although we noted "string vessels" indicative of vascular degenerations, not many abnormally looped, tortuous, crooked, or kinked vessels were noted in retinal vascular layers despite their attenuation in old age transgenic eyes. Similarly, multiple OCTA analyses in patients with AD have not reported morphologic changes other than decreased retinal vessel density.[119,121,124,126,128,130,132,136,278] This may suggests that retinal vascular structure is not identical to cerebral vasculature. Nevertheless, the vascular density pattern seen in our studies was analogous to the changes reported in deep CNS vessels during AD. We observed that age-related and AD-related rarefaction of retinal capillaries occurred differentially in these layers. In the transgenic model, all three vascular layers' density was significantly lower in old compared to young mice. However, in controls, only IVP and DVP density were significantly lower in old compared to young animals. The old transgenic animals had significantly lower SVP and DVP densities compared to their age-matched controls. This observation was compatible with most OCTA studies that showed significantly lower SVP and DVP densities in individuals with AD than age-matched controls. Besides, our findings were explainable with the known pathologic changes in the AD brain and its metabolic consequences. From a practical standpoint, we confirmed that retinal vascular density parameters could be quantified, and such quantification may identify AD-related changes in the retina. Our finding also suggested that a better understanding of longitudinal vascular changes in AD models and correlating them with cerebral pathologies and the crosstalk between the retina's vascular, neuronal, and glial elements may reveal additional therapeutic targets for AD.

There is strong evidence showing a geographic variation of retinal vascular densities in different retinal quadrants. Although previous studies have shown such differences using human histopathology and OCTA approaches, animal studies to model such differences are fallible because current retinal tissue preparation methods for histopathologic studies involve cutting through various retinal areas for flat-mount preparation or sections. To address this issue, we modified the existing methods for intact whole retina imaging by micro dissecting the sclera, choroid, and RPE, applying tissue optical clearing, and using lightsheet microscopy. After applying our tissue preparation

method, studying retinal vascular density and branching pattern and retinal microglia distribution and activation in the intact, uncut retina would give a better overview of the geographic variation of retinal neurovascular changes in AD and other degenerative and developmental diseases. An additional advantage of our novel method includes its potential for hyaloid vessel imaging in the developing eyes. We immunostained P1 mouse eyeballs using this novel method and showed, for the first time, hyaloid vessels in their intact undisturbed status. Thus, this method may help study retinal and vitreous cavity development and pathologies in diseases like retinopathy of prematurity. An interesting next plan would be to apply this method to the AD model retina and explore geographic variations in retinal vascular and glial densities in aging and disease states.

In summary, we identified various alterations in different components of the retinal neurovascular unit in an AD mouse model. Such alterations are detectable noninvasively in preclinical and clinical stages of AD and correlate with AD's reported pathologic burden. Based on the observations summarized above, we confirm that the retina is a complex structure involved in AD and possibly other neurodegenerations. A holistic approach that identifies alterations in various retinal neurovascular components may pave the road for more reliable noninvasive AD diagnosis and monitoring and a better understanding of AD's pathobiology.[212] The results of these studies highlight an urgent need for improving the precision and accuracy of currently available OCT-based diagnostic tests.

CONTRIBUTIONS TO THE CURRENT BODY OF KNOWLEDGE ON NEUROVASCULAR COUPLING IN THE RETINA DURING AD PROGRESSION.

The cerebral neurovascular unit in AD can be studied in four distinct but integrated levels: 1) Neuronal activity and life cycle. 2) synaptic communication at glial-vascular, glial-glia, glial-neurons, neuron-neurons levels. 3) Vascular structure and remodeling. 4) Neuroinflammation in the form of altered microglia and astrocyte function and morphology. In our studies, immunofluorescent approach was used to characterize these stages as function of age in retina of the 3xTg-AD model.

The human central nervous system consumes about one-fourth of the body's glucose and one-fifth of oxygen, far exceeding the body's average glucose and oxygen

consumption per unit of weight. Such remarkable glucose and oxygen demand require a vigorous blood supply. The brain's complex vascular system has evolved to a complex mechanism of communication between neurons, glia, and cerebral vasculature that spatially and temporally adjusts blood supply for neurons' constantly changing metabolic demands. Cerebral vessels may react to such changes in metabolic demand acutely by changing the diameter and adjusting the flow acutely. Or as a long-term change mainly in the form of changing vascular density. In AD, cerebral vascular changes were initially thought to be age-related alterations that concurrently accompany AD. However, vascular pathologies appeared early and persisted and worsened with AD, suggesting that cerebrovascular alterations and AD pathology are more directly linked. Advanced imaging techniques such as Transcranial Doppler (TCD- accuracy limited to the second and third distributary branches of major cerebral arteries), functional magnetic resonance imaging (fMRI), positron emission tomography (PET), Single Photon Emission Computer Tomography (SPECT), and near-infrared spectroscopy (that indirectly quantifies the oxygenated and deoxygenated hemoglobin levels based on the relative transparency of the tissue to near-infrared rays) are powerful tools to measure and trace regional alterations of brain metabolism and perfusion in the research setting as well as in various neurological conditions. Although these imaging studies' practical application is limited due to their expense, invasiveness, or convenience, they have been promising as tools for early diagnosis of neurodegenerative diseases. Nevertheless, better tools to track retinal vascular function in AD and other neurodegenerations are needed. Besides, AD brain histopathology studies have frequently landed on controversies, primarily due to variable methodologies and the challenge of conducting long-term longitudinal studies on at-risk individuals. For example, despite multiple animal and human studies reporting decreased vascular density in the hippocampus and increased vascular density and flow in the brain cortex,[279] Bourassa et al. did not observe a significant reduction in the total brain cortex's total amount capillaries in subjects with AD compared to non-AD controls.[205]

Recognizing that Cerebral and retinal neurovasculature have similarities in embryological origin, anatomical features, and physiological properties, there has been a growing interest in studying changes in retinal neurons and vessels to gain new insights into the pathophysiology of NVU accompanying AD progression with the goal of using

these changes as a biomarker to track disease progression and response to treatment. Although there is no long-term longitudinal study on retinal OCT features in normal at-risk individuals who may develop MCI and AD in the future, OCT studies on mouse models of AD have confirmed a preferential involvement of inner retinal layers during the early stages equivalent to preclinical AD.[57,170,171,181,182] However, instrumentation and segmentation differences have caused inconsistent reporting about the specific changes involving distinct retinal sublayers. In the 3xTg-AD model, we observed both RGC loss and RNFL thinning associated with a small, statistically insignificant increase in RGC thickness from young to middle age. This pattern of changes may be due to RGC loss that causes RNFL thinning, and a simultaneous AD-related neuroinflammation that neutralizes the thinning effect of AD neurodegeneration.[42] RNFL is a mostly acellular layer that, unlike cellular GCL-IPL, may not be influenced by the trophic processes such as microglia activation,[77] neuronal swelling,[183] and Müller cell hypertrophy.[42,184] In the meantime, vascular loss in the SVP layer (as we saw in our vascular study) would also contribute to RNFL thinning in the AD model. OCT studies in human patients suggest that neuronal loss may eventually overwhelm the trophic inflammatory processes in advanced AD stages and manifest as a decline in both inner retina and total retinal thickness.[102]

We observed early Aβ deposition in the retina compared to the hippocampus and brain cortex compatible with the previous observations[39,40,190,216] that suggested the retina, because of its unique biologic properties, is vulnerable to AD neurovascular degeneration earlier than the brain. However, the underlying cause of retinal predilection for Aβ and tau deposition remains obscured. An increased predisposition of specific neurons, e.g., GABAergic neurons of the dentate gyrus, to Aβ toxicity has been shown before and may partly explain prominent Aβ and tau pathologies in these regions of the brain.[280] However, increased vulnerability of retinal neurons to Aβ and tau deposition as seen in the current and similar studies [39,40,216] is less known. Retina shares cellular and functional elements with the brain; however, they have distinct developmental and structural differences that may explain the retina's increased susceptibility to Aβ and tau deposition. Glymphatic system has been recently known as an essential component of the brain's potentially neurotoxic waste product clearance system. Glymphatics are brain-wide paravascular spaces surrounding cerebral blood vessels along which cerebrospinal fluid (CSF)

recirculates through the brain parenchyma, facilitating the removal of toxic solutes such as Aβ.[281] Animal studies have shown evidence of an "ocular glymphatic system" in the optic nerve and retina.[281,282] A failure of the retina glymphatic system may explain earlier and more extensive development of Aβ depositions in our model.[283,284] Whether such differences in retinal and brain vascular development make the retina more vulnerable for AD-related pathologies needs to be further explored.

Human studies show that retinal vascular density and flow are lower in AD patients than those with MCI, who, in turn, have a lower retinal vascular density and flow compared to normal controls.[130] It is unclear whether retinal capillary attenuation is a consequence of Aβ and tau deposition, the result of decreased neuronal metabolic demand in a degenerating retina that has lost neurons secondary to the underlying pathology, or a consequence of enhanced vascular pruning by activated microglia/astrocytes.[212,277,285] However, such changes are common in other neurodegeneration and natural aging too. A set of specific AD markers in the retina that can be identified noninvasively is still missing. The retina is one of the highest energy-consuming organs, and its blood vessels grow and regress in reaction to changes in metabolic rate in normal and disease states.[52,286–288] Such coupling is the ultimate responsibility of the neurovascular unit. While our vascular study contributes to a better understanding of retinal neurovascular coupling, questions about the sequence of events and their inhibitory and excitatory mediators remain unanswered.

Published data regarding retinal capillary plexuses changes in rodents are sparse, and we are not aware of any publication showing retinal capillary morphology and density in AD models. In contrast, there has been a surge of human OCTA studies in individuals with MCI and AD, reporting decreased,[119,120,126,128,217] equal,[130] or even increased[132] retinal vascular densities. Such controversy highlights the uncertainty about the extent of retinal vascular changes in AD and their correlation to the brain's disease pathology. Our studies provided robust histopathologic confirmation that SVP and DVP densities were significantly lower in old transgenic mice than their age-matched controls. We are developing an OCTA algorithm to extract retinal vascular density data in live animals and confirm those density data with corresponding histopathologic evidence of retinal vascular network extension and density (Figure 5-1). However, more than a histopathologic confirmation for OCTA studies, our study may provide an overview of the pathologic

consequences of AD and aging on retinal vessels. It has been shown that retinal vascular distribution and flow couples with respective retinal layers' metabolic demand in the short and long terms.[218] Such coupling could occur in acute and chronic phases depending on the life length of such metabolic changes, focal growth factors' availability, localized damage to the vasculature, and concomitant cardiovascular pathologies.[221,229] In the 3xTg-AD mice where inner and middle retina pathologies are more prominent,[91,188] our observations of SVP and DVP attenuation show that retinal flow matched retinal layers' metabolic demands in the setting of AD neurodegeneration. Thus, SVP thinning in the AD model may indicate decreased metabolic demand due to RGC loss and amyloid and tau-mediated vascular damage. Similarly, decreased DVP density in the aged 3xTg-AD is possibly secondary to decreased metabolic demand[70,221] and capillary occlusion due to amyloid and tau deposition in and around deep retinal capillaries[188,230,231] While this sequence of events is possibly analogous to cerebral vascular pathologies seen in AD,[57,140,230,232] mediators of these events should be explored.

A
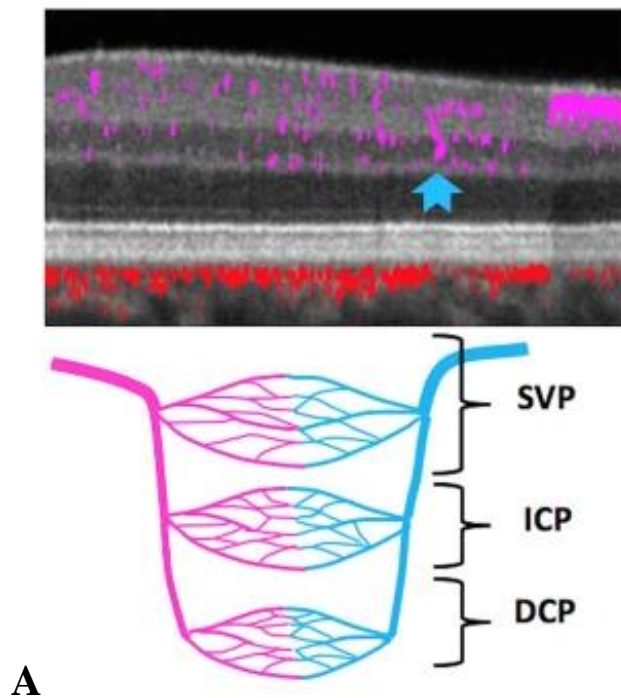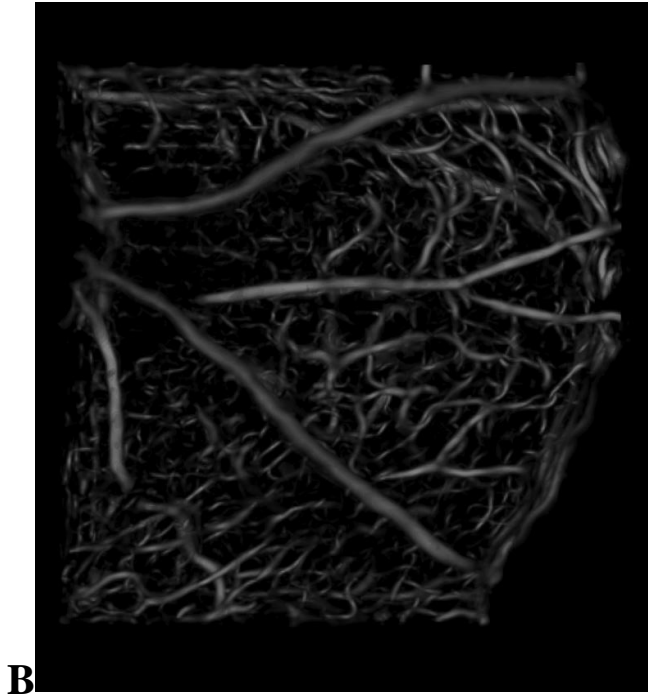
B

Figure 24. (A) Retinal capillary plexuses and their location in OCT scan. Signals from high-resolution SD-OCT scan (pink) are processed to yield OCTA images (reproduced with permission from reference #77 under Creative Commons Attribution License).[77] (B) OCTA rendering in Dr. Motamedi's lab shows retinal vascular layers in a 3xTg-AD mouse.

Although aging and cardiovascular diseases usually cause diffuse cerebral vascular pathologies,[233] Alzheimer's-related cerebral vasculopathy are skewed toward areas with a higher amyloid and tau burden, such as the hippocampus.[231,234–237] A similar pattern seen in the retina with its amyloid and tau deposition concentrated in GCL, IPL, OPL, and INL[187,216,238] is compatible with the observation of SVP and DVP loss both in human OCTA and our animal model studies. As mentioned above, such coupling of vascular damage and amyloid pathology burden should be explored.

Differentiating aging versus amyloid/tau pathology-induced neurovascular degeneration is challenging. Aging-associated decline in microvascular structure and function compromises CNS's capacity for coupling with alteration in the mentation-related increase in metabolic demand. Aging arteries are invariably vulnerable to cerebral amyloid angiopathy (CAA) that is characterized by amyloid deposition, mostly in medial-adventitial layers of leptomeningeal and intracranial cerebral arteries. CAA predisposes

arterioles and capillaries for spontaneous breakdown and focal bleedings contributing to aging and AD's cognitive dysfunction. Bell and Ball reported an age-dependent decrease in capillary density in various areas of the brain in individuals with AD.[289] Such capillary loss was suggested to be, at least in part, due to Aβ accumulations on capillaries that act as a molecular sink for angiogenic factor VEGF, reducing its availability in AD.[290] Besides, cholinergic shortages may also contribute to decreased cerebral flow in AD. We showed that inner retina is vulnerable to such decreased vascular density, possibly due to increased amyloid and tau burden in RGC. On the other hand, the DVP capillary network located in the trilaminar retinal vascular network's watershed zone is also vulnerable to decreased flow and occlusion. Such vulnerability predisposes IPL and ONL to unmet metabolic demand that may explain (at least in part) visual defects detected in patients with AD. With this hypothesis, preventing aging/atherosclerosis-associated vascular dysfunction may delay or prevent cognition loss in AD or vascular dementia. Under this hypothesis, hypertension, atherosclerosis, and other cardiovascular risk factors have been found associated with an increased risk of AD.[291]

Another aspect of AD pathology is neuroinflammation, mainly mediated via astrocytes and microglia. In a single-cell transcriptomic analysis from the prefrontal cortex of 48 individuals with varying degrees of AD, Mathys et al. identified transcriptionally distinct genes associated with regulators of myelination, inflammation, and neuron survival.[292] On the cellular level, CNS glial cells induce oxidative stress and faulty calcium homeostasis, leading to hyperactivation of kinase proteins and inactivation of phosphatases. As a result, tau protein becomes hyperphosphorylated and forms the neurofibrillary tangles accumulating in synapses and neuronal bodies. These structures enhance neuronal death by apoptosis and neurotransmitter loss. Besides, microglia release inflammatory mediators such as inflammatory cytokines, complement components, chemokines, and free radicals that are all known to contribute to Aβ production and accumulation. Besides, recent evidence show microglia mediate early synaptic loss in AD.[293] On the other hand, microglia are proposed to play a beneficial role in stimulating the clearance of amyloid plaques, at least in early AD.[294] In a detailed review, Hansen et al. proposed that "microglial function is normally protective in the brain, with microglia acting as housekeeping phagocytes to maintain tissue homeostasis and keep the

extracellular space clean of Aβ, thereby preventing AD." However, with increasing accumulation of Aβ, microglia compact Aβ aggregates in dense plaques and isolates them from neurons. However, the microglial function may become inadequate depending on age and genetic susceptibility. As microglia become overwhelmed with the deposition of toxic amyloid, tau pathology grows in stressed neurons and microglia initiating synaptic trimming and secretion of neurotoxic cytokines. Future potential treatments to stimulate microglial activity may help early AD stages but become disadvantageous in AD's proinflammatory late stages.[295]

The retina is developmentally part of the brain with its unique and distinct structure and biology. In the retina, muller cells constitute the main body of glial cells that, along with astrocytes and microglia, participate in retinal growth and neurogenesis, maintaining BBB, influencing synaptic connectivity by controlling the genesis and maintenance of synapses, and balancing nutrient and waste material homeostasis of photoreceptor and other neuronal elements.

Astrocytes have been heavily investigated for their role in AD. Astrocytes are mainly located in GCL and are in close interaction with the retina's superficial retinal vasculature. The astrocyte processes surround superficial retinal blood vessels.[76] Two distinct types of astrocytes exist in the retina: type I astrocytes identified by GFAP and connexin-43 expression and type II astrocytes identified by GFAP but no connexin-43 expression. Reactive astrocytes change their shape to become hypertrophic with enlarged soma, thicker processes, and enhanced GFAP immunoreactivity.[76] In AD, astrocytes are associated with amyloid plaques and show activation features.[296,297] Such enhanced immunoreactivity in the presence of Aβ has been shown to occur in parallel to enhanced apoptosis of the GCL in animal models of AD.[188,298] However, astrocytes' contribution to the maintenance and remodeling of SVP in AD neurodegeneration needs to be studied.

To explore astrocytes' role in maintaining NVU in the retina, we conducted limited preliminary studies on astrocytes' morphology and the expression of surface protein channels on astrocytes (Figures 25 to 27). These experiments were conducted as pilot hypothesis-generating studies. We attempted to quantify astrocyte morphology in the 3xTg-AD model using one of the methods described priorly.[299] Astrocytes were stained

with anti-GFAP antibody, and an outline was drawn around the astrocytes. The astrocytes' surface area was quantified in young and old transgenic and control retinas (Figure 27).
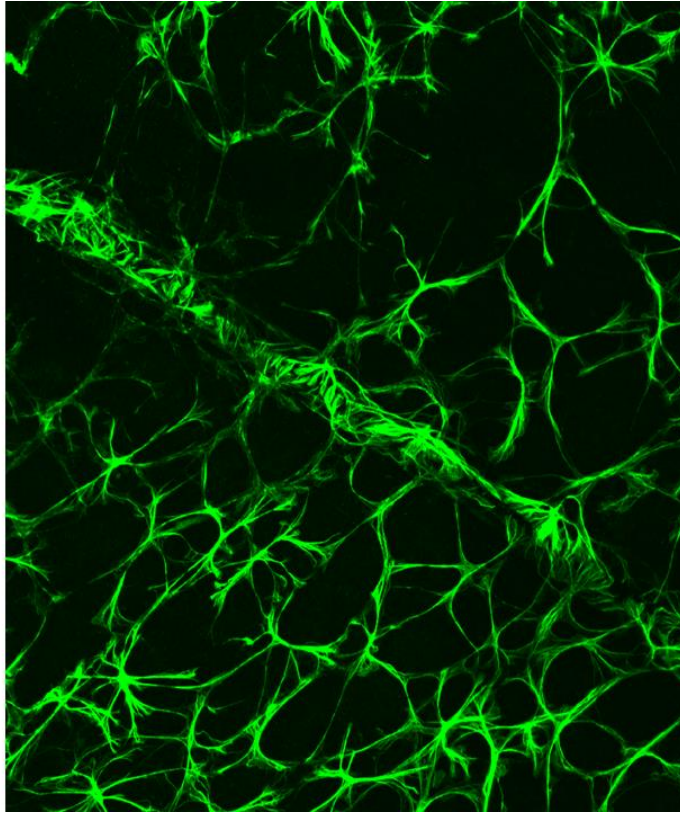
Figure 25. 3xTg-AD retina GFAP staining. Astrocyte footplates heavily surround large retinal vessels.
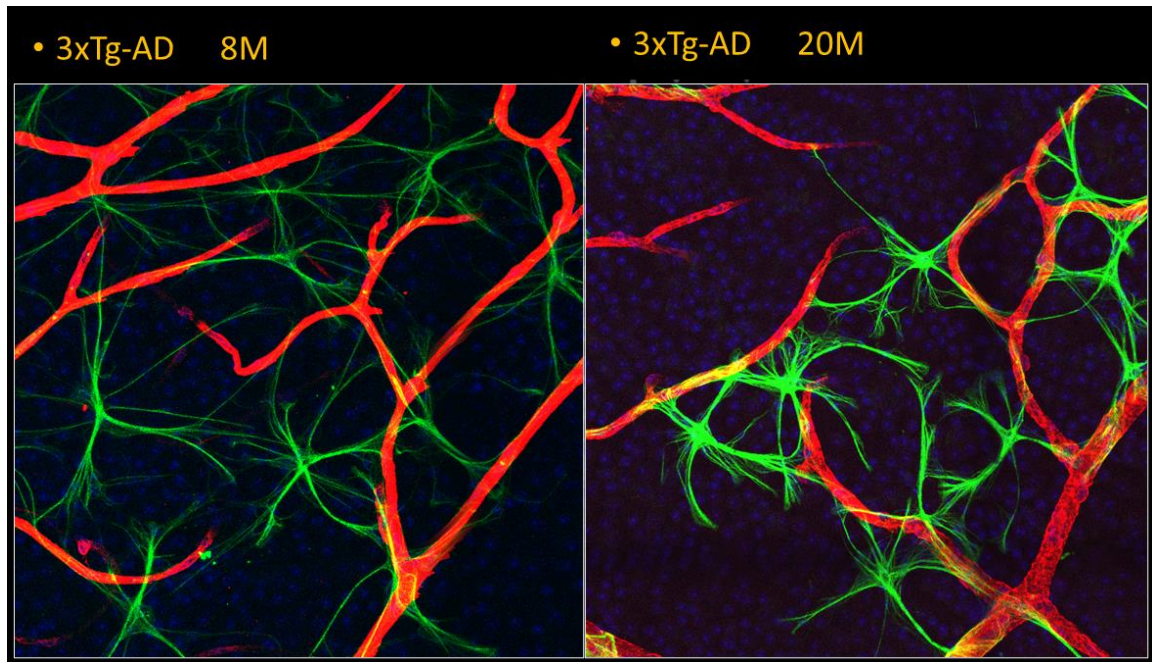
Figure 26. 3xTg-AD retina stained for collagen IV and GFAP. Astrocyte morphology changes in aged mouse.
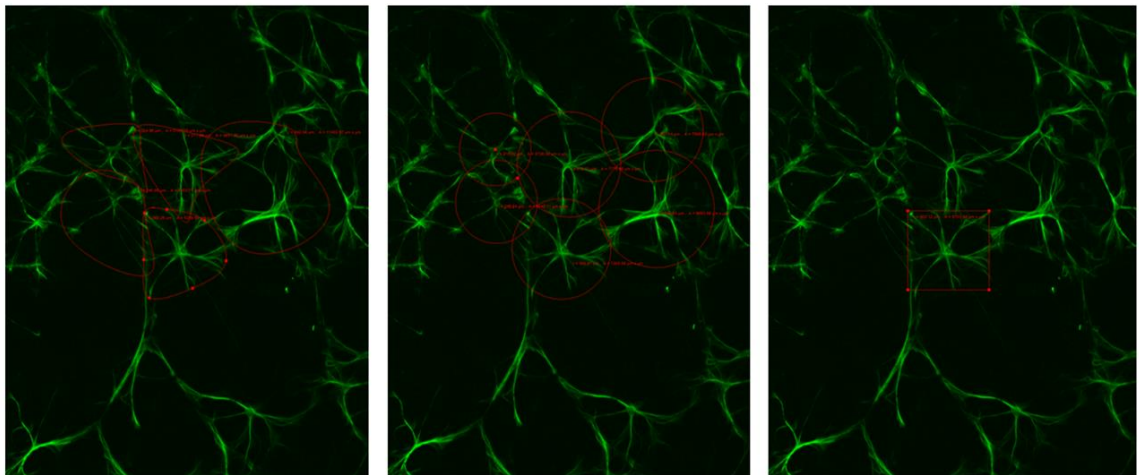
Figure 27. Preliminary studies. Experimenting with three outlining methods to delineate astrocyte perimeters. 3xTg-AD retina, GFAP staining. Astrocyte perimeters were delineated to quantify the area covered by the extensions.

We attempted to identify mechanistic targets that contribute to the interaction between astrocytes and capillary walls of NVU. Reactive astrocytes express pro-

inflammatory genes, NF-κB, complement components, and neurotoxins. Also, connexins 30 and 43, which are hemichannel protein complexes that play a pivotal role in cell-to-cell communication in the CNS, have been identified in mouse brain astrocytes, mostly on their footplates on pericytes.[300,301] We stained retina flat-mounts for connexin 43 expressions on astrocyte surface in young and old 3xTg-AD mouse retina (Figure 28), and showed possible age-dependent increased expression of connexin 43 on astrocyte footplates, where they adhere to superficial retinal arteries.
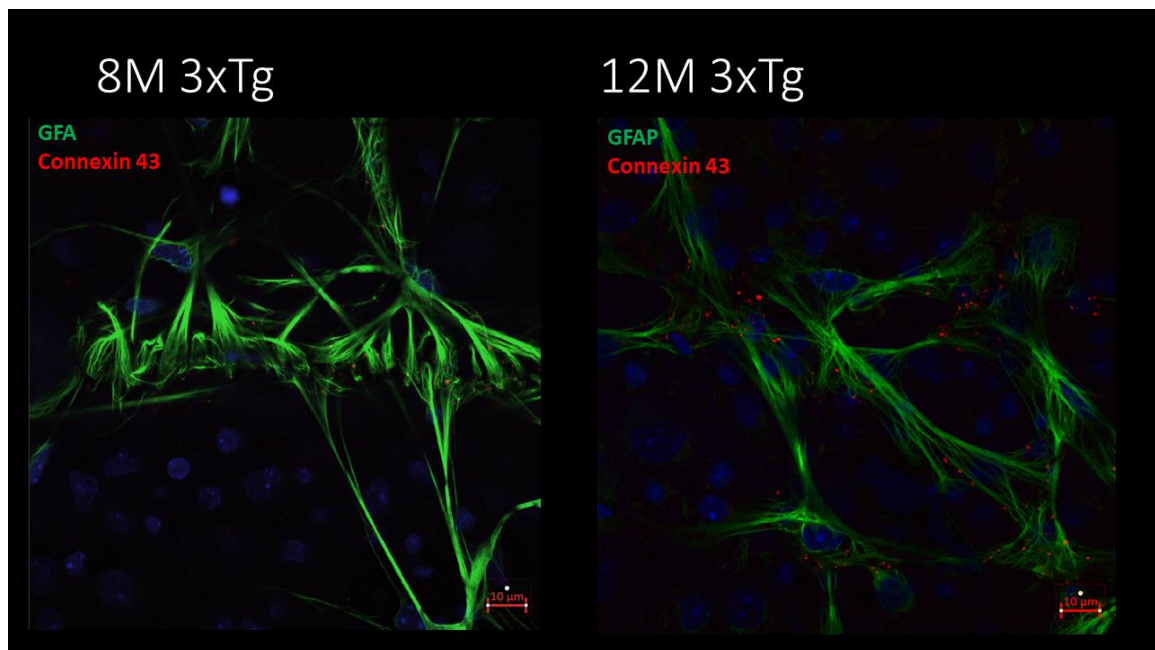
Figure 28. Connexin 43 expression on astrocyte footplates in 3xTg-AD mouse retina. More prominent Connexin 43 expression as animal aged.

In summary, our observations may be a confirmation for concurrent involvement of various retinal NVU elements in preclinical AD. In addition, we quantified retinal sublayer thicknesses in the 3xTg-AD retina with non-invasive OCT imaging and showed that RNFL thinning in the transgenic model correlated with the reduction in retinal GC numbers and an increasing retinal and brain AD pathology load. Our observations further supported decreased blood vessel distribution in the AD model and normal aging that matched decreased demand from neuronal loss, structural vascular damage due to amyloid,

tau, aging, or a combination of these phenomena. Our results indicated that neuronal, vascular, and glial components of NVU are altered in the retina of 3xTg-AD mice. Such alterations are distinct from age-dependent changes and can be detected in middle-age to old age. Our studies reiterate the questions already raised about the retina's role in AD and its correlation to brain pathologies. Future clinical studies should characterize longitudinal and temporal correlation of retinal NVU changes to those changes in the brain.

CONTRIBUTIONS TO NONINVASIVE DETECTION OF RETINAL NEURONAL LOSS IN AD.

The retina is one of the most intriguing parts of the CNS, and its structure and function can be interrogated using various invasive and noninvasive imaging studies. Although the retina's neuronal and vascular network has been studied before, the recent introduction of noninvasive in vivo imaging with OCT, OCTA, FAF, AO, DVA, and … illustrates the retina in unprecedented detail. However, controversial reports, limited ability to identify the preclinical disease, and considerable overlap between retinal presentations of various neurodegenerative diseases have limited the utility of retinal imaging in AD and similar diseases. A potential solution suggested by others and confirmed by our findings is to formulate a weighted functional and structural scoring system based incorporating multimodality retinal imaging. A prerequisite for such a scoring system is to improve the resolution and accuracy of current imaging systems and to correlate the findings with clinical features of the disease in the future (predictive values).

Clinical prediction or probability assessment systems are algorithms that include a combination of medical signs, symptoms, and laboratory or imaging findings to predict the probability of a specific disease or outcome. Such systems are commonly used in medicine to estimate the risks of diseases. Examples of such prediction systems are CHA2DS2-VASc score (clinical prediction rules for estimating the risk of stroke in patients with non-rheumatic atrial fibrillation) or APACHE II scoring system (severity-of-disease classification system for patients in intensive care units). In these systems, each item has an assigned weight or scores that will be added to give a final score that predicts the outcome. While we have multiple clinical, laboratory, and brain and ocular imaging systems available, almost none of them are pathognomonic for AD diagnosis or predicting its progression; but combining their findings and assigning an evidence-based score to

them may be able to predict AD more accurately. Multiple OCT imaging studies have shown significant RNFL thinning and macular volume loss in patients with mild to severe AD, suggesting that retinal thinning may occur early in the disease course.[302] However, no consensus has been achieved about the correlation of RNFL and other retinal sublayer thicknesses and cognitive loss. Besides, isolated studies have shown decreased SVP and DVP density in MCI and AD, decreased vascular flow response in DVA, and retinal photoreceptor loss with AO-based imaging in AD. A holistic approach that considers various modalities and assigns a score to their finding will be the future of AD diagnosis.

Our study confirmed the findings from the majority of current OCTA studies in terms of retinal vascular changes. Our data provided guidelines to differentiate aging- from AD-related vascular changes. Capillary density at any given time is influenced by at least four processes: the capillary network may proliferate or regress; and then tissue parenchyma may expand (by cell proliferation, hypertrophy, or edema) or shrink (by the reduction in number and size of cells, or by dehydration).[289] In AD, neuronal loss or glial proliferation may increase retinal sublayer thicknesses. Similarly, vascular dysfunction and leakage may increase the tissue volume, or a concomitant vascular loss may contribute to the loss of retinal sublayer thickness and volume. Retinal capillary bed is a mesh-like network, generally described as homogeneous and uniform for each layer and highly interconnected. Nevertheless, there is a center-to-periphery, macula-to-extra macula, and retinal quadrant-based variation in retinal neuronal and vascular densities and organization. While our whole-retinal imaging method offers a tissue preparation method to study retina samples for histology, ultrawide field imaging systems are becoming available for real clinical use. For example, Avanti Widefield OCT platform offers a field of view of 12 x 8 mm that covers a significant part of retina. Utilizing AO solutions to negate peripheral aberration to capture wider field retinal scans or software algorithms to stitch posterior pole and peripheral scan to a single retinal neuronal and vascular map.

Our findings have multiple implications when interpreting retinal imaging studies in patients with AD. Altered retinal vascular function (that may include blood-retinal barrier dysfunction, increased vascular leakage,[216] and toxic protein accumulation) possibly contributes to retinal thickness and volume as quantified by OCT and OCTA. Retinal thickness is determined by the sum of its vascular and neuronal mass; then, SVP

atrophy may enhance inner retinal thinning due to RNFL and GCL loss.[102] Meanwhile, a simultaneous increase in vascular permeability due to the amyloid/tau vasculopathy contracts the thinning effect of degenerative processes. The complex coexistence of trophic and atrophic processes that will ultimately determine the retinal sublayer thicknesses should be considered when interpreting retinal thickness and volume data.

In summary, our data supported OCT/OCTA-based noninvasive monitoring of retinal neuronal and vascular sublayers as a possible biomarker for AD progression in midlife, as a potential component of a decision-making tree to differentiate AD-neurodegeneration from retinal changes associated with normal aging, and as a likely outcome measure for future preclinical treatment intervention studies. Of course, these observations should be validated in human. While current data from human and animal studies support the association of noninvasive retinal imaging findings with neurodegeneration burden in AD, higher-resolution optical imaging tools are needed to redefine these associations and differentiate AD from aging and other neurovascular degeneration. From a practical standpoint, it appears that a combination of retinal and brain structural, functional, and molecular markers, together with cognitive assessments, might be the future diagnostic toolkit for identifying AD's pathologic burden.

CONCLUSION AND FUTURE DIRECTIONS

AD is a multifactorial disease with complex pathology. Commonly believed theory is based on the continuum of damaging processes that most likely begins with the accumulation of misfolded Aβ and HPT. Simultaneous inflammation, altered blood flow regulation, and synaptic loss participate in inducing neuronal death and causing AD cognitive symptoms. Currently available tools to probe and explore such targets in a noninvasive or minimally invasive, cost-effective, easily repeatable fashion are not adequate. Recent studies have suggested that cerebral blood flow abnormalities may precede the degeneration of neurons and synapses in the AD brain.[243] AD-related retinal neuronal and microvascular changes have been variably reported from individuals with preclinical AD.[122,132,244] Multiple studies indicate that the retina is possibly more vulnerable to AD pathology, thus a potential tool for identifying early disease. However, the extent of age-related versus AD-related pathologies in retinal vasculature is not clear yet. Besides,

the retina can help study the underlying mechanisms for impaired cerebral vascular clearance of Aβ, and whether vascular abnormalities trigger Aβ and tau deposition or Aβ/tau accumulation is the fundamental cause of cerebral vascular insufficiency. With an immunofluorescent study approach on the 3xTg-AD mouse model, we showed that retinal sublayer thicknesses change differently in young to middle age in transgenic and control animals. Further, we showed, for the first time, that loss of vascular density in superficial and deep retinal vascular plexuses may be able to differentiate old transgenic AD from age-matched controls. While our findings need validation in humans, it suggests that retinal vascular layers may reflect cerebral vasculature changes in the setting of AD.

We are also raising the following questions based on our observations and in the light of previous extensive work on retinal neurovascular pathologies in AD:

1) Do cerebrovascular changes drive the initial events leading to Aβ and tau deposition and neuronal injury, or Aβ and tau toxicity drives microvascular dysfunction and damage?

2) Do retinal vascular dysregulations in the setting of AD occur parallel to the cerebrovascular pathologies?

3) What molecular pathways and provoking and inhibitory mechanisms are involved in NVU dysfunction in the retina in AD?

4) Does the retina have a protective mechanism that protects it from AD pathology, or is it more prone to such pathologies?

5) To what extent retinal vascular reactivity alters with aging and AD? [57]

FUTURE PLAN:

We are validating mouse OCTA data with the corresponding histologic mapping of the retinal vascular layers using a costume OCTA algorithm has been developed in Dr. Motamedi's lab (Figure 24).

A crossbreed between 3xTg-AD and CX3CR1[GFP] has been developed in Dr. Zhang's lab. We plan to use this model for in vivo studying of microglia distribution in AD mouse model using SLO camera.

I am planning for clinical validation of the findings in patients with AD and other neurodegenerative disorders such as PD, FLDP, and senile/cardiovascular dementia. I have

already started scanning AD patients with OCTA and OCT. Communication with the University of Minnesota Department of Neurology led to an initial agreement to coordinate referrals; however, this project has been aborted since the COVID-19 pandemic. I am planning to resume the project with the Neurology team soon.

A possible avenue to explore retinal vascular mapping's clinical application is studying retinal vasculature changes in TBI. A protocol is being prepared to study college football team members with OCTA before and at the end of a game season. Using OCTA, we will analyze retinal vascular density and distributions.

Another potential avenue for research is to study photoreceptors and retinal vascular wall with adaptive optics and to correlate the findings with OCTA in normal aging, after TBI, and in AD.

Artificial intelligence-based deep learning procedures have offered novel clinical and research applications for retinal imaging. AI may facilitate screening, risk stratification, and monitoring of retinal vasculature changes.

Retinal vascular features may vary based on body habitus and ethnicity. Thus, predictive and monitoring values of retinal vascular imaging should be determined and validated in multiethnic cohorts. A future study about the utility of OCTA and other multimodal retinal imaging modalities should recruit individuals from various ethnic backgrounds.

Appendix

SUPPLEMENTAL VIDEO 1:

Intact whole retina imaging of a CX3CR^{-GFR} mouse.

SUPPLEMENTAL VIDEO 2:

Hyaloid vasculature and retrolental vascular plexus in a 4-day old mouse seen with intact whole retina tissue preparation method.

Bibliography

1.   Braak H, Braak E. Staging of alzheimer's disease-related neurofibrillary changes. *Neurobiol Aging*. 1995;16(3):271-278. doi:10.1016/0197-4580(95)00021-6

2.   Nelson AR, Sweeney MD, Sagare AP, Zlokovic B V. Neurovascular dysfunction and neurodegeneration in dementia and Alzheimer's disease. *Biochim Biophys Acta - Mol Basis Dis*. 2016;1862(5):887-900. doi:10.1016/j.bbadis.2015.12.016

3.   Ravi Teja KV, Tos Berendschot T, Steinbusch H, Carroll Webers AB, Praveen Murthy R, Mathuranath PS. Cerebral and Retinal Neurovascular Changes: A Biomarker for Alzheimer's Disease. *J Gerontol Geriatr Res*. 2017;6(4). doi:10.4172/2167-7182.1000447

4.   Goedert M, Wischik CM, Crowther RA, Walker JE, Klug A. Cloning and sequencing of the cDNA encoding a core protein of the paired helical filament of Alzheimer disease: Identification as the microtubule-associated protein tau. *Proc Natl Acad Sci U S A*. 1988;85(11):4051-4055. doi:10.1073/pnas.85.11.4051

5.   Glenner GG, Wong CW. Alzheimer's disease and Down's syndrome: Sharing of a unique cerebrovascular amyloid fibril protein. *Biochem Biophys Res Commun*. 1984;122(3):1131-1135. doi:10.1016/0006-291X(84)91209-9

6.   Nussbaum RL, Ellis CE. Alzheimer's Disease and Parkinson's Disease. *N Engl J Med*. 2003;348(14):1356-1364. doi:10.1056/nejm2003ra020003

7.   Georgiou M, Kalitzeos A, Patterson EJ, Dubra A, Carroll J, Michaelides M. Adaptive optics imaging of inherited retinal diseases. *Br J Ophthalmol*. 2018. doi:10.1136/bjophthalmol-2017-311328

8.   Hebert LE, Weuve J, Scherr PA, Evans DA. Alzheimer disease in the United States (2010-2050) estimated using the 2010 census. *Neurology*. 2013;80(19):1778-1783. doi:10.1212/WNL.0b013e31828726f5

9.   2018 Alzheimer's disease facts and figures. *Alzheimer's Dement*. 2018;14(3):367-429. doi:10.1016/j.jalz.2018.02.001

10.   Chen GF, Xu TH, Yan Y, et al. Amyloid beta: Structure, biology and structure-based therapeutic development. *Acta Pharmacol Sin*. 2017;38(9):1205-1235. doi:10.1038/aps.2017.28

11.   Grbovic OM, Mathews PM, Jiang Y, et al. Rab5-stimulated up-regulation of the endocytic pathway increases intracellular β-cleaved amyloid precursor protein carboxyl-terminal fragment levels and Aβ production. *J Biol Chem*. 2003;278(33):31261-31268. doi:10.1074/jbc.M304122200

12.   Yuksel M, Tacal O. Trafficking and proteolytic processing of amyloid precursor protein and secretases in Alzheimer's disease development: An up-to-date review. *Eur J Pharmacol*. 2019;856. doi:10.1016/j.ejphar.2019.172415

13.   Rasmussen MK, Mestre H, Nedergaard M. The glymphatic pathway in neurological disorders. *Lancet Neurol*. 2018;17(11):1016-1024. doi:10.1016/S1474-4422(18)30318-1

14.   Peng W, Achariyar TM, Li B, et al. Suppression of glymphatic fluid transport in a mouse model of Alzheimer's disease. *Neurobiol Dis*. 2016;93:215-225. doi:10.1016/j.nbd.2016.05.015

15.   Gandy S. The role of cerebral amyloid β accumulation in common forms of Alzheimer disease. *J Clin Invest*. 2005;115(5):1121-1129. doi:10.1172/jci25100

16.   Zlokovic B V. Neurovascular pathways to neurodegeneration in Alzheimer's disease and other disorders. *Nat Rev Neurosci*. 2011;12(12):723-738. doi:10.1038/nrn3114

17.   Mentis MJ, Alexander GE, Krasuski J, et al. Increasing required neural response to expose abnormal brain function in mild versus moderate or severe Alzheimer's disease: PET study using parametric visual stimulation. *Am J Psychiatry*. 1998;155(6):785-794. doi:10.1176/ajp.155.6.785

18.   Hamel E, Nicolakakis N, Aboulkassim T, Ongali B, Tong XK. Oxidative stress and cerebrovascular dysfunction in mouse models of Alzheimer's disease. In: *Experimental Physiology*. Vol 93. Blackwell Publishing Ltd; 2008:116-120. doi:10.1113/expphysiol.2007.038729

19.   Iadecola C, Zhang F, Niwa K, et al. SOD1 rescues cerebral endothelial dysfunction in mice overexpressing amyloid precursor protein. *Nat Neurosci*. 1999;2(2):157-161. doi:10.1038/5715

20.   Shi J, Perry G, Smith MA, Friedland RP. Vascular abnormalities: the insidious pathogenesis of Alzheimer's disease☆. *Neurobiol Aging*. 2000;21(2):357-361.

doi:10.1016/S0197-4580(00)00119-6

21.   Rosenblum WI. Why Alzheimer trials fail: Removing soluble oligomeric beta amyloid is essential, inconsistent, and difficult. *Neurobiol Aging*. 2014;35(5):969-974. doi:10.1016/j.neurobiolaging.2013.10.085

22.   Wirz KTS, Keitel S, Swaab DF, Verhaagen J, Bossers K. Early molecular changes in Alzheimer disease: Can we catch the disease in its presymptomatic phase? *J Alzheimer's Dis*. 2014;38(4):719-740. doi:10.3233/JAD-130920

23.   Sager MA, Hermann B, La Rue A. Middle-aged children of persons with Alzheimer's disease: APOE genotypes and cognitive function in the Wisconsin Registry for Alzheimer's Prevention. In: *Journal of Geriatric Psychiatry and Neurology*. Vol 18. J Geriatr Psychiatry Neurol; 2005:245-249. doi:10.1177/0891988705281882

24.   Stefaniak JD, Su L, Mak E, et al. Cerebral small vessel disease in middle age and genetic predisposition to late-onset Alzheimer's disease. *Alzheimer's Dement*. 2018;14(2):253-258. doi:10.1016/j.jalz.2017.08.017

25.   Mann DMA, Yates PO, Marcyniuk B, Ravindra CR. Loss of neurones from cortical and subcortical areas in Down's syndrome patients at middle age. Quantitative comparisons with younger Down's patients and patients with Alzheimer's disease. *J Neurol Sci*. 1987;80(1):79-89. doi:10.1016/0022-510X(87)90223-1

26.   Ritchie K, Carrière I, Howett D, et al. Allocentric and egocentric spatial processing in middle-aged adults at high risk of late-onset Alzheimer's disease: The PREVENT dementia study. *J Alzheimer's Dis*. 2018;65(3):885-896. doi:10.3233/JAD-180432

27.   Lautenschlager NT, Cupples LA, Rao VS, et al. Risk of dementia among relatives of Alzheimer's disease patients in the MIRAGE study: What is in store for the oldest old? *Neurology*. 1996;46(3):641-650. doi:10.1212/WNL.46.3.641

28.   Mayeux R, Saunders AM, Shea S, et al. Utility of the Apolipoprotein E Genotype in the Diagnosis of Alzheimer's Disease. *N Engl J Med*. 1998;338(8):506-511. doi:10.1056/NEJM199802193380804

29.   Goldman JS, Hahn SE, Catania JW, et al. Genetic counseling and testing for Alzheimer disease: Joint practice guidelines of the American College of Medical Genetics and the National Society of Genetic Counselors. *Genet Med*. 2011;13(6):597-

605. doi:10.1097/GIM.0b013e31821d69b8

30.   Schneider JA, Arvanitakis Z, Bang W, Bennett DA. Mixed brain pathologies account for most dementia cases in community-dwelling older persons. *Neurology*. 2007;69(24):2197-2204. doi:10.1212/01.wnl.0000271090.28148.24

31.   Sperling RA, Aisen PS, Beckett LA, et al. Toward defining the preclinical stages of Alzheimer's disease: Recommendations from the National Institute on Aging-Alzheimer's Association workgroups on diagnostic guidelines for Alzheimer's disease. *Alzheimer's Dement*. 2011;7(3):280-292. doi:10.1016/j.jalz.2011.03.003

32.   Hyman BT, Phelps CH, Beach TG, et al. National Institute on Aging-Alzheimer's Association guidelines for the neuropathologic assessment of Alzheimer's disease. *Alzheimer's Dement*. 2012;8(1):1-13. doi:10.1016/j.jalz.2011.10.007

33.   Kantarci K, Weigand SD, Przybelski SA, et al. Risk of dementia in MCI: Combined effect of cerebrovascular disease, volumetric MRI, and 1H MRS. *Neurology*. 2009;72(17):1519-1525. doi:10.1212/WNL.0b013e3181a2e864

34.   Grossberg GT, Christensen DD, Griffith PA, Kerwin DR, Hunt G, Hall EJ. The art of sharing the diagnosis and management of Alzheimer's disease with patients and caregivers: Recommendations of an expert consensus panel. *Prim Care Companion J Clin Psychiatry*. 2010;12(1). doi:10.4088/PCC.09cs00833oli

35.   Amram S, Frenkel D. Animal Models of Alzheimer's Disease. In: *Neuroprotection in Alzheimer's Disease*. Elsevier Inc.; 2017:31-58. doi:10.1016/B978-0-12-803690-7.00003-X

36.   LaFerla FM, Green KN. Animal models of Alzheimer disease. *Cold Spring Harb Perspect Med*. 2012;2(11). doi:10.1101/cshperspect.a006320

37.   Oddo S, Caccamo A, Kitazawa M, Tseng BP, LaFerla FM. Amyloid deposition precedes tangle formation in a triple transgenic model of Alzheimer's disease. *Neurobiol Aging*. 2003;24(8):1063-1070.

38.   Oddo S, Caccamo A, Shepherd JD, et al. Triple-transgenic model of Alzheimer's disease with plaques and tangles: intracellular Abeta and synaptic dysfunction. *Neuron*. 2003;39(3):409-421.

39.   Koronyo-Hamaoui M, Koronyo Y, Ljubimov A V., et al. Identification of amyloid plaques in retinas from Alzheimer's patients and noninvasive in vivo optical

imaging of retinal plaques in a mouse model. *Neuroimage*. 2011;54 Suppl 1(SUPPL. 1):S204-17. doi:10.1016/j.neuroimage.2010.06.020

40.   Chiasseu M, Alarcon-Martinez L, Belforte N, et al. Tau accumulation in the retina promotes early neuronal dysfunction and precedes brain pathology in a mouse model of Alzheimer's disease. *Mol Neurodegener*. 2017;12(1):58. doi:10.1186/s13024-017-0199-3

41.   Jankowsky JL, Zheng H. Practical considerations for choosing a mouse model of Alzheimer's disease. *Mol Neurodegener*. 2017;12(1). doi:10.1186/s13024-017-0231-7

42.   Edwards MM, Rodríguez JJ, Gutierrez-Lanza R, Yates J, Verkhratsky A, Lutty GA. Retinal macroglia changes in a triple transgenic mouse model of Alzheimer's disease. *Exp Eye Res*. 2014;127:252-260. doi:10.1016/j.exer.2014.08.006

43.   Drummond E, Wisniewski T. Alzheimer's disease: experimental models and reality. *Acta Neuropathol*. 2017;133(2):155-175. doi:10.1007/s00401-016-1662-x

44.   Sterniczuk R, Antle MC, Laferla FM, Dyck RH. Characterization of the 3xTg-AD mouse model of Alzheimer's disease: part 2. Behavioral and cognitive changes. *Brain Res*. 2010;1348:149-155. doi:10.1016/j.brainres.2010.06.011

45.   Cho SM, Lee S, Yang S-H, et al. Age-dependent inverse correlations in CSF and plasma amyloid-beta(1-42) concentrations prior to amyloid plaque deposition in the brain of 3xTg-AD mice. *Sci Rep*. 2016;6:20185. doi:10.1038/srep20185

46.   Drachman DA. The amyloid hypothesis, time to move on: Amyloid is the downstream result, not cause, of Alzheimer's disease. *Alzheimer's Dement*. 2014;10(3):372-380. doi:10.1016/j.jalz.2013.11.003

47.   Mir RH, Sawhney G, Pottoo FH, et al. Role of environmental pollutants in Alzheimer's disease: a review. *Environ Sci Pollut Res*. July 2020:1-19. doi:10.1007/s11356-020-09964-x

48.   Duggan E, Smith CA, Hooper ML, Chauhan BC. Colocalization of optical coherence tomography angiography with histology in the mouse retina. *Microvasc Res*. August 2020:104055. doi:10.1016/j.mvr.2020.104055

49.   Koronyo Y, Biggs D, Barron E, et al. Retinal amyloid pathology and proof-of-concept imaging trial in Alzheimer's disease. *JCI insight*. 2017;2(16):196-208.

doi:10.1172/jci.insight.93621

50.   Blanks JC, Torigoe Y, Hinton DR, Blanks RH. Retinal degeneration in the macula of patients with Alzheimer's disease. *Ann N Y Acad Sci*. 1991;640:44-46.

51.   Blanks JC, Torigoe Y, Hinton DR, Blanks RHI. Retinal pathology in Alzheimer's disease. I. Ganglion cell loss in foveal/parafoveal retina. *Neurobiol Aging*. 1996;17(3):377-384. doi:10.1016/0197-4580(96)00010-3

52.   Blanks JC, Hinton DR, Sadun AA, Miller CA. Retinal ganglion cell degeneration in Alzheimer's disease. *Brain Res*. 1989;501(2):364-372.

53.   Hinton DR, Sadun AA, Blanks JC, Miller CA. Optic-nerve degeneration in Alzheimer's disease. *N Engl J Med*. 1986;315(8):485-487. doi:10.1056/NEJM198608213150804

54.   Krantic S, Torriglia A. Retina: Source of the earliest biomarkers for Alzheimer's disease? *J Alzheimer's Dis*. 2014;40(2):237-243. doi:10.3233/JAD-132105

55.   Cheung C, Ong YT, Ikram MK, et al. Evidence of microvascular network alterations in the retinas of people with Alzheimer's disease. *Alzheimer's Dement*. 2013;1):P743. doi:http://dx.doi.org/10.1016/j.jalz.2013.05.1498

56.   Dorr A, Sahota B, Chinta L V., et al. Amyloid-β-dependent compromise of microvascular structure and function in a model of Alzheimer's disease. *Brain*. 2012;135(10):3039-3050. doi:10.1093/brain/aws243

57.   Chiquita S, Campos EJ, Castelhano J, et al. Retinal thinning of inner sub-layers is associated with cortical atrophy in a mouse model of Alzheimer's disease: A longitudinal multimodal in vivo study. *Alzheimer's Res Ther*. 2019;11(1). doi:10.1186/s13195-019-0542-8

58.   Hong S, Dissing-Olesen L, Stevens B. New insights on the role of microglia in synaptic pruning in health and disease. *Curr Opin Neurobiol*. 2016;36:128-134. doi:10.1016/j.conb.2015.12.004

59.   Chong MS, Sahadevan S. Preclinical Alzheimer's disease: diagnosis and prediction of progression. *Lancet Neurol*. 2005;4(9):576-579. doi:10.1016/S1474-4422(05)70168-X

60.   Cheung CYL, Ong YT, Ikram MK, et al. Microvascular network alterations in the retina of patients with Alzheimer's disease. *Alzheimer's Dement*.

2014;10(2):135-142. doi:10.1016/j.jalz.2013.06.009

61.   Snyder PJ, Johnson LN, Lim YY, et al. Nonvascular retinal imaging markers of preclinical Alzheimer's disease. *Alzheimer's Dement Diagnosis, Assess Dis Monit*. 2016;4. doi:10.1016/j.dadm.2016.09.001

62.   Bonnin S, Mané V, Couturier A, et al. NEW INSIGHT INTO THE MACULAR DEEP VASCULAR PLEXUS IMAGED BY OPTICAL COHERENCE TOMOGRAPHY ANGIOGRAPHY. *Retina*. 2015;35(11):2347-2352. doi:10.1097/IAE.0000000000000839

63.   Snodderly DM, Weinhaus RS, Chopb JC. *Neural-Vascular Relationships in Central Retina of Macaque Monkeys (Macaca Fascicularis)*. Vol 12.; 1992.

64.   Provis JM. Development of the primate retinal vasculature. *Prog Retin Eye Res*. 2001;20(6):799-821. doi:10.1016/S1350-9462(01)00012-X

65.   Tan PEZ, Yu PK, Balaratnasingam C, et al. Quantitative confocal imaging of the retinal microvasculature in the human retina. *Investig Ophthalmol Vis Sci*. 2012;53(9):5728-5736. doi:10.1167/iovs.12-10017

66.   Chan G, Balaratnasingam C, Yu PK, et al. Quantitative morphometry of perifoveal capillary networks in the human retina. *Investig Ophthalmol Vis Sci*. 2012;53(9):5502-5514. doi:10.1167/iovs.12-10265

67.   Simmons AB, Fuerst PG. Analysis of retinal vascular plexuses and interplexus connections. In: *Methods in Molecular Biology*. Vol 1753. Humana Press Inc.; 2018:317-330. doi:10.1007/978-1-4939-7720-8_22

68.   Campbell JP, Zhang M, Hwang TS, et al. Detailed Vascular Anatomy of the Human Retina by Projection-Resolved Optical Coherence Tomography Angiography. *Sci Rep*. 2017;7. doi:10.1038/srep42201

69.   Fruttiger M. Development of the retinal vasculature. *Angiogenesis*. 2007;10(2):77-88. doi:10.1007/s10456-007-9065-1

70.   Lavia C, Mecê P, Nassisi M, et al. Retinal Capillary Plexus Pattern and Density from Fovea to Periphery Measured in Healthy Eyes with Swept-Source Optical Coherence Tomography Angiography. *Sci Rep*. 2020;10(1):1-11. doi:10.1038/s41598-020-58359-y

71.   Onishi AC, Nesper PL, Roberts PK, et al. Importance of considering the

middle capillary plexus on OCT angiography in diabetic retinopathy. *Investig Ophthalmol Vis Sci*. 2018;59(5):2167-2176. doi:10.1167/iovs.17-23304

72.   Park JJ, Soetikno BT, Fawzi AA. CHARACTERIZATION of the MIDDLE CAPILLARY PLEXUS USING OPTICAL COHERENCE TOMOGRAPHY ANGIOGRAPHY in HEALTHY and DIABETIC EYES. *Retina*. 2016;36(11):2039-2050. doi:10.1097/IAE.0000000000001077

73.   Stone J, Itin A, Alon T, et al. Development of retinal vasculature is mediated by hypoxia-induced vascular endothelial growth factor (VEGF) expression by neuroglia. *J Neurosci*. 1995;15(7 I):4738-4747. doi:10.1523/jneurosci.15-07-04738.1995

74.   Arnold T, Betsholtz C. Erratum: The importance of microglia in the development of the vasculature in the central nervous system. *Vasc Cell*. 2013;5(1):1-7. doi:10.1186/2045-824X-5-12

75.   Usui Y, Westenskow PD, Kurihara T, et al. Neurovascular crosstalk between interneurons and capillaries is required for vision. *J Clin Invest*. 2015;125(6):2335-2346. doi:10.1172/JCI80297

76.   Vecino E, Rodriguez FD, Ruzafa N, Pereiro X, Sharma SC. Glia-neuron interactions in the mammalian retina. *Prog Retin Eye Res*. 2016;51:1-40. doi:10.1016/j.preteyeres.2015.06.003

77.   Ramirez AI, de Hoz R, Salobrar-Garcia E, et al. The role of microglia in retinal neurodegeneration: Alzheimer's disease, Parkinson, and glaucoma. *Front Aging Neurosci*. 2017;9(JUL):214. doi:10.3389/fnagi.2017.00214

78.   Risacher SL, WuDunn D, Pepin SM, et al. Visual contrast sensitivity in Alzheimer's disease, mild cognitive impairment, and older adults with cognitive complaints. *Neurobiol Aging*. 2013;34(4):1133-1144. doi:10.1016/j.neurobiolaging.2012.08.007

79.   Mendez MF, Martin RJ, Smyth KA, Whitehouse PJ. Disturbances of person identification in alzheimer's disease: A retrospective study. *J Nerv Ment Dis*. 1992;180(2):94-96. doi:10.1097/00005053-199202000-00005

80.   Kaeser PF, Ghika J, Borruat FX. Visual signs and symptoms in patients with the visual variant of Alzheimer disease. *BMC Ophthalmol*. 2015;15(1). doi:10.1186/s12886-015-0060-9

81. Polo V, Rodrigo MJ, Garcia-Martin E, et al. Visual dysfunction and its correlation with retinal changes in patients with Alzheimer's disease. *Eye*. 2017;31(7):1034-1041. doi:10.1038/eye.2017.23

82. Salamone G, Di Lorenzo C, Mosti S, et al. Color discrimination performance in patients with alzheimer's disease. *Dement Geriatr Cogn Disord*. 2009;27(6):501-507. doi:10.1159/000218366

83. Prettyman R, Bitsios P, Szabadi E. Altered pupillary size and darkness and light reflexes in Alzheimer's disease. *J Neurol Neurosurg Psychiatry*. 1997;62(6):665-668. doi:10.1136/jnnp.62.6.665

84. Coubard OA. What do we know about eye movements in Alzheimer's disease? The past 37 years and future directions. *Biomark Med*. 2016;10(7):677-680. doi:10.2217/bmm-2016-0095

85. Armstrong RA. Visual field defects in Alzheimer's disease patients may reflect differential pathology in the primary visual cortex. *Optom Vis Sci*. 1996;73(11):677-682. doi:10.1097/00006324-199611000-00001

86. Ivanova E, Alam NM, Prusky GT, Sagdullaev BT. Blood-retina barrier failure and vision loss in neuron-specific degeneration. *JCI Insight*. 2019;4(8). doi:10.1172/jci.insight.126747

87. Gameiro GR, Jiang H, Liu Y, et al. Retinal tissue hypoperfusion in patients with clinical Alzheimer's disease. *Eye Vis*. 2018;5(1):21. doi:10.1186/s40662-018-0115-0

88. Koronyo Y, Biggs D, Barron E, et al. Retinal amyloid pathology and proof-of-concept imaging trial in Alzheimer's disease. *JCI Insight*. 2017. doi:10.1172/jci.insight.93621

89. La Morgia C, Ross-Cisneros FN, Koronyo Y, et al. Melanopsin retinal ganglion cell loss in <scp>A</scp> lzheimer disease. *Ann Neurol*. 2016;79(1):90-109. doi:10.1002/ana.24548

90. den Haan J, Morrema THJ, Verbraak FD, et al. Amyloid-beta and phosphorylated tau in post-mortem Alzheimer's disease retinas. *Acta Neuropathol Commun*. 2018;6(1):147. doi:10.1186/s40478-018-0650-x

91. Shi H, Koronyo Y, Rentsendorj A, et al. Identification of early pericyte

loss and vascular amyloidosis in Alzheimer's disease retina. *Acta Neuropathol*. 2020;139(5):813-836. doi:10.1007/s00401-020-02134-w

92.   Asanad S, Ross-Cisneros FN, Nassisi M, Barron E, Karanjia R, Sadun AA. The retina in alzheimer's disease: Histomorphometric analysis of an ophthalmologic biomarker. *Investig Ophthalmol Vis Sci*. 2019;60(5):1491-1500. doi:10.1167/iovs.18-25966

93.   den Haan J, Morrema THJ, Rozemuller AJ, Bouwman FH, Hoozemans JJM. Different curcumin forms selectively bind fibrillar amyloid beta in post mortem Alzheimer's disease brains: Implications for in-vivo diagnostics. *Acta Neuropathol Commun*. 2018;6(1):75. doi:10.1186/s40478-018-0577-2

94.   den Haan J, Janssen SF, van de Kreeke JA, Scheltens P, Verbraak FD, Bouwman FH. Retinal thickness correlates with parietal cortical atrophy in early-onset Alzheimer's disease and controls. *Alzheimer's Dement Diagnosis, Assess Dis Monit*. 2018;10:49-55. doi:10.1016/j.dadm.2017.10.005

95.   Lad EM, Mukherjee D, Stinnett SS, et al. Evaluation of inner retinal layers as biomarkers in mild cognitive impairment to moderate Alzheimer's disease. *PLoS One*. 2018;13(2). doi:10.1371/journal.pone.0192646

96.   Uchida A, Pillai JA, Bermel R, et al. **Outer Retinal Assessment Using Spectral-Domain Optical Coherence Tomography in Patients With Alzheimer's and Parkinson's Disease**. *Investig Opthalmology Vis Sci*. 2018;59(7):2768. doi:10.1167/iovs.17-23240

97.   Gao LY, Liu Y, Li XH, Bai QH, Liu P. Abnormal retinal nerve fiber layer thickness and macula lutea in patients with mild cognitive impairment and Alzheimer's disease. *Arch Gerontol Geriatr*. 2015;60(1):162-167. doi:10.1016/j.archger.2014.10.011

98.   Parisi V, Restuccia R, Fattapposta F, Mina C, Bucci MG, Pierelli F. Morphological and functional retinal impairment in Alzheimer's disease patients. *Clin Neurophysiol*. 2001;112(10):1860-1867. doi:10.1016/S1388-2457(01)00620-4

99.   Cheung CYL, Ong YT, Hilal S, et al. Retinal ganglion cell analysis using high-definition optical coherence tomography in patients with mild cognitive impairment and alzheimer's disease. *J Alzheimer's Dis*. 2015;45(1):45-56. doi:10.3233/JAD-141659

100.   Kesler A, Vakhapova V, Korczyn AD, Naftaliev E, Neudorfer M. Retinal

thickness in patients with mild cognitive impairment and Alzheimer's disease. *Clin Neurol Neurosurg*. 2011;113(7):523-526. doi:10.1016/j.clineuro.2011.02.014

101. Liu D, Zhang L, Li Z, et al. Thinner changes of the retinal nerve fiber layer in patients with mild cognitive impairment and Alzheimer's disease. *BMC Neurol*. 2015;15(1):14. doi:10.1186/s12883-015-0268-6

102. Ascaso FJ, Cruz N, Modrego PJ, et al. Retinal alterations in mild cognitive impairment and Alzheimer's disease: an optical coherence tomography study. doi:10.1007/s00415-014-7374-z

103. Kwon JY, Yang JH, Han JS, Kim DG. Analysis of the Retinal Nerve Fiber Layer Thickness in Alzheimer Disease and Mild Cognitive Impairment. *Korean J Ophthalmol*. 2017;31(6):548. doi:10.3341/kjo.2016.0118

104. Cunha JP, Proença R, Dias-Santos A, et al. OCT in Alzheimer's disease: thinning of the RNFL and superior hemiretina. *Graefe's Arch Clin Exp Ophthalmol*. 2017;255(9):1827-1835. doi:10.1007/s00417-017-3715-9

105. Kirbas S, Turkyilmaz K, Anlar O, Tufekci A, Durmus M. Retinal nerve fiber layer thickness in patients with Alzheimer sisease. *J Neuro-Ophthalmology*. 2013;33(1):58-61. doi:10.1097/WNO.0b013e318267fd5f

106. Kromer R, Serbecic N, Hausner L, Froelich L, Aboul-Enein F, Beutelspacher SC. Detection of Retinal Nerve Fiber Layer Defects in Alzheimer's Disease Using SD-OCT. *Front Psychiatry*. 2014;5(FEB):22. doi:10.3389/fpsyt.2014.00022

107. Mutlu U, Colijn JM, Ikram MA, et al. Association of Retinal Neurodegeneration on Optical Coherence Tomography with Dementia: A Population-Based Study. *JAMA Neurol*. 2018;75(10):1256-1263. doi:10.1001/jamaneurol.2018.1563

108. Paquet C, Boissonnot M, Roger F, Dighiero P, Gil R, Hugon J. Abnormal retinal thickness in patients with mild cognitive impairment and Alzheimer's disease. *Neurosci Lett*. 2007;420(2):97-99. doi:10.1016/j.neulet.2007.02.090

109. Chan VTT, Sun Z, Tang S, et al. Spectral-Domain OCT Measurements in Alzheimer's Disease: A Systematic Review and Meta-analysis. *Ophthalmology*. 2019;126(4):497-510. doi:10.1016/j.ophtha.2018.08.009

110. Song A, Johnson N, Ayala A, Thompson AC. Optical Coherence

Tomography in Patients with Alzheimer's Disease: What Can It Tell Us? *Eye Brain*. 2021;Volume 13:1-20. doi:10.2147/eb.s235238

111.   Song A, Johnson N, Ayala A, Thompson AC. Optical Coherence Tomography in Patients with Alzheimer's Disease: What Can It Tell Us? *Eye Brain*. 2021;Volume 13:1-20. doi:10.2147/eb.s235238

112.   Trebbastoni A, Marcelli M, Mallone F, et al. Attenuation of Choroidal Thickness in Patients With Alzheimer Disease: Evidence From an Italian Prospective Study. *Alzheimer Dis Assoc Disord*. 2017;31(2):128-134. doi:10.1097/WAD.0000000000000176

113.   Gharbiya M, Trebbastoni A, Parisi F, et al. Choroidal thinning as a new finding in Alzheimer's Disease: Evidence from enhanced depth imaging spectral domain optical coherence tomography. *J Alzheimer's Dis*. 2014;40(4):907-917. doi:10.3233/JAD-132039

114.   Robbins CB, Grewal DS, Thompson AC, et al. Choroidal Structural Analysis in Alzheimer Disease, Mild Cognitive Impairment, and Cognitively Healthy Controls. *Am J Ophthalmol*. 2021;223:359-367. doi:10.1016/j.ajo.2020.09.049

115.   Bayhan HA, Aslan Bayhan S, Celikbilek A, Tanık N, Gürdal C. Evaluation of the chorioretinal thickness changes in Alzheimer's disease using spectral-domain optical coherence tomography. *Clin Experiment Ophthalmol*. 2015;43(2):145-151. doi:10.1111/ceo.12386

116.   Marchesi VT. Alzheimer's dementia begins as a disease of small blood vessels, damaged by oxidative-induced inflammation and dysregulated amyloid metabolism: implications for early detection and therapy. *FASEB J*. 2011;25(1):5-13. doi:10.1096/fj.11-0102ufm

117.   Miao J, Vitek MP, Xu F, Previti M Lou, Davis J, Van Nostrand WE. Reducing cerebral microvascular amyloid-β protein deposition diminishes regional neuroinflammation in vasculotropic mutant amyloid precursor protein transgenic mice. *J Neurosci*. 2005;25(27):6271-6277. doi:10.1523/JNEUROSCI.1306-05.2005

118.   Tsai Y, Lu B, Ljubimov A V., et al. Ocular changes in TGF344-AD rat model of Alzheimer's disease. *Investig Ophthalmol Vis Sci*. 2014;55(1):523-534. doi:10.1167/iovs.13-12888

119.   Bulut M, Kurtuluş F, Gözkaya O, et al. Evaluation of optical coherence tomography angiographic findings in Alzheimer's type dementia. *Br J Ophthalmol*. 2018;102(2):233-237. doi:10.1136/bjophthalmol-2017-310476

120.   Yoon SP, Grewal DS, Thompson AC, et al. Retinal Microvascular and Neurodegenerative Changes in Alzheimer's Disease and Mild Cognitive Impairment Compared with Control Participants. *Ophthalmol Retin*. 2019;3(6):489-499. doi:10.1016/j.oret.2019.02.002

121.   Yoon SP, Thompson AC, Polascik BW, et al. Correlation of OctA and volumetric MRI in mild cognitive impairment and Alzheimer's disease. *Ophthalmic Surg Lasers Imaging Retin*. 2019;50(11):709-718. doi:10.3928/23258160-20191031-06

122.   Jiang H, Wei Y, Shi Y, et al. Altered Macular Microvasculature in Mild Cognitive Impairment and Alzheimer Disease. *J Neuro-Ophthalmology*. 2018;38(3):292-298. doi:10.1097/WNO.0000000000000580

123.   Jiang H, Liu Y, Wei Y, et al. Impaired retinal microcirculation in patients with Alzheimer's disease. Mogi M, ed. *PLoS One*. 2018;13(2):e0192154. doi:10.1371/journal.pone.0192154

124.   Zabel P, Kaluzny JJ, Wilkosc-Debczynska M, et al. Comparison of retinal microvasculature in patients with Alzheimer's disease and primary open-angle glaucoma by optical coherence tomography angiography. *Investig Ophthalmol Vis Sci*. 2019;60(10):3447-3455. doi:10.1167/IOVS.19-27028

125.   Zhang YS, Zhou N, Knoll BM, et al. Parafoveal vessel loss and correlation between peripapillary vessel density and cognitive performance in amnestic mild cognitive impairment and early Alzheimer's Disease on optical coherence tomography angiography. Vavvas DG, ed. *PLoS One*. 2019;14(4):e0214685. doi:10.1371/journal.pone.0214685

126.   Lahme L, Esser EL, Mihailovic N, et al. Evaluation of Ocular Perfusion in Alzheimer's Disease Using Optical Coherence Tomography Angiography. *J Alzheimer's Dis*. 2018;66(4):1745-1752. doi:10.3233/JAD-180738

127.   Grewal DS, Polascik BW, Hoffmeyer GC, Fekrat S. Assessment of differences in retinal microvasculature using OCT angiography in Alzheimer's disease: A twin discordance report. *Ophthalmic Surg Lasers Imaging Retin*. 2018;49(6):440-444.

doi:10.3928/23258160-20180601-09

128.   Zhang YS, Zhou N, Knoll BM, et al. Parafoveal vessel loss and correlation between peripapillary vessel density and cognitive performance in amnestic mild cognitive impairment and early Alzheimer's Disease on optical coherence tomography angiography. Vavvas DG, ed. *PLoS One*. 2019;14(4):e0214685. doi:10.1371/journal.pone.0214685

129.   O'Bryhim BE, Lin JB, Van Stavern GP, Apte RS. OCTA Findings in Pre-Clinical Alzheimer's Disease: 3 Year Follow-Up. *Ophthalmology*. February 2021. doi:10.1016/j.ophtha.2021.02.016

130.   Querques G, Borrelli E, Sacconi R, et al. Functional and morphological changes of the retinal vessels in Alzheimer's disease and mild cognitive impairment. *Sci Rep*. 2019;9(1):1-10. doi:10.1038/s41598-018-37271-6

131.   Haan J, Kreeke JA, Berckel BN, et al. Is retinal vasculature a biomarker in amyloid proven Alzheimer's disease? *Alzheimer's Dement Diagnosis, Assess Dis Monit*. 2019;11(1):383-391. doi:10.1016/j.dadm.2019.03.006

132.   Van De Kreeke JA, Nguyen HT, Konijnenberg E, et al. Optical coherence tomography angiography in preclinical Alzheimer's disease. *Br J Ophthalmol*. 2019;104(2):157-161. doi:10.1136/bjophthalmol-2019-314127

133.   Haan J den, van de Kreeke JA, van Berckel BN, et al. Is retinal vasculature a biomarker in amyloid proven Alzheimer's disease? *Alzheimer's Dement Diagnosis, Assess Dis Monit*. 2019;11:383-391. doi:10.1016/j.dadm.2019.03.006

134.   Zhang YS, Zhou N, Knoll BM, et al. Parafoveal vessel loss and correlation between peripapillary vessel density and cognitive performance in amnestic mild cognitive impairment and early Alzheimer's Disease on optical coherence tomography angiography. Vavvas DG, ed. *PLoS One*. 2019;14(4):e0214685. doi:10.1371/journal.pone.0214685

135.   Pellegrini M, Vagge A, Ferro Desideri L, et al. Optical Coherence Tomography Angiography in Neurodegenerative Disorders. *J Clin Med*. 2020;9(6):1706. doi:10.3390/jcm9061706

136.   Grewal DS, Polascik BW, Hoffmeyer GC, Fekrat S. Assessment of differences in retinal microvasculature using OCT angiography in Alzheimer's disease: A

twin discordance report. *Ophthalmic Surg Lasers Imaging Retin*. 2018;49(6):440-444. doi:10.3928/23258160-20180601-09

137.   van de Kreeke JA, Nguyen H-T, Konijnenberg E, et al. Optical coherence tomography angiography in preclinical Alzheimer's disease. *Br J Ophthalmol*. May 2019:bjophthalmol-2019-314127. doi:10.1136/bjophthalmol-2019-314127

138.   Salas M, Augustin M, Ginner L, et al. Visualization of micro-capillaries using optical coherence tomography angiography with and without adaptive optics. *Biomed Opt Express*. 2017;8(1):207. doi:10.1364/boe.8.000207

139.   Yu PK, Mammo Z, Balaratnasingam C, Yu DY. Quantitative study of the macular microvasculature in human donor eyes. *Investig Ophthalmol Vis Sci*. 2018;59(1):108-116. doi:10.1167/iovs.17-22542

140.   Balaratnasingam C, An D, Sakurada Y, et al. Comparisons Between Histology and Optical Coherence Tomography Angiography of the Periarterial Capillary-Free Zone. *Am J Ophthalmol*. 2018;189:55-64. doi:10.1016/j.ajo.2018.02.007

141.   Kokona D, Schneider N, Giannakaki-Zimmermann H, Jovanovic J, Ebneter A, Zinkernagel M. Noninvasive quantification of retinal microglia using widefield autofluorescence imaging. *Investig Ophthalmol Vis Sci*. 2017;58(4):2160-2165. doi:10.1167/iovs.16-20916

142.   Sadda SVR, Borrelli E, Fan W, et al. A pilot study of fluorescence lifetime imaging ophthalmoscopy in preclinical Alzheimer's disease. *Eye*. 2019;33(8):1271-1279. doi:10.1038/s41433-019-0406-2

143.   Jentsch S, Schweitzer D, Schmidtke KU, et al. Retinal fluorescence lifetime imaging ophthalmoscopy measures depend on the severity of Alzheimer's disease. *Acta Ophthalmol*. 2015;93(4):e241-e247. doi:10.1111/aos.12609

144.   Normando EM, Yap TE, Maddison J, et al. A CNN-aided method to predict glaucoma progression using DARC (Detection of Apoptosing Retinal Cells). *Expert Rev Mol Diagn*. 2020;20(7):737-748. doi:10.1080/14737159.2020.1758067

145.   Iadecola C. The Neurovascular Unit Coming of Age: A Journey through Neurovascular Coupling in Health and Disease. *Neuron*. 2017;96(1):17-42. doi:10.1016/j.neuron.2017.07.030

146.   Mawuenyega KG, Sigurdson W, Ovod V, et al. Decreased clearance of

CNS β-amyloid in Alzheimer's disease. *Science (80-)*. 2010;330(6012):1774. doi:10.1126/science.1197623

147.   Janelidze S, Hertze J, Nägga K, et al. Increased blood-brain barrier permeability is associated with dementia and diabetes but not amyloid pathology or APOE genotype. *Neurobiol Aging*. 2017;51:104-112. doi:10.1016/j.neurobiolaging.2016.11.017

148.   Montagne A, Barnes SR, Sweeney MD, et al. Blood-Brain barrier breakdown in the aging human hippocampus. *Neuron*. 2015;85(2):296-302. doi:10.1016/j.neuron.2014.12.032

149.   Janelidze S, Hertze J, Nägga K, et al. Increased blood-brain barrier permeability is associated with dementia and diabetes but not amyloid pathology or APOE genotype. *Neurobiol Aging*. 2017;51:104-112. doi:10.1016/j.neurobiolaging.2016.11.017

150.   Roher AE, Tyas SL, Maarouf CL, et al. Intracranial atherosclerosis as a contributing factor to Alzheimer's disease dementia. *Alzheimer's Dement*. 2011;7(4):436-444. doi:10.1016/j.jalz.2010.08.228

151.   Toledo JB, Arnold SE, Raible K, et al. Contribution of cerebrovascular disease in autopsy confirmed neurodegenerative disease cases in the National Alzheimer's Coordinating Centre. *Brain*. 2013;136(9):2697-2706. doi:10.1093/brain/awt188

152.   Iadecola C. The Neurovascular Unit Coming of Age: A Journey through Neurovascular Coupling in Health and Disease. *Neuron*. 2017;96(1):17-42. doi:10.1016/j.neuron.2017.07.030

153.   Tong XK, Nicolakakis N, Kocharyan A, Hamel E. Vascular remodeling versus amyloid β-induced oxidative stress in the cerebrovascular dysfunctions associated with alzheimer's disease. *J Neurosci*. 2005;25(48):11165-11174. doi:10.1523/JNEUROSCI.4031-05.2005

154.   Park L, Uekawa K, Garcia-Bonilla L, et al. Brain Perivascular Macrophages Initiate the Neurovascular Dysfunction of Alzheimer Aβ Peptides. *Circ Res*. 2017;121(3):258-269. doi:10.1161/CIRCRESAHA.117.311054

155.   Niwa K, Kazama K, Younkin L, Younkin SG, Carlson GA, Iadecola C.

Cerebrovascular autoregulation is profoundly impaired in mice overexpressing amyloid precursor protein. *Am J Physiol - Hear Circ Physiol*. 2002;283(1 52-1). doi:10.1152/ajpheart.00022.2002

156.	Grimmer T, Faust M, Auer F, et al. White matter hyperintensities predict amyloid increase in Alzheimer's disease. *Neurobiol Aging*. 2012;33(12):2766-2773. doi:10.1016/j.neurobiolaging.2012.01.016

157.	Braak H, Braak E. Frequency of stages of Alzheimer-related lesions in different age categories. *Neurobiol Aging*. 1997;18(4):351-357. doi:10.1016/S0197-4580(97)00056-0

158.	Pratico D, Clark CM, Liun F, Rokach J, Lee VY-M, Trojanowski JQ. Increase of brain oxidative stress in mild cognitive impairment: a possible predictor of Alzheimer disease. *Arch Neurol*. 2002;59(6):972-976.

159.	Bateman RJ, Xiong C, Benzinger TLS, et al. Clinical and Biomarker Changes in Dominantly Inherited Alzheimer's Disease. *N Engl J Med*. 2012;367(9):795-804. doi:10.1056/NEJMoa1202753

160.	Fagan AM, Xiong C, Jasielec MS, et al. Longitudinal change in CSF biomarkers in autosomal-dominant Alzheimer's disease. *Sci Transl Med*. 2014;6(226). doi:10.1126/scitranslmed.3007901

161.	Salobrar-García E, De Hoz R, Ramírez AI, et al. Changes in visual function and retinal structure in the progression of Alzheimer's disease. *PLoS One*. 2019;14(8). doi:10.1371/journal.pone.0220535

162.	Risacher SL, Wudunn D, Tallman EF, et al. Visual contrast sensitivity is associated with the presence of cerebral amyloid and tau deposition. doi:10.1093/braincomms/fcaa019

163.	Gupta VK, Chitranshi N, Gupta VB, et al. Amyloid β accumulation and inner retinal degenerative changes in Alzheimer's disease transgenic mouse. *Neurosci Lett*. 2016;623:52-56. doi:10.1016/j.neulet.2016.04.059

164.	Lu Y, Li Z, Zhang X, et al. Retinal nerve fiber layer structure abnormalities in early Alzheimer's disease: Evidence in optical coherence tomography. *Neurosci Lett*. 2010;480(1):69-72. doi:10.1016/j.neulet.2010.06.006

165.	Kromer R, Serbecic N, Hausner L, Froelich L, Aboul-Enein F,

Beutelspacher SC. Detection of retinal nerve fiber layer defects in Alzheimer's disease using SD-OCT. *Front Psychiatry*. 2014;5(FEB). doi:10.3389/fpsyt.2014.00022

166.   Marziani E, Pomati S, Ramolfo P, et al. Evaluation of retinal nerve fiber layer and ganglion cell layer thickness in Alzheimer's disease using spectral- domain optical coherence tomography. *Investig Ophthalmol Vis Sci*. 2013;54(9):5953-5958. doi:10.1167/iovs.13-12046

167.   Liu YL, Hsieh YT, Chen TF, et al. Retinal ganglion cell–inner plexiform layer thickness is nonlinearly associated with cognitive impairment in the community-dwelling elderly. *Alzheimer's Dement Diagnosis, Assess Dis Monit*. 2019;11:19-27. doi:10.1016/j.dadm.2018.10.006

168.   Dubois B, Hampel H, Feldman HH, et al. Preclinical Alzheimer's disease: Definition, natural history, and diagnostic criteria. *Alzheimer's Dement*. 2016;12(3):292-323. doi:10.1016/j.jalz.2016.02.002

169.   Buccarello L, Sclip A, Sacchi M, et al. The c-jun N-terminal kinase plays a key role in ocular degenerative changes in a mouse model of alzheimer disease suggesting a correlation between ocular and brain pathologies. *Oncotarget*. 2017;8(47):83038-83051. doi:10.18632/oncotarget.19886

170.   Georgevsky D, Retsas S, Raoufi N, Shimoni O, Golzan SM. A longitudinal assessment of retinal function and structure in the APP/PS1 transgenic mouse model of Alzheimer's disease. *Transl Neurodegener*. 2019;8(1). doi:10.1186/s40035-019-0170-z

171.   Lim JKH, Li Q-X, He Z, et al. Retinal Functional and Structural Changes in the 5xFAD Mouse Model of Alzheimer's Disease. *Front Neurosci*. 2020;14:862. doi:10.3389/fnins.2020.00862

172.   Cunha LP, Lopes LC, Costa-Cunha LVF, et al. Macular thickness measurements with frequency domain-oct for quantification of retinal neural loss and its correlation with cognitive impairment in Alzheimer?S disease. *PLoS One*. 2016;11(4). doi:10.1371/journal.pone.0153830

173.   Grimaldi A, Brighi C, Peruzzi G, et al. Inflammation, neurodegeneration and protein aggregation in the retina as ocular biomarkers for Alzheimer's disease in the 3xTg-AD mouse model. *Cell Death Dis*. 2018;9(6):685. doi:10.1038/s41419-018-0740-5

174. Williams PA, Thirgood RA, Oliphant H, et al. Retinal ganglion cell dendritic degeneration in a mouse model of Alzheimer's disease. *Neurobiol Aging*. 2013;34(7):1799-1806. doi:10.1016/j.neurobiolaging.2013.01.006

175. Gupta VK, Chitranshi N, Gupta VB, et al. Amyloid β accumulation and inner retinal degenerative changes in Alzheimer's disease transgenic mouse. *Neurosci Lett*. 2016;623:52-56. doi:10.1016/j.neulet.2016.04.059

176. Carroll JC, Rosario ER, Kreimer S, et al. Sex differences in beta-amyloid accumulation in 3xTg-AD mice: role of neonatal sex steroid hormone exposure. *Brain Res*. 2010;1366:233-245. doi:10.1016/j.brainres.2010.10.009

177. Ferguson LR, Dominguez JM, Balaiya S, Grover S, Chalam K V. Retinal Thickness Normative Data in Wild-Type Mice Using Customized Miniature SD-OCT. *PLoS One*. 2013;8(6). doi:10.1371/journal.pone.0067265

178. Gao H, Hollyfield JG. Aging of the human retina: Differential loss of neurons and retinal pigment epithelial cells. *Investig Ophthalmol Vis Sci*. 1992;33(1):1-17.

179. Bell K, Rosignol I, Sierra-Filardi E, et al. Age related retinal Ganglion cell susceptibility in context of autophagy deficiency. *Cell Death Discov*. 2020;6(1):21. doi:10.1038/s41420-020-0257-4

180. Lin B, Peng EB. Retinal Ganglion Cells are Resistant to Photoreceptor Loss in Retinal Degeneration. Lewin A, ed. *PLoS One*. 2013;8(6):e68084. doi:10.1371/journal.pone.0068084

181. Gardner MR, Baruah V, Vargas G, Motamedi M, Milner TE, Rylander HG. Scattering Angle Resolved Optical Coherence Tomography Detects Early Changes in 3xTg Alzheimer's Disease Mouse Model. *Transl Vis Sci Technol*. 2020;9(5). https://doi.org/10.1167/tvst.9.5.18. Accessed August 31, 2020.

182. Harper DJ, Augustin M, Lichtenegger A, et al. Retinal analysis of a mouse model of Alzheimer's disease with multicontrast optical coherence tomography. *Neurophotonics*. 2020;7(01):1. doi:10.1117/1.nph.7.1.015006

183. Fujino Y, DeLucia MW, Davies P, Dickson DW. Ballooned neurones in the limbic lobe are associated with Alzheimer type pathology and lack diagnostic specificity. *Neuropathol Appl Neurobiol*. 2004;30(6):676-682. doi:10.1111/j.1365-

2990.2004.00593.x

184.   Reichenbach A, Wurm A, Pannicke T, Iandiev I, Wiedemann P, Bringmann A. Müller cells as players in retinal degeneration and edema. *Graefe's Arch Clin Exp Ophthalmol*. 2007;245(5):627-636. doi:10.1007/s00417-006-0516-y

185.   Oliveira-Souza FG, DeRamus ML, van Groen T, Lambert AE, Bolding MS, Strang CE. Retinal changes in the Tg-SwDI mouse model of Alzheimer's disease. *Neuroscience*. 2017;354. doi:10.1016/j.neuroscience.2017.04.021

186.   Hill JM, Dua P, Clement C, Lukiw WJ. An evaluation of progressive amyloidogenic and pro-inflammatory change in the primary visual cortex and retina in Alzheimer's disease (AD). *Front Neurosci*. 2014;8(OCT):347. doi:10.3389/fnins.2014.00347

187.   Grimaldi A, Pediconi N, Oieni F, et al. Neuroinflammatory Processes, A1 Astrocyte Activation and Protein Aggregation in the Retina of Alzheimer's Disease Patients, Possible Biomarkers for Early Diagnosis. *Front Neurosci*. 2019;13:925. doi:10.3389/fnins.2019.00925

188.   Ning A, Cui J, To E, Ashe KH, Matsubara J. Amyloid-β deposits lead to retinal degeneration in a mouse model of Alzheimer disease. *Investig Ophthalmol Vis Sci*. 2008;49(11):5136-5143. doi:10.1167/iovs.08-1849

189.   Chidlow G, Wood JPM, Manavis J, Finnie J, Casson RJ. Investigations into Retinal Pathology in the Early Stages of a Mouse Model of Alzheimer's Disease. *J Alzheimer's Dis*. 2017;56(2):655-675. doi:10.3233/JAD-160823

190.   Cho SM, Lee S, Yang SH, et al. Age-dependent inverse correlations in CSF and plasma amyloid-β(1-42) concentrations prior to amyloid plaque deposition in the brain of 3xTg-AD mice. *Sci Rep*. 2016;6(1):1-9. doi:10.1038/srep20185

191.   Shariati MA, Park JH, Liao YJ. Optical coherence tomography study of retinal changes in normal aging and after ischemia. *Investig Ophthalmol Vis Sci*. 2015;56(5):2790-2797. doi:10.1167/iovs.14-15145

192.   Cenni MC, Bonfanti L, Martinou JC, Ratto GM, Strettoi E, Maffei L. Long-term survival of retinal ganglion cells following optic nerve section in adult bcl-2 transgenic mice. *Eur J Neurosci*. 1996;8(8):1735-1745. doi:10.1111/j.1460-9568.1996.tb01317.x

193.   Samuel MA, Zhang Y, Meister M, Sanes JR. Age-related alterations in neurons of the mouse retina. *J Neurosci*. 2011;31(44):16033-16044. doi:10.1523/JNEUROSCI.3580-11.2011

194.   Barron AM, Garcia-Segura LM, Caruso D, et al. Ligand for Translocator Protein Reverses Pathology in a Mouse Model of Alzheimer's Disease. *J Neurosci*. 2013;33(20):8891-8897. doi:10.1523/JNEUROSCI.1350-13.2013

195.   Peng J, Liang G, Inan S, et al. Dantrolene ameliorates cognitive decline and neuropathology in Alzheimer triple transgenic mice. *Neurosci Lett*. 2012;516(2):274-279. doi:10.1016/j.neulet.2012.04.008

196.   Rothman SM, Herdener N, Camandola S, et al. 3xTgAD mice exhibit altered behavior and elevated Aβ after chronic mild social stress. *Neurobiol Aging*. 2012;33(4):830.e1-830.e12. doi:10.1016/j.neurobiolaging.2011.07.005

197.   Galindo-Romero C, Avilés-Trigueros M, Jiménez-López M, et al. Axotomy-induced retinal ganglion cell death in adult mice: Quantitative and topographic time course analyses. 2011. doi:10.1016/j.exer.2011.02.008

198.   Berisha F, Feke GT, Trempe CL, McMeel JW, Schepens CL. Retinal abnormalities in early Alzheimer's disease. *Investig Ophthalmol Vis Sci*. 2007;48(5):2285-2289. doi:10.1167/iovs.06-1029

199.   Kesler A, Vakhapova V, Korczyn AD, Naftaliev E, Neudorfer M. Retinal thickness in patients with mild cognitive impairment and Alzheimer's disease. *Clin Neurol Neurosurg*. 2011;113(7):523-526. doi:10.1016/j.clineuro.2011.02.014

200.   He XF, Liu YT, Peng C, Zhang F, Zhuang S, Zhang JS. Optical coherence tomography assessed retinal nerve fiber layer thickness in patients with Alzheimer's disease: A meta-analysis. *Int J Ophthalmol*. 2012;5(3). doi:10.3980/j.issn.2222-3959.2012.03.30

201.   Castillo-Carranza DL, Nilson AN, Van Skike CE, et al. Cerebral Microvascular Accumulation of Tau Oligomers in Alzheimer's Disease and Related Tauopathies. *Aging Dis*. 2017;8(3):257-266. doi:10.14336/AD.2017.0112

202.   Grammas P. Neurovascular dysfunction, inflammation and endothelial activation: implications for the pathogenesis of Alzheimer's disease. *J Neuroinflammation*. 2011;8(1):26. doi:10.1186/1742-2094-8-26

203.	Koizumi K, Wang G, Park L. Endothelial Dysfunction and Amyloid-β-Induced Neurovascular Alterations. *Cell Mol Neurobiol*. 2016;36(2):155-165. doi:10.1007/s10571-015-0256-9

204.	Sagare AP, Bell RD, Zlokovic B V. Neurovascular defects and faulty amyloid-β vascular clearance in Alzheimer's disease. Perry G, Zhu X, Smith MA, Sorensen A, Avila J, eds. *J Alzheimers Dis*. 2013;33 Suppl 1(s1):S87-100. doi:10.3233/JAD-2012-129037

205.	Bourassa P, Tremblay C, Schneider JA, Bennett DA, Calon F. Beta-amyloid pathology in human brain microvessel extracts from the parietal cortex: relation with cerebral amyloid angiopathy and Alzheimer's disease. *Acta Neuropathol*. 2019;137(5):801-823. doi:10.1007/s00401-019-01967-4

206.	Sakai K, Boche D, Carare R, et al. Aβ immunotherapy for Alzheimer's disease: effects on apoE and cerebral vasculopathy. *Acta Neuropathol*. 2014;128(6):777-789. doi:10.1007/s00401-014-1340-9

207.	Wang Z, Das SR, Xie SX, Arnold SE, Detre JA, Wolk DA. Arterial spin labeled MRI in prodromal Alzheimer's disease: A multi-site study. *NeuroImage Clin*. 2013;2(1):630-636. doi:10.1016/j.nicl.2013.04.014

208.	Duggan E, Smith CA, Hooper ML, Chauhan BC. Colocalization of optical coherence tomography angiography with histology in the mouse retina. *Microvasc Res*. 2020;132:104055. doi:10.1016/j.mvr.2020.104055

209.	Paques M, Tadayoni R, Sercombe R, et al. Structural and Hemodynamic Analysis of the Mouse Retinal Microcirculation. *Investig Ophthalmol Vis Sci*. 2003;44(11):4960-4967. doi:10.1167/iovs.02-0738

210.	Ganesan P, He S, Xu H. Development of an image-based model for capillary vasculature of retina. *Comput Methods Programs Biomed*. 2011;102(1):35-46. doi:10.1016/j.cmpb.2010.12.009

211.	Hagino N, Kobayashi S, Tsutsumi T, et al. Vascular change of hippocampal capillary is associated with vascular change of retinal capillary in aging. *Brain Res Bull*. 2004;62(6):537-547. doi:10.1016/S0361-9230(03)00082-0

212.	Ravi Teja KV, Berendschot TJM T, Steinbusch H, Webers AB C, Murthy R P, PS M. Cerebral and Retinal Neurovascular Changes: A Biomarker for Alzheimer's

Disease. *J Gerontol Geriatr Res*. 2017;06(04). doi:10.4172/2167-7182.1000447

213.   Lesage SR, Mosley TH, Wong TY, et al. Retinal microvascular abnormalities and cognitive decline: The ARIC 14-year follow-up study. *Neurology*. 2009;73(11):862-868. doi:10.1212/WNL.0b013e3181b78436

214.   Dutescu RM, Li Q-X, Crowston J, Masters CL, Baird PN, Culvenor JG. Amyloid precursor protein processing and retinal pathology in mouse models of Alzheimer's disease. *Graefes Arch Clin Exp Ophthalmol*. 2009;247(9):1213-1221. doi:10.1007/s00417-009-1060-3

215.   Liu B, Rasool S, Yang Z, et al. Amyloid-peptide vaccinations reduce {beta}-amyloid plaques but exacerbate vascular deposition and inflammation in the retina of Alzheimer's transgenic mice. *Am J Pathol*. 2009;175(5):2099-2110. doi:10.2353/ajpath.2009.090159

216.   Fan Xia, Yonju Ha, Shuizhen Shi, Yi Li, Shengguo Li, Jonathan Luisi, Rakez Kayed, Massoud Motamedi, Hua Liu WZ. Early alterations of neurovascular unit in the retina in mouse models of tauopathy. *Mol Neurodegener*. 2021.

217.   Grewal DS, Polascik BW, Hoffmeyer GC, Fekrat S. Assessment of Differences in Retinal Microvasculature Using OCT Angiography in Alzheimer's Disease: A Twin Discordance Report. *Ophthalmic Surgery, Lasers Imaging Retin*. 2018;49(6):440-444. doi:10.3928/23258160-20180601-09

218.   Kornfield TE, Newman EA. Regulation of blood flow in the retinal trilaminar vascular network. *J Neurosci*. 2014;34(34):11504-11513. doi:10.1523/JNEUROSCI.1971-14.2014

219.   Carroll JC, Rosario ER, Kreimer S, et al. Sex differences in β-amyloid accumulation in 3xTg-AD mice: Role of neonatal sex steroid hormone exposure. *Brain Res*. 2010;1366:233-245. doi:10.1016/j.brainres.2010.10.009

220.   Hossein Nazari, Maxim Ivannikov, Lorenzo Ochoa, Gracie Vargas MM. Microsurgical Dissection and Tissue Clearing for High Resolution Intact Whole Retina and Vitreous Imaging. *J Vis Exp*. 2021:e61595. doi:10.3791/61595 (2021).

221.   Fernández-Sánchez L, Esquiva G, Pinilla I, Lax P, Cuenca N. Retinal Vascular Degeneration in the Transgenic P23H Rat Model of Retinitis Pigmentosa. *Front Neuroanat*. 2018;12:55. doi:10.3389/fnana.2018.00055

222.   Zudaire E, Gambardella L, Kurcz C, Vermeren S. A computational tool for quantitative analysis of vascular networks. *PLoS One*. 2011;6(11):27385. doi:10.1371/journal.pone.0027385

223.   Sugano Y, Sekiryu T, Furuta M, et al. Morphometrical evaluation of the choriocapillaris imaged by swept-source optical coherence tomography angiography. *Clin Ophthalmol*. 2018;12:2267-2276. doi:10.2147/OPTH.S179634

224.   Singh JN, Nowlin TM, Seedorf GJ, Abman SH, Shepherd DP. Quantifying three-dimensional rodent retina vascular development using optical tissue clearing and light-sheet microscopy. *J Biomed Opt*. 2017;22(7):076011. doi:10.1117/1.jbo.22.7.076011

225.   Wälchli T, Mateos JM, Weinman O, et al. Quantitative assessment of angiogenesis, perfused blood vessels and endothelial tip cells in the postnatal mouse brain. *Nat Protoc*. 2015;10(1):53-74. doi:10.1038/nprot.2015.002

226.   Zudaire E, Gambardella L, Kurcz C, Vermeren S. A computational tool for quantitative analysis of vascular networks. *PLoS One*. 2011;6(11). doi:10.1371/journal.pone.0027385

227.   Pinheiro J, Bates D, R-core. nlme: Linear and Nonlinear Mixed Effects Models. 2020.

228.   R Core Team. R: A Language and Environment for Statistical Computing. 2020.

229.   Sapieha P, Sirinyan M, Hamel D, et al. The succinate receptor GPR91 in neurons has a major role in retinal angiogenesis. *Nat Med*. 2008;14(10):1067-1076. doi:10.1038/nm.1873

230.   Nortley R, Korte N, Izquierdo P, et al. Amyloid b oligomers constrict human capillaries in Alzheimer's disease via signaling to pericytes. *Science (80-)*. 2019;365(6450). doi:10.1126/science.aav9518

231.   Bennett RE, Robbins AB, Hu M, et al. Tau induces blood vessel abnormalities and angiogenesis-related gene expression in P301L transgenic mice and human Alzheimer's disease. *Proc Natl Acad Sci U S A*. 2018;115(6):E1289-E1298. doi:10.1073/pnas.1710329115

232.   Meyer EP, Ulmann-Schuler A, Staufenbiel M, Krucker T. Altered

morphology and 3D architecture of brain vasculature in a mouse model for Alzheimer's disease. *Proc Natl Acad Sci U S A*. 2008;105(9):3587-3592. doi:10.1073/pnas.0709788105

233.   Schager B, Brown CE. Susceptibility to capillary plugging can predict brain region specific vessel loss with aging. *J Cereb Blood Flow Metab*. 2020;40(12):2475-2490. doi:10.1177/0271678X19895245

234.   Buée L, Hof PR, Bouras C, et al. Pathological alterations of the cerebral microvasculature in Alzheimer's disease and related dementing disorders. *Acta Neuropathol*. 1994;87(5):469-480. doi:10.1007/BF00294173

235.   Fischer VW, Siddiqi A, Yusufaly Y. Altered angioarchitecture in selected areas of brains with Alzheimer's disease. *Acta Neuropathol*. 1990;79(6):672-679. doi:10.1007/BF00294246

236.   Zhang X, Yin X, Zhang J, et al. High-resolution mapping of brain vasculature and its impairment in the hippocampus of Alzheimer's disease mice. *Natl Sci Rev*. 2019;6(6):1223-1238. doi:10.1093/nsr/nwz124

237.   Paris D, Patel N, Delledonne A, Quadros A, Smeed R, Mullan M. Impaired angiogenesis in a transgenic mouse model of cerebral amyloidosis. *Neurosci Lett*. 2004;366(1):80-85. doi:10.1016/j.neulet.2004.05.017

238.   Kornfield TE, Newman EA. Regulation of Blood Flow in the Retinal Trilaminar Vascular Network. 2014. doi:10.1523/JNEUROSCI.1971-14.2014

239.   Lau JCM, Linsenmeier RA. Oxygen consumption and distribution in the Long-Evans rat retina. *Exp Eye Res*. 2012;102:50-58. doi:10.1016/j.exer.2012.07.004

240.   Curcio CA. Photoreceptor topography in ageing and age-related maculopathy. *Eye*. 2001;15(3):376-383. doi:10.1038/eye.2001.140

241.   Cunea A, Powner MB, Jeffery G. Death by color: Differential cone loss in the aging mouse retina. *Neurobiol Aging*. 2014;35(11):2584-2591. doi:10.1016/j.neurobiolaging.2014.05.012

242.   Garrity ST, Iafe NA, Phasukkijwatana N, Chen X, Sarraf D. Quantitative analysis of three distinct retinal capillary plexuses in healthy eyes using optical coherence tomography angiography. *Investig Ophthalmol Vis Sci*. 2017;58(12):5548-5555. doi:10.1167/iovs.17-22036

243.   Feke GT, Hyman BT, Stern RA, Pasquale LR. Retinal blood flow in mild cognitive impairment and Alzheimer's disease. *Alzheimer's Dement (Amsterdam, Netherlands)*. 2015;1(2):144-151. doi:10.1016/j.dadm.2015.01.004

244.   O'Bryhim BE, Apte RS, Kung N, Coble D, Van Stavern GP. Association of Preclinical Alzheimer Disease With Optical Coherence Tomographic Angiography Findings. *JAMA Ophthalmol*. 2018;136(11):1242. doi:10.1001/jamaophthalmol.2018.3556

245.   Akula JD, Hansen RM, Martinez-Perez ME, Fulton AB. Rod photoreceptor function predicts blood vessel abnormality in retinopathy of prematurity. *Investig Ophthalmol Vis Sci*. 2007;48(9):4351-4359. doi:10.1167/iovs.07-0204

246.   Usui Y, Westenskow PD, Kurihara T, et al. Neurovascular crosstalk between interneurons and capillaries is required for vision. *J Clin Invest*. 2015;125(6):2335-2346. doi:10.1172/JCI80297

247.   Prahst C, Ashrafzadeh P, Mead T, et al. Mouse retinal cell behaviour in space and time using light sheet fluorescence microscopy. *Elife*. 2020;9. doi:10.7554/eLife.49779

248.   Henning Y, Osadnik C, Malkemper EP. *EyeCi: Optical Clearing and Imaging of Immunolabeled Mouse Eyes Using Light-Sheet Fluorescence Microscopy*. Vol 180. Academic Press; 2019:137-145. doi:10.1016/j.exer.2018.12.001

249.   Chang C-C, Chu A, Meyer S, et al. Selective Plane Illumination Microscopy and Computing Reveal Differential Obliteration of Retinal Vascular Plexuses. *bioRxiv*. May 2020:2020.05.06.081463. doi:10.1101/2020.05.06.081463

250.   Vigouroux RJ, César Q, Chédotal A, Nguyen-Ba-Charvet KT. Revisiting the role of DCC in visual system development with a novel eye clearing method. *Elife*. 2020;9. doi:10.7554/eLife.51275

251.   Kim SY, Assawachananont J. A new method to visualize the intact subretina from retinal pigment epithelium to retinal tissue in whole mount of pigmented mouse eyes. *Transl Vis Sci Technol*. 2016;5(1):1-8. doi:10.1167/tvst.5.1.6

252.   Kayatz P, Thumann G, Luther TT et al. Oxidation causes melanin fluorescence. *Invest Ophthalmol Vis Sci*. 2001;42(1):241-246.

253.   Iwai-Takekoshi L, Ramos A, Schaler A, Weinreb S, Blazeski R, Mason C.

Retinal pigment epithelial integrity is compromised in the developing albino mouse retina. *J Comp Neurol*. 2016;524(18):3696-3716. doi:10.1002/cne.24025

254.   Alexander RA, Cree IA FA. The immunoalkaline phosphatase technique in immunohistochemistry: the effect of permanganate-oxalate melanin bleaching upon four final reaction products. *Br J Biomed Sci*. 1996;53(2):170-171.

255.   Ueda HR, Dodt HU, Osten P, Economo MN, Chandrashekar J, Keller PJ. Whole-Brain Profiling of Cells and Circuits in Mammals by Tissue Clearing and Light-Sheet Microscopy. *Neuron*. 2020;106(3):369-387. doi:10.1016/j.neuron.2020.03.004

256.   Hillman EMC, Voleti V, Li W, Yu H. Light-Sheet Microscopy in Neuroscience. *Annu Rev Neurosci*. 2019;42(1):295-313. doi:10.1146/annurev-neuro-070918-050357

257.   Jing D, Zhang S, Luo W, et al. Tissue clearing of both hard and soft tissue organs with the pegasos method. *Cell Res*. 2018;28(8):803-818. doi:10.1038/s41422-018-0049-z

258.   Tainaka K, Kubota SI, Suyama TQ, et al. Whole-body imaging with single-cell resolution by tissue decolorization. *Cell*. 2014;159(4):911-924. doi:10.1016/j.cell.2014.10.034

259.   Hohberger B, Baumgart C, Bergua A. Optical clearing of the eye using the See Deep Brain technique. *Eye (Lond)*. 2017;31(10):1496-1502. doi:10.1038/eye.2017.83

260.   Kuwajima T, Sitko AA, Bhansali P, Jurgens C, Guido W, Mason C. ClearT: A detergent- and solvent-free clearing method for neuronal and non-neuronal tissue. *Dev*. 2013;140(6):1364-1368. doi:10.1242/dev.091844

261.   Lee H, Park JH, Seo I, Park SH, Kim S. Improved application of the electrophoretic tissue clearing technology, CLARITY, to intact solid organs including brain, pancreas, liver, kidney, lung, and intestine. *BMC Dev Biol*. 2014;14(1). doi:10.1186/s12861-014-0048-3

262.   Pan C, Cai R, Quacquarelli FP, et al. Shrinkage-mediated imaging of entire organs and organisms using uDISCO. *Nat Methods*. 2016;13(10):859-867. doi:10.1038/nmeth.3964

263.   Hegde S, Srivastava O. Different gene knockout/transgenic mouse models manifesting persistent fetal vasculature: Are integrins to blame for this pathological

condition? 2016. doi:10.1016/j.lfs.2016.12.019

264.   Hartnett ME, Penn JS. Mechanisms and Management of Retinopathy of Prematurity. *N Engl J Med*. 2012;367(26):2515-2526. doi:10.1056/NEJMra1208129

265.   Pierce EA, Foley ED, Smith LEH. Regulation of vascular endothelial growth factor by oxygen in a model of retinopathy of prematurity. *Arch Ophthalmol*. 1996;114(10):1219-1228. doi:10.1001/archopht.1996.01100140419009

266.   Ash J, McLeod DS, Lutty GA. Transgenic expression of leukemia inhibitory factor (LIF) blocks normal vascular development but not pathological neovascularization in the eye. *Mol Vis*. 2005;11:298-308. http://www.ncbi.nlm.nih.gov/pubmed/15889014. Accessed January 21, 2020.

267.   Reichel MB, Ali RR, D'Esposito F, et al. High frequency of persistent hyperplastic primary vitreous and cataracts in p53-deficient mice. *Cell Death Differ*. 1998;5(2):156-162. doi:10.1038/sj.cdd.4400326

268.   Gage GJ, Kipke DR, Shain W. Whole animal perfusion fixation for rodents. *J Vis Exp*. 2012;(65). doi:10.3791/3564

269.   Kirshner H, Aguet F, Sage D, Unser M. 3-D PSF fitting for fluorescence microscopy: Implementation and localization application. *J Microsc*. 2013;249(1):13-25. doi:10.1111/j.1365-2818.2012.03675.x

270.   Hörl D, Rojas Rusak F, Preusser F, et al. BigStitcher: reconstructing high-resolution image datasets of cleared and expanded samples. *Nat Methods*. 2019;16(9):870-874. doi:10.1038/s41592-019-0501-0

271.   Susaki EA, Ueda HR. Whole-body and Whole-Organ Clearing and Imaging Techniques with Single-Cell Resolution: Toward Organism-Level Systems Biology in Mammals. *Cell Chem Biol*. 2016;23(1):137-157. doi:10.1016/j.chembiol.2015.11.009

272.   Tian B, Liu Z, Litvinov J, et al. Efficacy of novel highly specific bromodomain-containing protein 4 inhibitors in innate inflammation–driven airway remodeling. *Am J Respir Cell Mol Biol*. 2019;60(1):68-83. doi:10.1165/rcmb.2017-0445OC

273.   Zaman RT, Rajaram N, Nichols BS, et al. Changes in morphology and optical properties of sclera and choroidal layers due to hyperosmotic agent. *J Biomed*

Opt. 2011;16(7):077008. doi:10.1117/1.3599985

274.   Staudt T, Lang MC, Medda R, Engelhardt J, Hell SW. 2,2′-Thiodiethanol: A new water soluble mounting medium for high resolution optical microscopy. *Microsc Res Tech*. 2007;70(1):1-9. doi:10.1002/jemt.20396

275.   Aoyagi Y, Kawakami R, Osanai H, Hibi T, Nemoto T. A rapid optical clearing protocol using 2,2′-thiodiethanol for microscopic observation of fixed mouse brain. *PLoS One*. 2015;10(1). doi:10.1371/journal.pone.0116280

276.   Icha J, Schmied C, Sidhaye J, Tomancak P, Preibisch S, Norden C. Using Light Sheet Fluorescence Microscopy to Image Zebrafish Eye Development. *J Vis Exp*. 2016;(110):53966. doi:10.3791/53966

277.   Hohsfield LA, Daschil N, Orädd G, Strömberg I, Humpel C. Vascular pathology of 20-month-old hypercholesterolemia mice in comparison to triple-transgenic and APPSwDI Alzheimer's disease mouse models. *Mol Cell Neurosci*. 2014;63:83-95. doi:10.1016/j.mcn.2014.10.006

278.   Chua J, Hu Q, Ke M, et al. Retinal Microvascular Alterations in Alzheimer's Disease and Mild Cognitive Impairment. doi:10.21203/rs.3.rs-37801/v1

279.   Bennett RE, Robbins AB, Hu M, et al. Tau induces blood vessel abnormalities and angiogenesis-related gene expression in P301L transgenic mice and human Alzheimer's disease. *Proc Natl Acad Sci U S A*. 2018;115(6):E1289-E1298. doi:10.1073/pnas.1710329115

280.   Krantic S, Isorce N, Mechawar N, et al. Hippocampal GABAergic neurons are susceptible to amyloid-β toxicity in vitro and are decreased in number in the Alzheimer's disease TgCRND8 mouse model. *J Alzheimers Dis*. 2012;29(2):293-308. doi:10.3233/JAD-2011-110830

281.   Wostyn P, Killer HE, De Deyn PP. Glymphatic stasis at the site of the lamina cribrosa as a potential mechanism underlying open-angle glaucoma. *Clin Experiment Ophthalmol*. 2017;45(5):539-547. doi:10.1111/ceo.12915

282.   Wang X, Lou N, Eberhardt A, et al. An ocular glymphatic clearance system removes β-amyloid from the rodent eye. *Sci Transl Med*. 2020;12(536). doi:10.1126/scitranslmed.aaw3210

283.   Wostyn P, De Groot V, Van Dam D, Audenaert K, Killer HE, De Deyn

PP. Age-related macular degeneration, glaucoma and Alzheimer's disease: amyloidogenic diseases with the same glymphatic background? *Cell Mol Life Sci*. 2016;73(22):4299-4301. doi:10.1007/s00018-016-2348-1

284.   Sen S, Saxena R, Tripathi M, Vibha D, Dhiman R. Neurodegeneration in Alzheimer's disease and glaucoma: overlaps and missing links. *Eye*. 2020;34(9):1546-1553. doi:10.1038/s41433-020-0836-x

285.   Di Marco LY, Venneri A, Farkas E, Evans PC, Marzo A, Frangi AF. Vascular dysfunction in the pathogenesis of Alzheimer's disease--A review of endothelium-mediated mechanisms and ensuing vicious circles. *Neurobiol Dis*. 2015;82:593-606. doi:10.1016/j.nbd.2015.08.014

286.   Joyal JS, Gantner ML, Smith LEH. Retinal energy demands control vascular supply of the retina in development and disease: The role of neuronal lipid and glucose metabolism. *Progress in Retinal and Eye Research*. 2017.

287.   Lim JKH, Li Q-X, He Z, et al. The Eye As a Biomarker for Alzheimer's Disease. *Front Neurosci*. 2016;10:536. doi:10.3389/fnins.2016.00536

288.   London A, Benhar I, Schwartz M. The retina as a window to the brain-from eye research to CNS disorders. *Nat Rev Neurol*. 2013;9(1):44-53. doi:10.1038/nrneurol.2012.227

289.   Bell MA, Ball MJ. *Acta Neuropathologica Morphometric Comparison of Hippocampal Microvasculature in Ageing and Demented People: Diameters and Densities*. Vol 53.; 1981.

290.   Yang SP, Bae DG, Kang HJ, Gwag BJ, Gho YS, Chae CB. Co-accumulation of vascular endothelial growth factor with β-amyloid in the brain of patients with Alzheimer's disease. *Neurobiol Aging*. 2004;25(3):283-290. doi:10.1016/S0197-4580(03)00111-8

291.   Casserly I, Topol E. Convergence of atherosclerosis and Alzheimer's disease: Inflammation, cholesterol, and misfolded proteins. *Lancet*. 2004;363(9415):1139-1146. doi:10.1016/S0140-6736(04)15900-X

292.   Pennesi ME, Michaels K V., Magee SS, et al. Long-term characterization of retinal degeneration in rd1 and rd10 mice using spectral domain optical coherence tomography. *Investig Ophthalmol Vis Sci*. 2012;53(8):4644-4656. doi:10.1167/iovs.12-

9611

293.   Hong S, Beja-Glasser VF, Nfonoyim BM, et al. Complement and microglia mediate early synapse loss in Alzheimer mouse models. *Science (80-)*. 2016;352(6286):712-716. doi:10.1126/science.aad8373

294.   Cai Z, Hussain MD, Yan LJ. Microglia, neuroinflammation, and beta-amyloid protein in Alzheimer's disease. *Int J Neurosci*. 2014;124(5):307-321. doi:10.3109/00207454.2013.833510

295.   Hansen D V., Hanson JE, Sheng M. Microglia in Alzheimer's disease. *J Cell Biol*. 2018;217(2):459-472. doi:10.1083/jcb.201709069

296.   Beach TG, McGeer EG. Lamina-specific arrangement of astrocytic gliosis and senile plaques in Alzheimer's disease visual cortex. *Brain Res*. 1988;463(2):357-361. doi:10.1016/0006-8993(88)90410-6

297.   Mrak RE, Sheng JG, Griffin WST. Correlation of astrocytic S100β expression with dystrophie neurites in amyloid plaques of Alzheimer's disease. *J Neuropathol Exp Neurol*. 1996;55(3):273-279. doi:10.1097/00005072-199603000-00002

298.   Blanks JC, Schmidt SY, Torigoe Y, Porrello K V., Hinton DR, Blanks RHI. Retinal pathology in Alzheimer's disease. II. Regional neuron loss and glial changes in GCL. *Neurobiol Aging*. 1996;17(3):385-395. doi:10.1016/0197-4580(96)00009-7

299.   Pekny M, Pekna M. Reactive gliosis in the pathogenesis of CNS diseases. *Biochim Biophys Acta - Mol Basis Dis*. 2016;1862(3):483-491. doi:10.1016/j.bbadis.2015.11.014

300.   Zhao Y, Xin Y, He Z, Hu W. Function of connexins in the interaction between glial and vascular cells in the central nervous system and related neurological diseases. *Neural Plast*. 2018;2018. doi:10.1155/2018/6323901

301.   Arranz AM, De Strooper B. The role of astroglia in Alzheimer's disease: pathophysiology and clinical implications. *Lancet Neurol*. 2019;18(4):406-414. doi:10.1016/S1474-4422(18)30490-3

302.   Hart NJ, Koronyo Y, Black KL, Koronyo-Hamaoui M. Ocular indicators of Alzheimer's: exploring disease in the retina. *Acta Neuropathol*. 2016;132(6):767-787. doi:10.1007/s00401-016-1613-6

<h1 align="center">Vita</h1>

Hossein Nazari, MD, PhD

Department of Ophthalmology and Visual Neurosciences

University of Minnesota

516 Delaware St SE, Floor 9

Minneapolis, MN 55455

Phone: 3107741366

Email: nazari@umn.edu   h.nazari.k@gmail.com

Education:

2015-2021: PhD in Neurosciences; UTMB, Galveston, Texas

2019-2020: Vitreoretinal Surgery Fellowship, University of Minnesota, Minneapolis, Minnesota

2016-2019: Ophthalmology Residency; UTMB, Galveston, Texas

2015-2016: Internship; UTMB, Galveston, Texas

2006-2007: Vitreoretinal Surgery Fellowship: Iran University of Medical Sciences (IUMS), Tehran, Iran

2000-2004: Ophthalmology Residency: Tabriz University of Medical Sciences, Tabriz, Iran

1991-1998: Undergraduate and Medical School: Zanjan University of Medical Sciences, Zanjan, Iran

Professional and teaching experience:

2020-cont' Assistant Professor, Vitreoretinal Surgery Service, Department of Ophthalmology and Visual Neurosciences, University of Minnesota, Minneapolis, MN

2014-2015 Adjunct faculty, Department of Ophthalmology, University of Southern California, Los Angeles

2010-2014 Research fellow, University of Southern California, Los Angeles, California

2007-2010 Assistant professor, Department of Ophthalmology, IUMS, Tehran, Iran

2004-2006 Comprehensive ophthalmology, Iran

Honors:

Rapid Response Grant, University of Minnesota; 2020

Fellowship research award: University of Minnesota; 2020

Surgical Video presentation, Vit-Buckle Society annual meeting; 2020

Research Scholarship Award, UTMB Ophthalmology Residency Program; 2019

Silver Scalpel Award; UTMB Ophthalmology Residency Program; 2019

Academic Achievement Award, UTMB Ophthalmology Residency Program; 2019

Academic Achievement Award; UTMB Ophthalmology Residency Program; 2018

Academic Achievement Award; UTMB Ophthalmology Residency Program; 2017

First presentation award, Sun and Science: National Eye Resident Research Conference, UTMB, 2016

National Institute of Health (NEI)/Association for Research in Vision and Ophthalmology (ARVO) travel award, ARVO annual meeting 2014

Doheny Eye Institute Basic Science Award, 2013

California Institute for Regenerative Medicine (CIRM) training award for stem cell research 2012

Publications (current h-index 20):

A. Papers in peer reviewed journals:

1. Nazari H, Ivannikov M, Ochoa L, Vargas G, Motamedi M. Microsurgical Dissection and Tissue Clearing for High Resolution Intact Whole Retina and Vitreous Imaging. J Vis Exp. 2020. doi: 10.3791/61595

2. Naravane A, Mundae R, Zhou Y, Santilli C, van Kuijk F, Nazari H, Yamanuha J, Emerson G, Koozekanani D, Montezuma S. Short term visual and structural outcomes of anti-vascular endothelial growth factor (anti-VEGF) treatment delay during the first COVID-19 wave: A pilot study. PLoS One 2021 Feb 17;16(2):e0247161

3. Nazari H, Emerson G, Tang PH. Intractable pain and diplopia after scleral buckle surgery. Retin Cases Brief Rep. 2020 Dec 7. doi: 10.1097/ICB.0000000000001104.

4. Nakatsuka A, Nazari H, Merkley K. Fishhook injury of the anterior chamber angle of the eye. Hawai'I Journal of Medicine and public Health. 2019 Jun; 78 (6):200-201

5.   Nakatsuka A, <u>Nazari H</u>, Lam Q, El Annan J. Intranasal Corticosteroids and Central Serous Chorioretinopathy: A Report and Review of the Literature. Hawai'i Journal of Medicine and Public Health. 2019 May; 78(5): 151-154

6.   <u>Nazari H</u>, Nakatsuka A, Soliman M. Optic Nerve Head Elevation in an Asymptomatic Child: Worry or Watch? Pediatr Neurol. 2018 May;82:55-56

7.   Sadaka A, Iqbal C, <u>Nazari H</u>, et al. Positive visual phenomena following the Argus II Retinal Prosthesis implantation. Ophthalmic Surg Lasers Imaging Retina 2017 Dec 1; 48 (12): 1022-1025

8.   <u>Nazari H</u>, Kim-Binh M, Yalamanchili S, Chang E. Metallic Filament Embolization of the Retinal Artery. JAMA Ophthalmol. 2017 Nov 1;135(11):1279-1281

9.   <u>Nazari H</u>, Falabella P, Yue L, Weiland J, Humayun M. Retinal Prostheses. Journal of Vitreoretinal Diseases 2017. 1-10

10.   <u>Nazari H</u>, Nakatsuka A, El Annan J. Smartphone fundus photography. J Vis Exp. 2017 Jul 6;(125).

11.   Thomas B, Zhu L, Zhang L, Thomas PB, <u>Nazari H</u>, et al. Survival and Functionality of hESC Derived Retinal Pigment Epithelium Cells Cultured as a Monolayer on Polymer Substrates Transplanted in RCS Rats. IOVS 2016; 57 (6):2877-87

12.   Murali K, Kang D, <u>Nazari H</u>, et al. Spatial Variations in Vitreous Oxygen Consumption. PLoS One. 2016 Mar 1;11(3):e0149961.

13.   Ishikawa K, Sreekumar PG, Spee C, <u>Nazari H</u>, et al. αB-crystallin regulates subretinal fibrosis by modulation of epithelial-mesenchymal transition. AJP 2016; 1864):859-73

14.   Abri Aghdam K, Joshaghani M, <u>Nazari H</u>, et al. Comparison of the effect of cycloplegic versus NSAID eye drops on pain after photorefractive keratectomy. J Curr Ophthalmol 2016. 27 (3-4):87-91

15.   Roybal CN, Sanfilippo CJ, <u>Nazari H</u>, et al. Multimodal imaging of the retinal and choroid in systemic amyloidosis. Retin Cases Brief Rep. 2015;9(4):339-46.

16.   He S, Barron E, Ishikawa K, <u>Nazari H</u>, et al. Inhibition of DNA Methylation and Methyl-CpG-Binding Protein 2 Suppresses RPE Transdifferentiation: Relevance to Proliferative Vitreoretinopathy. Invest Ophthalmol Vis Sci. 2015 Aug;56(9):5579-89

17.   Ghasemi Falavarjani K, <u>Nazari Khanamiri H</u>, et al. Determination of the

toxicity of intravitreal minocycline in rabbit eyes. Cutaneous and Ocular Toxicology 2016;35(3):233-6.

18. Nazari H, Zhang L, et al. Stem cell based therapies for age-related macular degeneration: The promises and the challenges. Prog Retin Eye Res. 2015; 48:1-39

19. Olmos L, Nazari H, Rodger D, Humayun M. Stem Cell Therapy for the Treatment of Dry Age-Related Macular Degeneration. Current Ophthalmology Reports 2015;

20. Hirsch L, Nazari H, Sreekumar PG, Kannan R, Dustin L, Zhu D, Barron E, Hinton DR. TGF-β2 secretion from RPE decreases with polarization and becomes apically oriented. Cytokine. 2015;71(2):394-6

21. Ishikawa K, He S, Terasaki H, Nazari H, et al. Resveratrol inhibits epithelial-to-mesenchymal transition of retinal pigment epithelium and development of proliferative vitreoretinopathy. Sci Rep 2015; 5: 16386

22. Naseripour M, Jaberi R, Sedaghat A, Azma Z, Nojomi M, Falavarjani KG, Nazari H. Ruthenium-106 brachytherapy for thick uveal melanoma: reappraisal of apex and base dose radiation and dose rate. J Contemp Brachytherapy. 2016 Feb;8(1):66-73.

23. Ghasemi Falavarjani K, Alemzadeh SA, Modarres M, Parvaresh MM, Hashemi M, Naseripour M, Nazari HK, Askari S. Scleral buckling surgery for rhegmatogenous retinal detachment with subretinal proliferation.Eye (Lond). 2015 Apr;29(4):509-14.

24. Askari M, Nikpoor AR, Nazari H, et al. Association of Apolipoprotein E Alleles with Susceptibility to Age-Related Macular Degeneration in Iranian Patients. Research in Molecular Medicine 2015; (3) 2:22-27.

25. Askari M, Nikpoor AR, Nazari H, et al. Association of Htra1 gene polymorphisms with the risk of developing AMD in Iranian population. Rep Biochem Mol Biol. 2015 Oct;4(1):43-9.

26. Nazari H, Karakousis P, Rao N. Replication of Mycobacterium tuberculosis in Retinal Pigment Epithelium. JAMA Ophthalmol 2014 June;132(6):724-9. PMID: 24723139

27. Nazari H, Ghasemi Falavarjani K, Sanati MH, Aryan A, Irani A, Hashemi M, Modarres M, Parvaresh MM, Nikeghbali A. Complement Factor H Y402H and LOC387715 A69S Polymorphisms in Association with Age-Related Macular Degeneration in Iran. Journal of Ophthalmic and Vision Research 2014;9(2):181-7.

28. Nazari H, Hariri A, Hu Z, et al. Choroidal atrophy and loss of choriocapillaris in convalescent stage of Vogt-Koyanagi-Harada disease: In vivo documentation. J Ophthalmic Inflamm Infect. 2014 Mar 22;4(1):9.

29. Parvaresh MM, Ghasemi Falavarjani K, Modarres M, Nazari H, Saiepour N. Transscleral Diode Laser Photocoagulation for Type 1 Prethreshold Retinopathy of Prematurity. Journal of Ophthalmic and Vision Research 2013; 8 (4):298-302.

30. Hong B, Nazari Khanamiri H, Rao N. The Role of Ultra-Widefield Fluorescein Angiography in the Management of Uveitis. Can J Ophthalmol 2013 Dec;48(6):489-93.

31. Nazari H, Rao NA. Serpiginous choroiditis and infectious multifocal serpiginoid choroiditis. Survey of Ophthalmology. 2013;58(3):203-32.

32. Nazari H, Dustin L, Heussen FM, Sadda SV, Rao N. Morphometric analysis of optical coherence tomography predicts visual outcome in uveitis patients with epiretinal membrane. American Journal of Ophthalmology 2012 Jul: 154(1):78-86.

33. Nazari H, Rao NA. Antitubercular therapy is not required in latent tuberculosis. Br J Ophthalmol 2012;96(3):463.

34. Nazari H, Rao NA. Longitudinal morphometric analysis of epiretinal membrane in patients with uveitis. Ocular Immunology and inflammation 2013;21(1):2-7.

35. Nazari H, Rao NA. Resolution of subretinal fluid with systemic corticosteroids treatment in acute Vogt-Koyanagi-Harada Disease. Br J Ophthalmol 2012;96(11):1410-4

36. Tayil S, Albini T, Nazari H, Moshfeghi AA, Parel JM, Rao NA, Karakousis PC. Local ischemia and increased expression of vascular endothelial growth factor following ocular dissemination of mycobacterium tuberculosis. PLoS ONE, 2011;6(12):e28383.

37. Ghasemi Falavarjani K, Hashemi M, Jalili Fazel A, Modarres M, Nazari H, Parvaresh M. Pars Plana vitrectomy and intravitreal phacoemulsification for Dropped Nuclei. J Ophthalmic Vis Res. 2012; 7 (2): 125-129.

38. Nazari H, Nilforushan N, Sedaghat A, Soudi R, Irani A, Gordiz, A, Hatamkhani S. Intraocular pressure after exposure to moderate altitude. Graefes Archives for Clinical and Experimental Ophthalmology 2013;251(1):123-7.

39. Joshaghani M, Nazari H, Ghasemi Falavarjani K, et al. Effect of Homatropine eye drops on pain after photorefractive keratectomy; a pilot study. Saudi Journal of

Ophthalmology 2013;27(2):83-87.

40.   M Naroi Nejad, M Yousefi, <u>Nazari H</u>, A Ghasempoor. Comparing carotid intima-media thickness in type 2 diabetes between patients with and without retinopathy. Tehran University Medical Journal (TUMJ) 2012; 70 (3):150-155.

41.   Modarres M, <u>Nazari H</u>, Rezaei Kanavi M, et al. Determination of safety of escalating doses of Intravitreal Erythropoietin in Rabbit Eyes. Iranian Journal of Ophthalmology. 2012;24(2):26-32.

42.   <u>Nazari H</u>, SM Modareszadeh, R Soudi, A Maleki, H Mirzajani. A review article of pharmacologic vitreolysis. Razi Journal of Medical Sciences 18 (82), 32-43

43.   Modarres M, Falavarjani KG, <u>Nazari H</u>, et al. Intravitreal erythropoietin injection for the treatment of non-arteritic anterior ischaemic optic neuropathy. Br J Ophthalmol. 2011;95(7):992-5.

44.   <u>Nazari H</u>, Modarres M, Parvaresh MM, Ghasemi Falavarjani K. Intravitreal bevacizumab in combination with laser therapy for the treatment of severe retinopathy of prematurity (ROP) associated with vitreous or retinal hemorrhage; Graefe's Archive for Clinical and Experimental Ophthalmology 2010;248(12):1713-8.

45.   <u>Nazari H</u>, Moddares M, Maleki A; Pharmacologic vitreolysis. J Ophthalmic Vis Res 2010; 5 (1): 44-52.

46.   Falavarjani KG, Modarres M, <u>Nazari H</u>, Naseripour M, Parvaresh MM. Diabetic macular edema following panretinal photocoagulation. Arch Ophthalmol. 2010;128(2):262.

47.   Nazari H. Laser prophylaxis for peripheral retinal lesions. Lasers in Medicine 2009; 6(3): 29-34.

48.   Modarres M, <u>Nazari H</u>, Falavarjani KG, et al. Intravitreal injection of bevacizumab before vitrectomy for proliferative diabetic retinopathy. Eur J Ophthalmol 2009;19(5): 848 – 852.

49.   Razpa E, <u>Nazari H</u>, et al. Prevalence of head and neck abnormalities among people with consanguineous parents. Tehran University Medical Journal 2008; 66: 515-520.

50.   Falavarjani KG, Modarres M, <u>Nazari H</u>. Therapeutic effect of bevacizumab injected into the silicone oil in eyes with neovascular glaucoma after vitrectomy for advanced diabetic retinopathy. Eye. 2010;24(4):717-719.

51. <u>Nazari H</u>, Modarres M, Naseripour M, et al. Central retinal artery perfusion following 0.1 ml intravitreal injection of Bevacizumab. Iranian J Ophthalmol 2009;21(2): 13-18.

52. Naseripour M, <u>Nazari H</u>, Bakhtiari P, et al. Ruthenium-106 plaque radiotherapy for retinal vasoproliferative tumors. Iranian J Ophthalmol 2009;21:31-35.

53. Naseripour M, <u>Nazari H</u>, Bakhtiari P, et al. Retinoblastoma in Iran: outcomes in terms of patients' survival and globe survival. Br J Ophthalmol 2009;93(1):28-32.

54. Mohammadreza H, <u>Nazari H</u>, et al. Measurement of Choroidal Neovascular Area in Age-Related Macular Degeneration using Modified Otsu's Thresholding Method; Iranian J Med Phys 2008; 20,21: 77-84.

55. Naseripour M, <u>Nazari H</u>, Bakhtiari P, et al. Outcomes and prognosis of treatment for retinoblastoma with primary chemotherapy and focal treatment. Bina J Ophthalmol 2008;14(1):3-9.

56. Nabei R, <u>Nazari H</u>. Okihiro syndrome: A Duane's syndrome variant. Bina J Ophthalmol 2004;10(1):55-59.

B. Book chapters:

1. "Recent Advances in Ocular Imaging in Management of Uveitis and Related Intraocular Inflammations" Nazari H, Rao N. In "Advances in Ophthalmology and Optometry" Edited by Myron Yanoff; p435–457 ; 2017; Elsevier

2. "Artificial Vision" Weiland J, Nazari H, Humayun H. in "Ryan's Retina" 6th edition. 2017 Elsevier

3. "Argus II Retinal Prosthesis System". Falabella P, Nazari H. Weiland J, Humayun M. in "Artificial Vision, a clinical guide". Springer. 2017

4. "Scaffolds for Cell Transplantation" George M, Nazari H, Mitra D, Clegg D, Hinton D, Humayun M. In "Cellular Therapies for Retinal Disease" edited by Schwartz, Nagiel, Lanza; P: 45-54; Springer

5. "Multifocal Choroiditis/Serpiginous Choroiditis and Related Entities" Nazari H, Rao N. in "Advances in Intraocular Inflammation Imaging and Treatment" edited by Narsing Rao and Damien Rodger, and Julie Schallhorn; Springer 2019

C. Patent

Tai Y, Scianmarello N, Kang D, Park J, Humayun M, Murali K, Kashani A, Nazari Khanamiri H; Small molecular transport device for drug delivery or waste removal. USPTO # 9655774 B2. 2017

Abstracts in the past three years:

1. Nazari H, Karamaghaei C. Montalbano M, Taglialatela G, Vargas G, Zhang W, Motamedi M. Differential loss of retinal microvascular layers in Alzheimer's disease. ARVO 2020 Poster

2. Nazari H, El-Annan J. Central serous chorioretinopathy in a patient receiving intranasal corticosteroid. ASRS 2019 Poster

3. Nazari H, Montalbano M, Luisi J, Taglialatela G, Vargas G, Motamedi M. Age-dependent structural and microvascular changes in retina associated with progressive amyloid-β and tau deposition in triple transgenic mouse model of Alzheimer's disease. ARVO 2018 Poster

4. Nazari H, Sharifi A, Singh M, Kornblau I, El-Annan J, Carvounis P. Optical Density of Intraretinal Fluid in Diabetic Macular Edema. Retina Society Meeting 2018 Poster

Papers in preparation for submission:

1. H Nazari, M Montalbano, G Taglialatela, H Rylander, G Vargas, W Zhang, M Motamedi. Monitoring retinal sublayer thickness as a biomarker for Alzheimer's disease progression in young to middle age triple transgenic mouse model of AD. Prepared for submission to "Translational Vision Science and Technology"

2. H Nazari, R van de Merwe, C Karamaghaei, G Taglialatela, G Vargas, W Zhang, M Motamedi. Retinal vascular plexus attenuation in the triple transgenic mouse model of Alzheimer's Disease. Prepared for submission to "Eye and Brain"

Revised: May 2021